

Chapter 7

The ventilation of the Central and Eastern North Atlantic Ocean

7.1 Introduction

The ventilation of the permanent thermocline or pycnocline is thought to result from the subduction, or “drawdown” into the ocean interior, of water masses formed through air-sea interaction near the ocean surface. This idea, that fluid in the ocean interior can originate at the sea surface, is an old one, and ISELIN (1939), for example, proposed that water would be pushed downwards along sloping isopycnals from the base of the Ekman layer by the wind-induced vertical Ekman pumping velocity (related directly to the wind stress curl). More recently, there has been a development of idealised models of the thermocline circulation in which processes occurring above the seasonal pycnocline have not been considered explicitly. For instance, LUYTEN et al. (1983) prescribed the distribution of Ekman pumping velocity at the base of a flat Ekman layer which connected directly with the permanent pycnocline beneath. Their model, based on Sverdrup dynamics applied to a layered ocean, was successful in illuminating the character of the circulation patterns in the permanent thermocline, in particular leading to the classification of the so-called “pool”, “ventilated” and “shadow” regions. However, the lack of a realistic mixed layer, varying in time and space, was limiting. For instance, under the action of mechanical and buoyancy forcing, the mixed layer seasonally shallows and deepens, and STOMMEL (1979) recognised that it is only fluid leaving the mixed layer when it is deep during winter and spring that can irreversibly enter the permanent pycnocline, whereas fluid subducted from the summer mixed layer may be typically re-entrained during the following winter — the “mixed layer demon” hypothesis. This biases the T/S prop-

erties of the main thermocline toward those of the deep winter mixed layer, which had already been noted to be the case by ISELIN (1939).

Consequently, although Ekman pumping has traditionally been viewed as setting the rate at which the surface waters are transferred down into the pycnocline, it is actually the flow through the base of the winter mixed layer, which is often much deeper than the base of the Ekman layer and may possess large gradients in its depth, that ventilates the underlying ocean. As pointed out by WOODS (1985), the absence of a mixed layer in the idealised thermocline models precludes the possibility of lateral induction across the sloping base of the mixed layer, in which water parcels might be swept from the mixed layer into the permanent pycnocline by horizontal velocities, which themselves would result partly from the wind forcing, and partly from the buoyancy forcing. Subsequently, WILLIAMS (1989) extended the work of LUYTEN et al. (1983) to include a spatially-varying but time-constant mixed layer in which the density was prescribed. He found that the volume of ventilated fluid within the subtropical gyre was indeed increased because of the presence of the sloping mixed layer base. This result is also supported by the observational tracer studies of SARMIENTO (1983) and JENKINS (1987), which suggest that the subduction rate in the North Atlantic is actually two or three times greater than can be accounted for by Ekman pumping alone, so that the lateral induction would indeed seem to make an important contribution. This idea has been further tested by MARSHALL et al. (1993), who were able to infer the subduction rate over the North Atlantic from observations of wind stress and hydrography. They showed that whereas the Ekman pumping velocity in the subtropical gyre may be typically between 25–50 m/y, the total subduction rate reached around 100 m/y in a band stretching across the central North Atlantic, and that this enhancement was largely due to the lateral induction of fluid across the base of the sloping mixed layer.

Since the thermocline models referred to above are unable to duplicate the full complexity of ventilation from a time-varying mixed layer (and also cannot accommodate the recirculation in the Gulf Stream system), and since, due to uncertainties in the climatological observations, MARSHALL et al. (1993) were only able to provide a rather “blurred” view, we now turn our attention to studies with Ocean General Circulation Models. COX and BRYAN (1984) and COX (1985), for instance, provided a detailed investigation of the ventilation process in a primitive-equation level model of the North Atlantic, but their studies employed a simplified basin geometry and idealised (zonally-averaged) surface flux fields, together with a rudimentary mixed layer (relaxing the density of the upper level, 30m thick, to a prescribed field). BLECK et al (1989), on the other hand, used an isopycnic-coordinate model to study

the ventilation into the various model layers, but the model, although possessing an embedded mixed layer, used only a square, flat-bottomed ocean, and possessed a coarse horizontal resolution (about 2°). NEW et al. (1995) then went on to study the subduction process in a medium-resolution (about 1°) simulation of the Atlantic Ocean, and confirmed the result that the ventilation of the subtropical gyre was mostly due to the lateral induction across the sloping mixed layer base. However, their model was not of “eddy-permitting” resolution, and the ventilation patterns appeared somewhat smooth and idealised.

In summary, the ventilation of the North Atlantic subtropical gyre has not so far been investigated in detail in any realistic simulation with an eddy-permitting model, although BECKMANN et al. (1994) have compared a section at 30°W from a $1/3^\circ$ resolution model with observations. As a result, the main goals of this chapter are to describe the way in which the three high-resolution state-of-the-art DYNAMO models describe the circulation patterns and ventilation of the North Atlantic subtropical gyre, to assess these descriptions by comparing them with available observations, and to seek new insights into the mechanisms governing the ventilation of the gyre in nature.

In the real world, the ventilation of the North Atlantic subtropical gyre is characterised by the subduction of large quantities of relatively homogeneous “mode” waters, each of which is characterised by a certain sector of the temperature-salinity diagram for which there exists a relatively large volume when compared with other sectors (WRIGHT and WORTHINGTON, 1970; MCCARTNEY and TALLEY, 1982). These water masses result from relatively deep winter-time mixing (to several hundred metres) of the near-surface water masses in certain regions of the central North Atlantic. One well-defined mode is the so-called 18°C water which forms in the Sargasso Sea (Worthington, 1959) with a density of around 26.5. This water mass has been called the “subtropical” mode water by MASUZAWA (1969) and is subducted southwards and southwestwards to ventilate the ocean to depths of 400–500 m. Heavier modes, of densities in the range 27.0–27.3 have been observed northeast of the Azores (MCCARTNEY and TALLEY, 1982; POLLARD and PU, 1985), and are thought to be drawn slowly into the ocean interior (at speeds of order 0.5 cm/s) by geostrophic advection. These water masses can be traced to depths of 800–900 m, and have been called “subpolar” mode waters by MCCARTNEY and TALLEY (1982), even though they ventilate the subtropical gyre. More recently, however, the terminology “Eastern North Atlantic Water (ENAW)”, has been applied to them by POLLARD et al. (1996), who in a detailed observational study concluded that the primary direction of ventilation was (somewhat surprisingly) to the west, from a formation region in and to the west of the Bay of Biscay. There is by contrast relatively little support in the observations

for the production of mode waters in the central subtropical gyre (i.e. near the Mid-Atlantic ridge), but this is where the Azores Current (AC) cuts across the North Atlantic. The Azores Current is a major current feature which is thought to separate from the Gulf Stream near the Grand Banks, and then to move southwards and eastwards to meet the Mid-Atlantic ridge at about 35°N , after which it runs almost zonally, between $32\text{--}35^{\circ}\text{N}$, perhaps reaching as far as the Moroccan coast, but with branches off to the south (STRAMMA, 1984; GOULD, 1985; SY, 1988; KLEIN and SIEDLER, 1989; FERNANDEZ and PINGREE, 1996; CROMWELL et al., 1996; KÄSE and KRAUSS, 1996; PINGREE, 1997). It appears that the AC may inhibit the relatively deep wintertime mixing in the central north Atlantic, so that mode waters are not produced in large quantities there.

The present chapter investigates the ventilation of the subtropical gyre in the three high resolution DYNAMO models, chiefly by comparing maps of potential vorticity on density surfaces (which can be used as a tracer to infer the circulation pathways) with those presented in the observations. Throughout, we pay particular attention to the influence of the Azores Current on the ventilation process, and lay special emphasis on the ENAW (Eastern North Atlantic Water) water mass, giving the study a special relevance for the oceanography of the seas near the European margins. Although the emphasis is on the intercomparison phase (mean conditions over the last five years) of the various model integrations, when the models are more nearly in a state of equilibrium, attention is also paid to some aspects of the spin-up behaviour. The chapter is laid out as follows. In section 7.2 we describe the characteristics of the wintertime mixed layers of the models, since (from the above reasoning), this is the critical time of year for setting the properties which are subducted into the ocean interior. We then discuss the near-surface circulation patterns in section 7.3, and in particular the form of the Azores Current, since this affects the ventilation pathways into the gyre. Section 7.4 then investigates the patterns of potential vorticity on density surfaces, comparing with observations where appropriate. Finally, section 7.5 discusses the model solutions near 30°W , again comparing with observations, and section 7.6 summarises our conclusions.

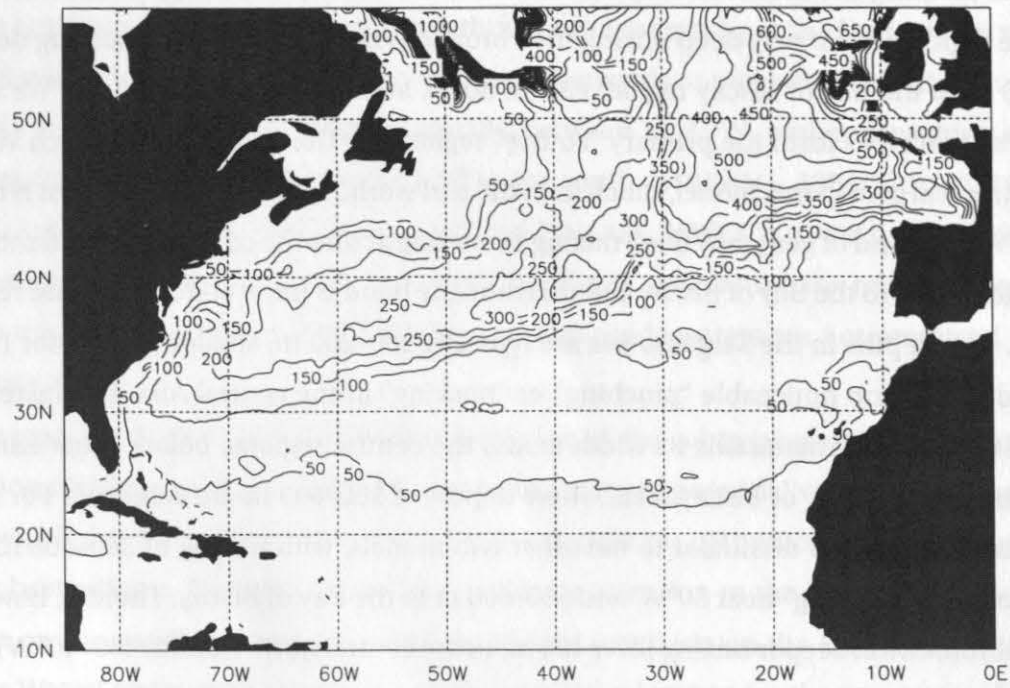
7.2 Winter Mixed Layer Characteristics

Figure 7.1 compares the climatological winter mixed layer depth fields (averaged between January–March over the intercomparison phase) between the three models. For ISOPYCNIC, there is a well defined area of relatively deep mixing, to 350–400 m, in the Sargasso Sea (i.e. west of about 50°W , and between $30\text{--}42^{\circ}\text{N}$). This region then pinches to a “neck” at about

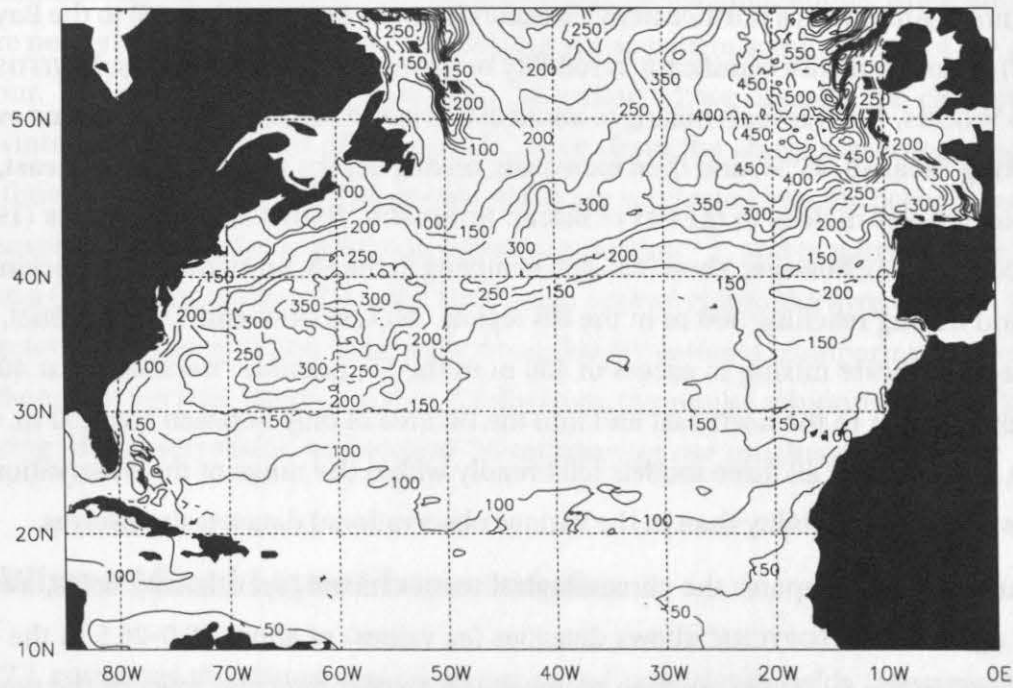
45°W, 35°N, where the mixing reaches only 200 m or so (which is in fact where one of the branches forming the model Azores Current runs, see below). Moving towards the northeast, the region of relatively deep mixing then broadens out and deepens, reaching depths of 500–600 m in the Bay of Biscay region, east of 30°W, and between 42–52°N say. We will see that these two areas form the primary “source” regions for the mode waters which ventilate the subtropical gyre in this model, much as in the real world. For LEVEL, the pattern is broadly similar, with a band of generally deep mixing extending across the central north Atlantic from the Sargasso Sea to the Bay of Biscay, but this time the band is more continuous and regularly varying. The depths in the Sargasso Sea are typically 200–250 m, shallower than for ISOPYCNIC, and there is no noticeable “pinching” or “necking” in the central Atlantic. Instead, the band of deep mixing maintains its width across the central regions, before broadening and deepening into the Bay of Biscay area, where depths of 500–600 m are achieved. For SIGMA, the situation is not too dissimilar to the other two models, with mixing of 300–400 m in the Sargasso Sea, a “necking” near 50°W, and 500–600 m in the Bay of Biscay. There is, however, a region of somewhat deeper mixing (over 400 m) in the central north Atlantic (30–40°W) which is not apparent in the other models.

The observations also show a broad band of deep wintertime mixing stretching across the central north Atlantic in a northeasterly direction from the Sargasso Sea (SS) to the Bay of Biscay (BB) region, but with significant variability between the various datasets. LEVITUS (1982; see also WOODS, 1987) reveals mixing to about 250 m in the Sargasso Sea, with some evidence of “necking” near 40–45°W, and then increasing mixing depths towards the northeast, reaching about 300–600 m deep in the Bay of Biscay. ROBINSON, BAUER and SCHROEDER (1979, see also WOODS, 1987), however, show 300–400 m mixing in the SS, no evidence of “necking” near 40°W, and mixing reaching 900 m in the BB region. MCCARTNEY and TALLEY (1982), on the other hand, indicate mixing in excess of 400 m in the SS, possible “necking” near 40–45°W, but mixing further to the northeast and into the BB area of only between 200–400 m. Consequently, it seems that all three models fall broadly within the range of the observations, and perhaps with less variability than in the various observational datasets themselves.

Figure 7.2 now compares the climatological winter mixed layer density fields, and there is close agreement. ISOPYCNIC shows densities (σ_0 values) of about 26.0–26.5 in the area of deep mixing in the SS. There are then progressively heavier densities towards the northeast, reaching 27.0–27.2 in the BB region. LEVEL possesses similar densities in the SS area, but slightly heavier in the BB (27.2–27.4). SIGMA also shows values between 26.0–26.5 in the SS, increasing to 27.0–27.2 in the BB, in close agreement with ISOPYCNIC.



(a) LEVEL



(b) ISOPYCNIC

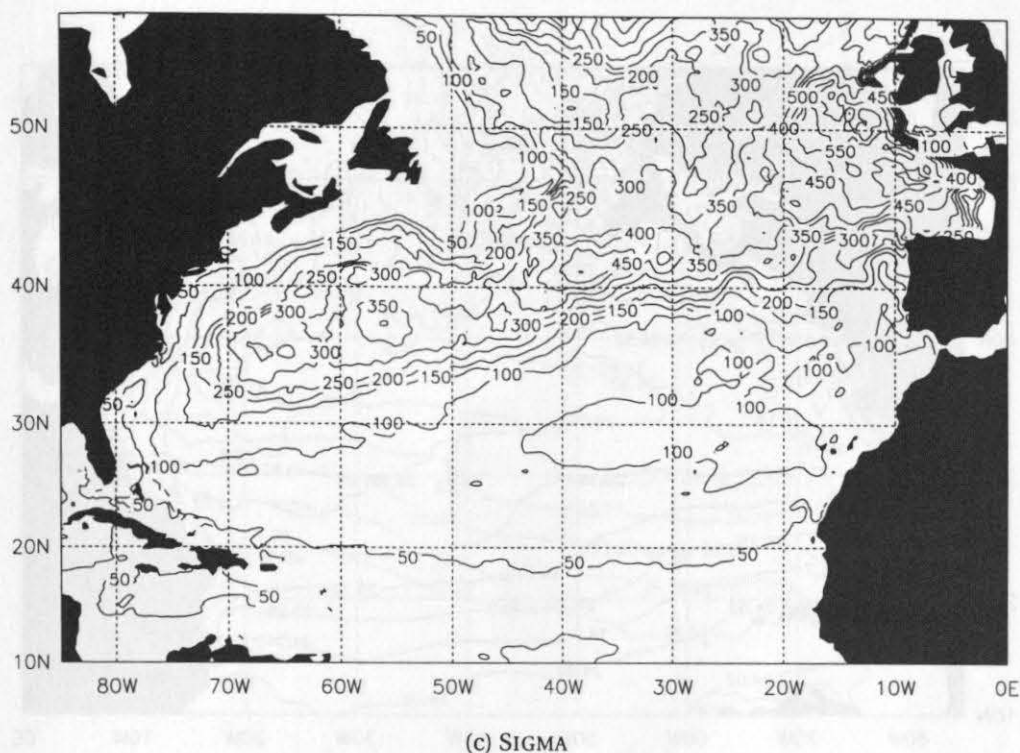
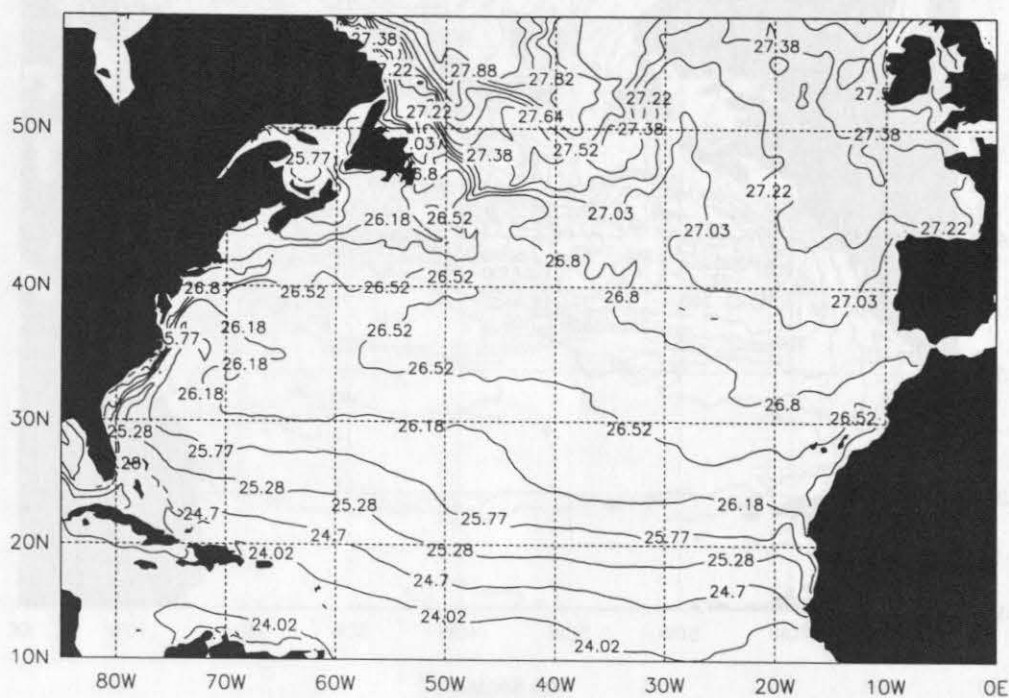
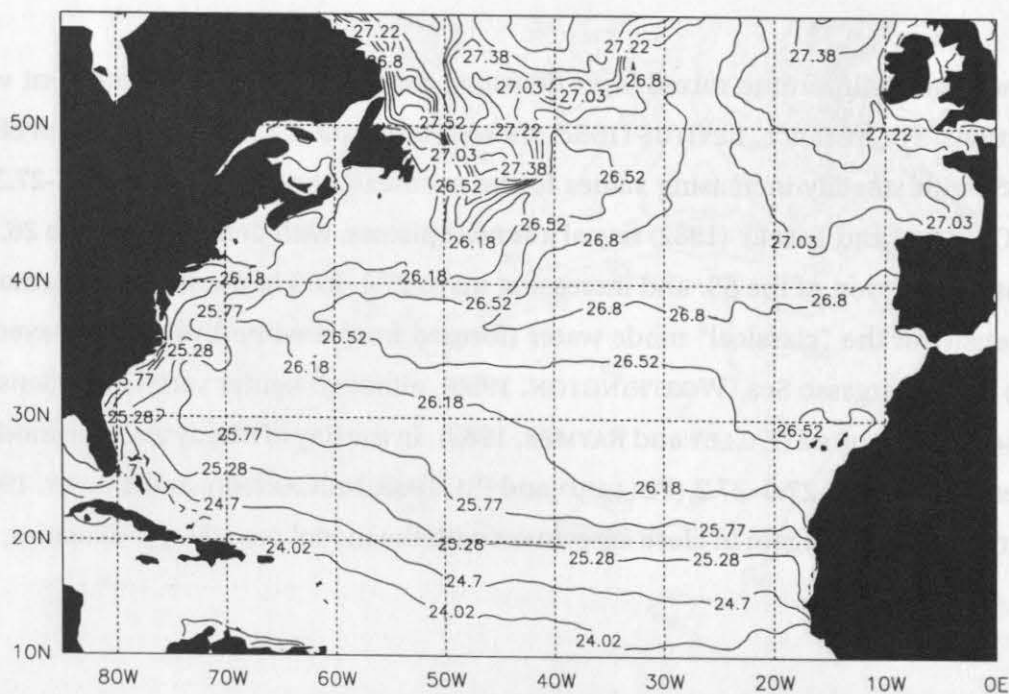


Figure 7.1: Winter climatological mixed layer depth (m), contours from 0 to 1000 at interval of 50

These model wintertime mixed layer densities are also in excellent agreement with the observations. For instance, LEVITUS (1982) shows wintertime densities of between 26.0–26.5 in the SS, with steadily increasing values to the northeast, reaching about 27.0–27.3 in the BB. MCCARTNEY and TALLEY (1982) reveal a similar picture, with densities close to 26.5 in the northeastern portion of the SS, and increasing up to 27.1–27.3 in the BB. Furthermore, 26.5 is the density of the "classical" mode water (formed from a wintertime mixed layer of this density) in the Sargasso Sea (WORTHINGTON, 1959), although lighter varieties of density 26.4 have also been reported (TALLEY and RAYMER, 1982). In the Bay of Biscay also, the mode water densities are between 27.0–27.2 (POLLARD and PU, 1985, MCCARTNEY and TALLEY, 1982, and POLLARD et al., 1996), again in close agreement with the model mixed layer densities.



(a) LEVEL



(b) ISOPYCNIC

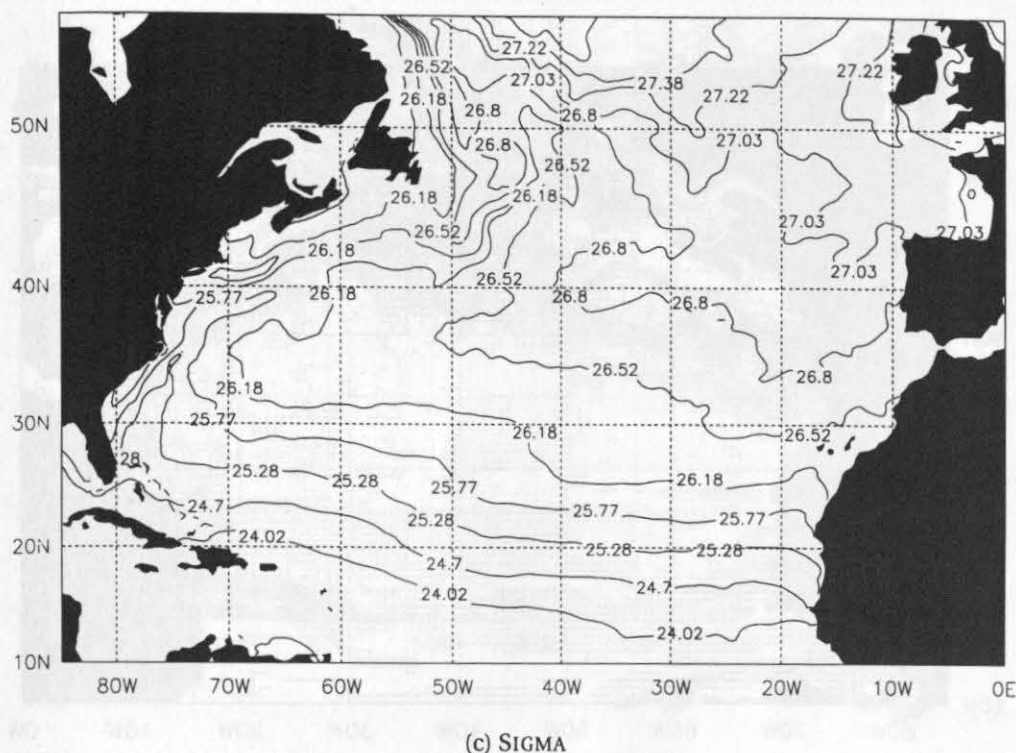
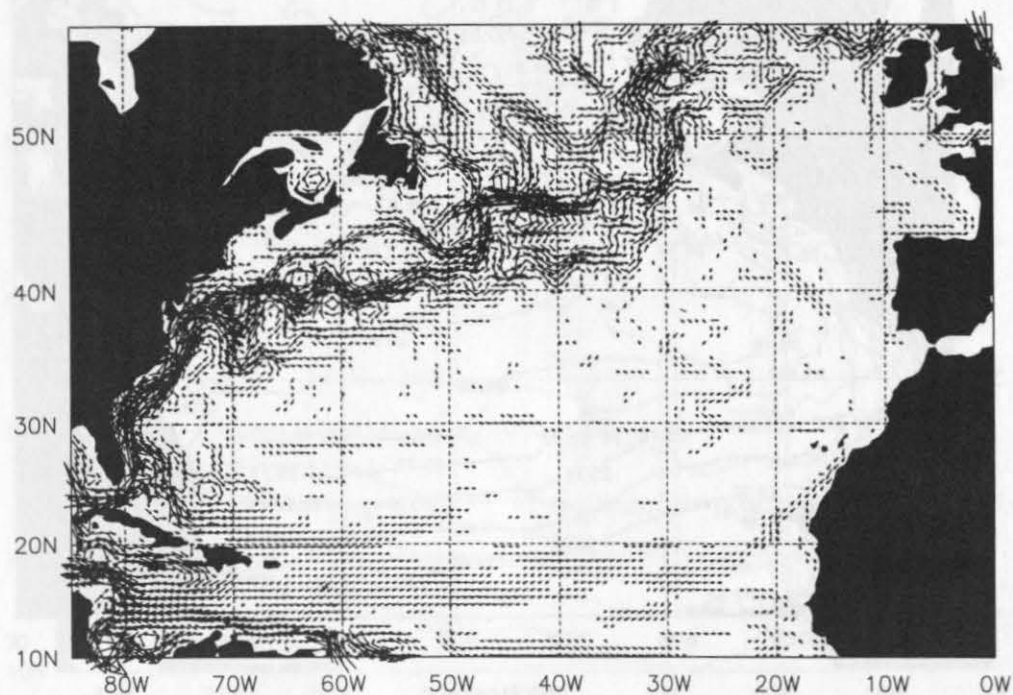


Figure 7.2: Winter climatological mixed layer density (σ_0 units), contours from 24.02 to 28.12

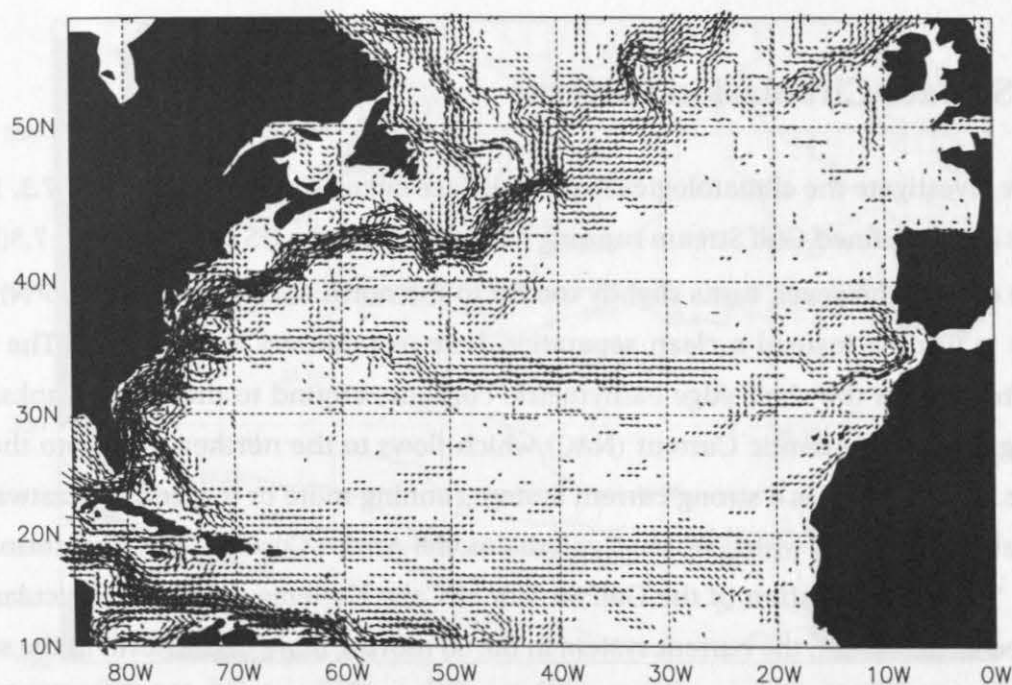
7.3 Surface Circulation Patterns

We now investigate the climatological winter surface circulation patterns in Fig. 7.3. ISOPYCNIC has a well-defined Gulf Stream running northwards up the US coastline (Fig. 7.3(b)).

The current, however, turns slightly too far to the north at Cape Hatteras (35°N), observations indicating instead a clean separation here (e.g. BROWN et al., 1986). The current thereafter follows the shelf-edge bathymetric contours around to the Grand Banks, before forming the North Atlantic Current (NAC) which flows to the northeast out into the North Atlantic. Also present is a strong current system running more or less zonally eastwards between about $32\text{--}35^\circ\text{N}$, which we shall call the model Azores Current (AC). This forms partly from a “partial” separation of the Gulf Stream at Cape Hatteras (which is particularly pronounced in the winter, the current system in the SS moving more to the north in the summer months), and partially from a current which branches off from the Gulf Stream/NAC system near the Grand Banks, flowing initially towards the southwest, but then turning to the southeast, before joining the AC system near 45°W , 35°N (close to the “necking” in the mixed layer depths referred to above). The model AC then appears to run more or less zonally all the way



(a) LEVEL



(b) ISOPYCNIC

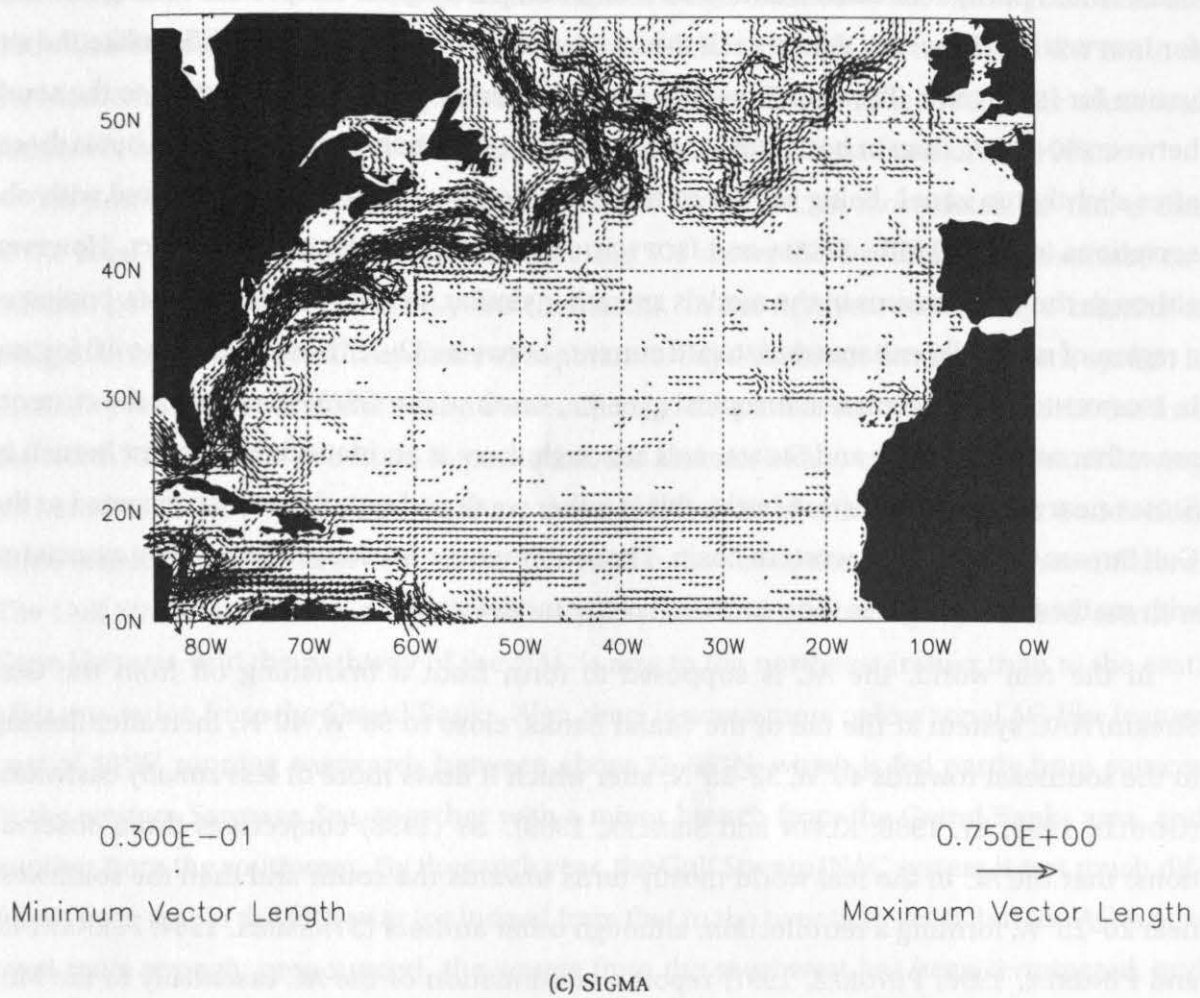


Figure 7.3: Winter climatological surface (53m) circulation patterns. Every second point plotted. Velocity cutoff at 3 cm/s.

to the Moroccan coast, before turning both to the north (mostly) and also to the south, so forming countercurrents. However, there is an over-strong cyclonic circulation cell immediately west of the Gibraltar Straits in ISOPYCNIC which may be associated with the sinking of Mediterranean Water, and which may be partly responsible for “pulling” the AC to the Moroccan coast. We also note an identifiable branch breaking off from the AC near 25°W and flowing initially southwards, then turning to the southwest and west. Overall, there is a general anticyclonic circulation in the subtropical gyre, which these currents are superimposed upon, and part of.

In both the LEVEL and SIGMA models, the Gulf Stream (GS) also turns somewhat too far to the north at Cape Hatteras. For LEVEL, there is a large current meander near Cape Hat-

terras, which partly recirculates anticyclonically, and partly gives a separation along 35°N (as for ISOPYCNIC). However, this branch then moves north to join the main GS, unlike the situation for ISOPYCNIC. The Gulf Stream in LEVEL is then perhaps slightly further to the south between 50 – 65°W , than in both ISOPYCNIC and SIGMA, and hence more realistic, but is thereafter slightly too zonal, being too far to the south between 30 – 40°W as compared with observations (e.g. SY, 1988). SIGMA and ISOPYCNIC are more realistic in this respect. However, although the Gulf Streams in the models are rather similar, neither LEVEL or SIGMA possesses a region of markedly enhanced eastward currents between 32 – 35°N , similar to the AC feature in ISOPYCNIC. In the central subtropical gyre (i.e. south of the GS/NAC system), the currents are rather weak in LEVEL and SIGMA, and although there is an identifiable current branch in SIGMA near 30°N in the eastern basin, this is rather weak and not obviously connected to the Gulf Stream system in the western basin. These differences are found below to be associated with marked differences in the ventilation of the model gyres.

In the real world, the AC is supposed to form from a branching off from the Gulf Stream/NAC system at the tail of the Grand Banks, close to 50°W , 40°N , thereafter flowing to the southeast towards 40°W , 32 – 35°N , after which it flows more or less zonally eastwards (GOULD, 1985; SY, 1988; KLEIN and SIEDLER, 1989). SY (1988) conjectures (from observations) that the AC in the real world mostly turns towards the south and then the southwest near 20 – 25°W , forming a retroflexion, although other authors (STRAMMA, 1984; FERNANDEZ and PINGREE, 1996; PINGREE, 1997) report a continuation of the AC essentially to the Moroccan coast, albeit with a diminishing transport. In the western basin (west of about 50°W), some authors (SCHMITZ and MCCARTNEY, 1993) show a tight (inertial) westward recirculation immediately south of the Gulf Stream system (near 30 – 35°N), although this is not apparent in the circulation patterns inferred from drifters by RICHARDSON (1983), which instead shows an eastward flow in a broad Gulf Stream system between about 35 – 40°N in the western basin.

In ISOPYCNIC, it is therefore unclear as to how realistic the “double” separation of the Gulf Stream at Cape Hatteras is (which has been seen before in preliminary runs with this model at this resolution), giving eastward flow near 35°N . It may be that this separation is related to some feature of the wind stress field (separation usually occurring near the zero wind stress curl line). Or it may be that if the (northward branch of the) Gulf Stream itself were correctly placed in this model (further south in this region), then the two separation features would become indistinguishable, giving a realistic separation pattern. The branching off from the Grand Banks, however, is broadly supported by the observations, albeit with some differences in the precise current pathway between 50°W , 40°N and 40°W , 32 – 35°N . Further, the AC in

ISOPYCNIC is at the correct latitude in the eastern basin (east of 40°W, where it crosses the mid-Atlantic ridge), and is therefore reasonably realistic, although the turning to the north at the Moroccan coast seems stronger than occurs in nature. The retroflection to the south and southwest near 25°W in ISOPYCNIC is also supported by the observations of SY (1988).

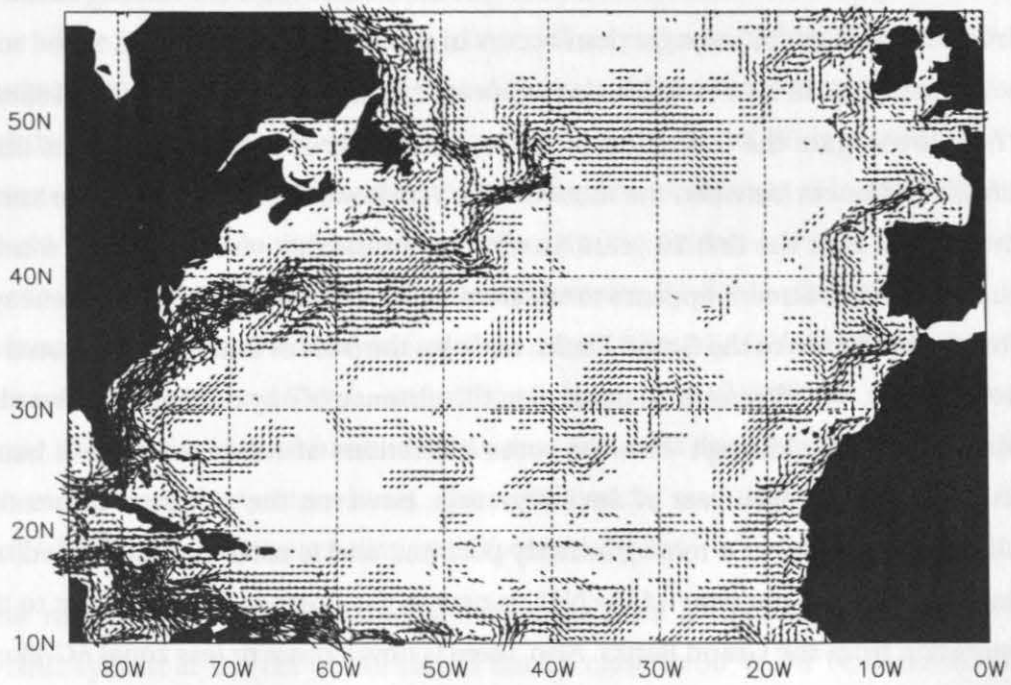
We now investigate the formation of the AC in ISOPYCNIC in more detail, as this is one of the chief differences between the models. Fig. 7.4 shows the evolution of the surface circulation patterns over the first 10 years (in march). In the first year (after only 6 months of integration), the Gulf Stream appears to separate at Cape Hatteras, but the current system is thereafter too broad out to the Grand Banks, and also the path of the NAC is too zonal out into the North Atlantic. We also note, in particular, the absence of any coherent eastward flowing jet between 32–35°N, although there are some indications of enhanced current bands near these latitudes. By the fifth year of the integration, however, the picture is rather different. The Gulf Stream now takes a more northerly position, and is more tightly defined, north of Cape Hatteras, and the pathway of the NAC is now to the northeast (rather than to the east) after separation from the Grand Banks. Also, there is now a more or less zonal AC-like feature east of 40°W, running eastwards between about 32–35°N, which is fed partly from sources in the western Sargasso Sea, together with a minor branch from the Grand Banks area, and another from the southwest. By the tenth year, the Gulf Stream/NAC system is not much different from that in the fifth year (or indeed from that in the twentieth year), but the AC is now even more strongly pronounced, the source from the southwest has been terminated, and the retroflection to the south near 25°W is also in evidence. In summary, the AC in ISOPYCNIC is not present in the first year, but forms quickly during the first 5 years, strengthening out to year 10, by which time a more or less stable flow pattern has become established.

7.4 Isopycnic Potential Vorticity

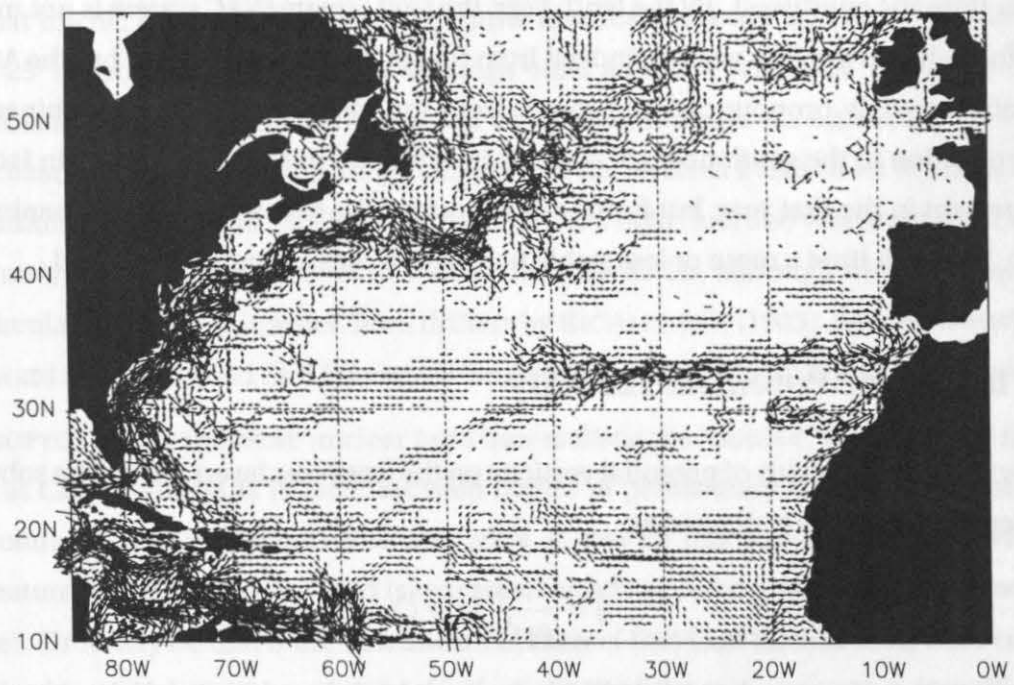
We now consider the fields of potential vorticity on the isopycnic layers within the subtropical gyre. Potential vorticity is defined as

$$q = \frac{1}{\rho_0} \frac{d\rho}{dz} (f + \zeta) \quad (7.1)$$

where ρ_0 is a reference density (1026.5 kg/m³), and ζ is the relative vorticity. An appropriate finite-difference form of the potential vorticity for the layered ISOPYCNIC model uses the layer thickness and density difference to define the local density gradient. This is a dynamical quantity which is conserved along fluid trajectories in the absence of external forcing and



(a) Year 0



(b) Year 4

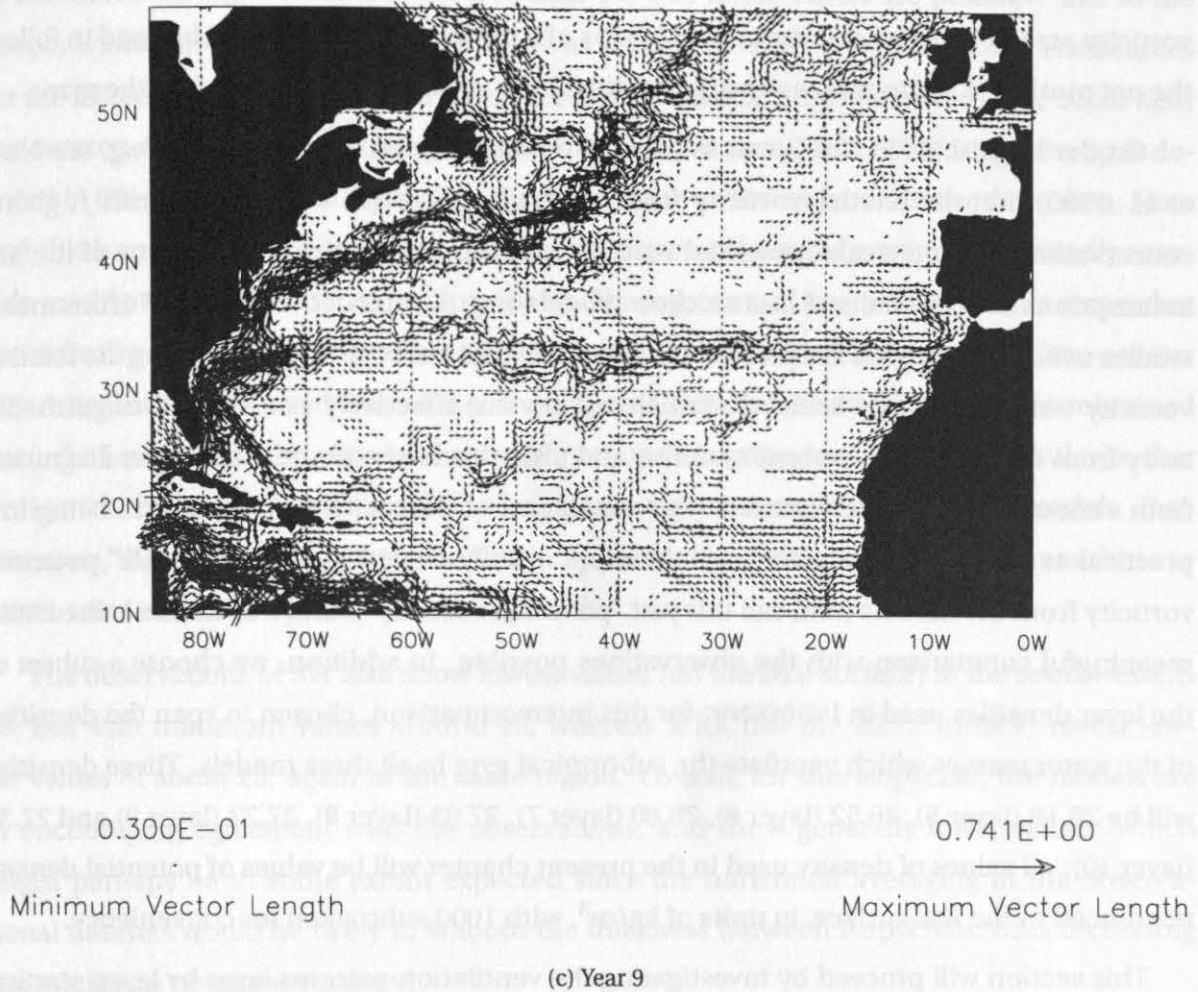


Figure 7.4: ISOPYCNIC surface circulation patterns (snapshots) at month 6 (March) of (a) Year 0, (b) Year 4 and (c) Year 9. Every second point plotted. Velocity cutoff at 3 cm/s.

dissipative effects (that is, once the water parcels are removed, by subduction, from the influence of the surface forcing, and in the absence of any mixing in the interior of the ocean). If density is also conserved along fluid trajectories (usually a good approximation), then the lines of constant q on density surfaces coincide with the fluid trajectories, so that the potential vorticity can be used to trace the circulation of water masses (confined to constant density layers). For a given isopycnic layer, the potential vorticity will be lowest near the region where that water mass is detrained from the wintertime mixed layer (since the mixed layer becomes deep, forming a large volume of a homogeneous “mode” water of low potential vorticity), which we consider as the source region. We thereafter expect that this low- q water would ventilate into the gyre with some slight increase in q as the mixing in the ocean

interior gradually destroys the thickness of the water mass in question. In this way, potential vorticity acts as a Lagrangian tracer, and maps of q on density surfaces can be used to follow the net motion of water masses and to illuminate the ventilation pathways into the gyre.

On the large scale in the ocean interior, it is often a good approximation (e.g. see NEW et al. 1995) that the relative vorticity term can be neglected in comparison with f , giving conservation of “large-scale” potential vorticity on fluid trajectories, which is one of the key assumptions of the idealised thermocline models (e.g. LUYTEN et al., 1983). Furthermore, studies using output from the present models show that fields of “full” (including the relative vorticity term) and “large-scale” potential vorticity are effectively visually indistinguishable away from the boundary current systems, and also, this latter quantity has been diagnosed from various observational datasets (the calculation of the relative vorticity term being impractical as yet). In the following, we therefore usually consider the “large-scale” potential vorticity from the models (and call this just “potential vorticity”), and this makes a direct and meaningful comparison with the observations possible. In addition, we choose a subset of the layer densities used in ISOPYCNIC for this intercomparison, chosen to span the densities of the water masses which ventilate the subtropical gyre in all three models. These densities will be 26.18 (layer 5), 26.52 (layer 6), 26.80 (layer 7), 27.03 (layer 8), 27.22 (layer 9) and 27.38 (layer 10): all values of density used in the present chapter will be values of potential density referenced to the sea-surface, in units of kg/m^3 , with 1000 subtracted for convenience.

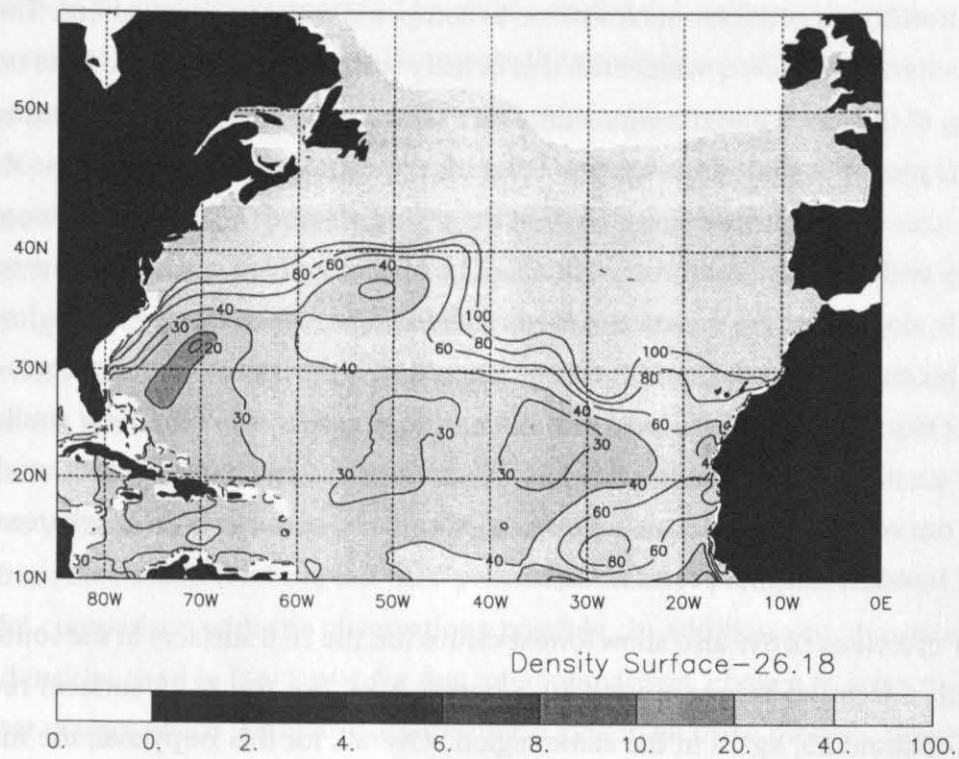
This section will proceed by investigating the ventilation patterns layer by layer, starting with the lightest layers first, and throughout, all values of potential vorticity will be in units of $10^{-11} \text{ m}^{-1}\text{s}^{-1}$. For each layer we will firstly consider the q -field in the initial model state (which represents the situation for the LEVITUS (1982) observational dataset), and compare this with the situation for the climatological winter means for the models. We choose winter as the time for the presentation of the model datasets as this also reveals the positions of the layer outcrops into the winter mixed layer, from where the water masses are detrained. We will also make comparisons primarily with the diagnoses from the observational datasets of KEFFER (1985, to be referred to as K in the following) and STAMMER and WOODS (1987, to be referred to as SW). We will also refer to some extent to the work of MCDOWELL et al. (1982, to be referred to as MRK, which can be considered as an earlier version of the Keffer datasets), where extra density surfaces are presented.

Fig. 7.5 shows the situation for the 26.18 isopycnal surface. In the initial state (i.e. for the LEVITUS, 1982, observations), the region of lowest q is in the southwestern Sargasso Sea, where values lower than 20 occur. For ISOPYCNIC in winter, the lowest values are still in more

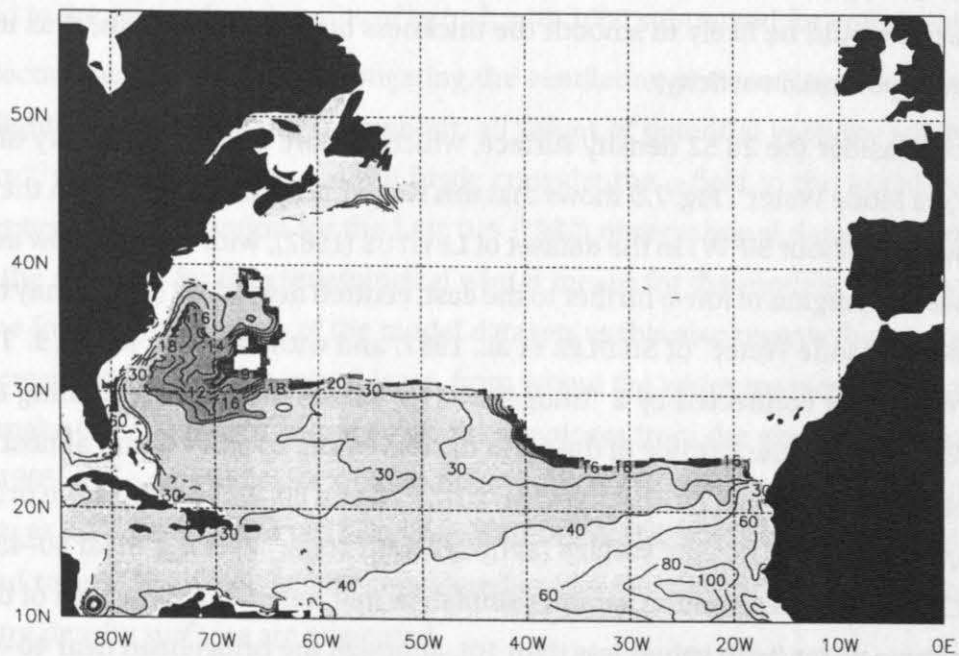
or less the same region, but are now less than 10. The lower values are probably due to the deeper wintertime mixed layer in ISOPYCNIC as compared with the observations. The sources for the injection of this low- q water onto this density surface from the mixed layer occur near the outcrop of this layer into the wintertime mixed layer near 30°N , 60°W (the outcrop is denoted in the plot by the line separating the region with contours from that with no data. Note that this is a mean wintertime picture so that the region of lowest q need not necessarily coincide exactly with the mean outcrop position). The injection of low- q water occurs somewhat sporadically, depending on the state of the local eddy field, which also twists the low- q water into complex and distorted shapes (i.e. as compared with the overly smooth picture obtained from the Levitus dataset). For LEVEL and SIGMA the situation is qualitatively similar to that in ISOPYCNIC, except that the region of low- q is not quite so extensive in these models. Furthermore, the ventilation pathway in SIGMA appears to be to the southeast, whereas those in LEVEL and ISOPYCNIC appear to be anticyclonic.

The observations of SW also show lowest values (on the 26.0 surface) in the southwestern SS, but with minimum values around 40, whereas MRK (for the 26.15 surface) reveal lowest values of about 25, again in the same region. Overall, for this isopycnal, the models are in encouraging agreement with the observations, and show generally lower values (which might perhaps be to some extent expected since the horizontal averaging in the observational datasets would be likely to smooth the thickness between isopycnals, thus increasing the minimum potential vorticity).

We now consider the 26.52 density surface, which is more or less the density of classical “Sargasso Sea Mode Water”. Fig. 7.6 shows that this water mass exists primarily in the Sargasso Sea (extending to about 50°W) in the dataset of LEVITUS (1982), with values as low as 7. There is also, however, a region of low- q further to the east, centred near 30°W (which may be related to the “Madeira Mode Water” of SIEDLER et al., 1987) and with values as low as 9. These two regions are possibly connected by a “bridgehead” of values less than 12, running east–west near $30\text{--}32^{\circ}\text{N}$, close to the latitude of the AC in the real world, so that we may almost consider most of the subtropical gyre, i.e. that between $20\text{--}35^{\circ}\text{N}$, and $80\text{--}25^{\circ}\text{W}$, to be more or less filled with low- q water on this density surface (although with some “necking” near $40\text{--}45^{\circ}\text{W}$). For ISOPYCNIC in winter, the situation is rather similar, in that nearly the same area of the gyre is filled with low- q water (with values less than 10), although the bridgehead near $40\text{--}45^{\circ}\text{W}$ has been lost, and the lowest values are now in the centre of the gyre, near $40\text{--}50^{\circ}\text{W}$, rather than in the Sargasso Sea. (In fact, the pattern in Levitus for this layer falls between the patterns for the surfaces 26.18 and 26.52 in ISOPYCNIC, so indicating that the ISOPYCNIC mixed layer



(a) Initial state for ISOPYCNIC, and all models



(b) winter climatological means for LEVEL

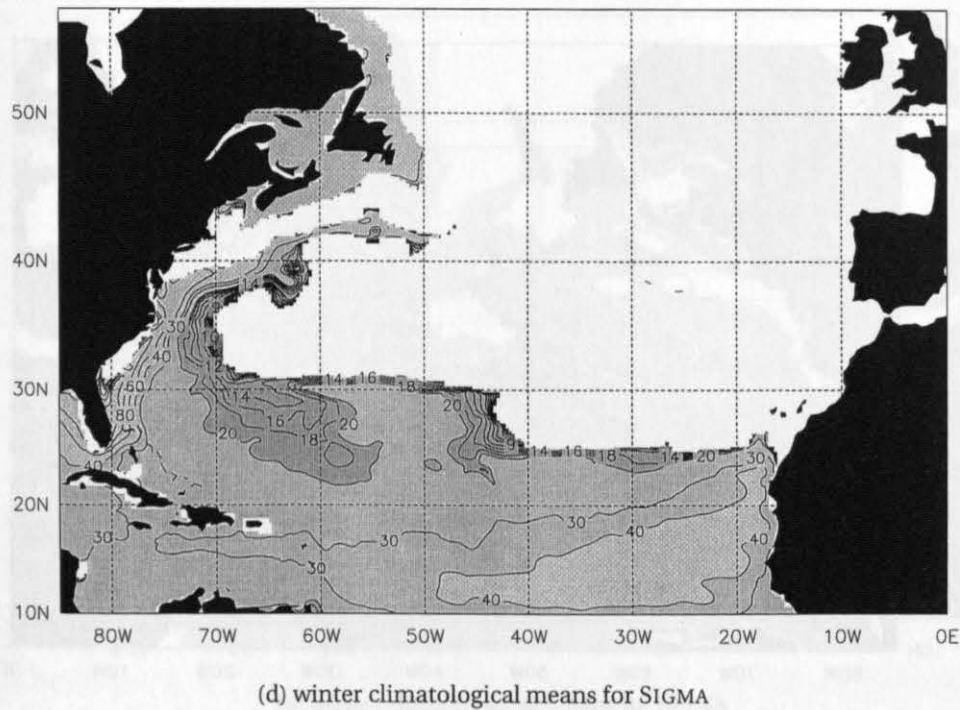
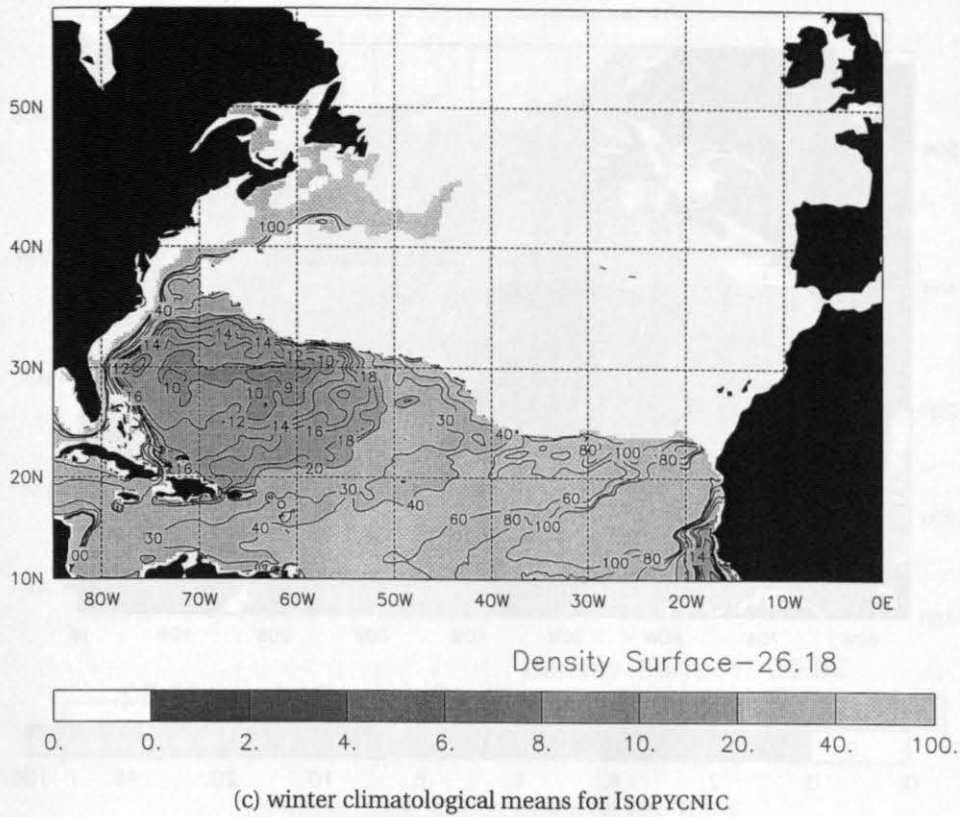
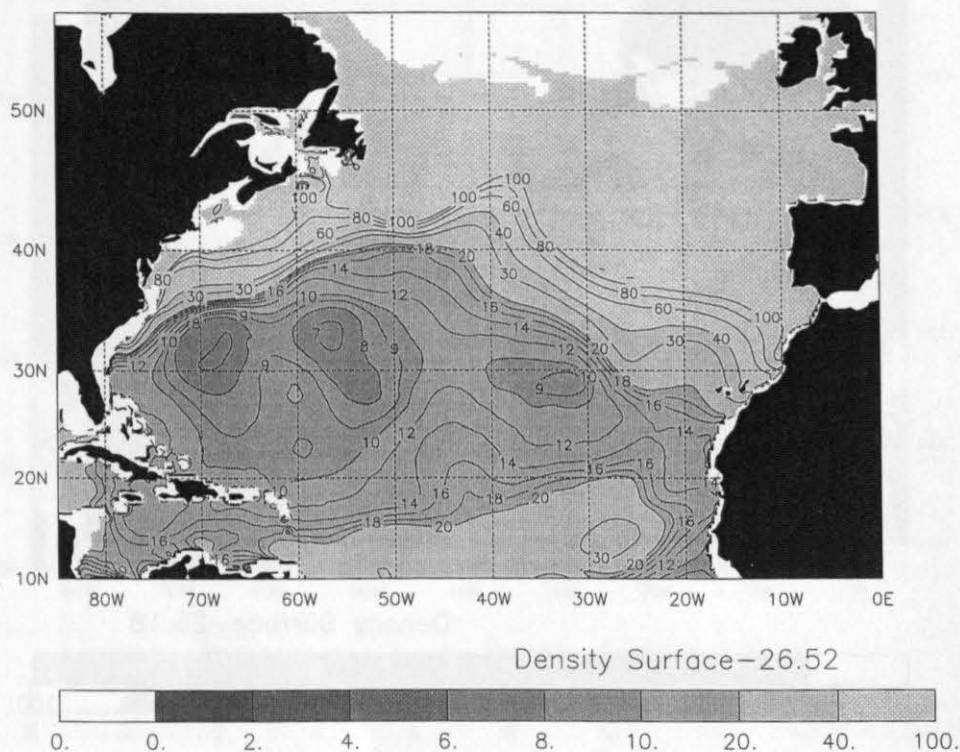
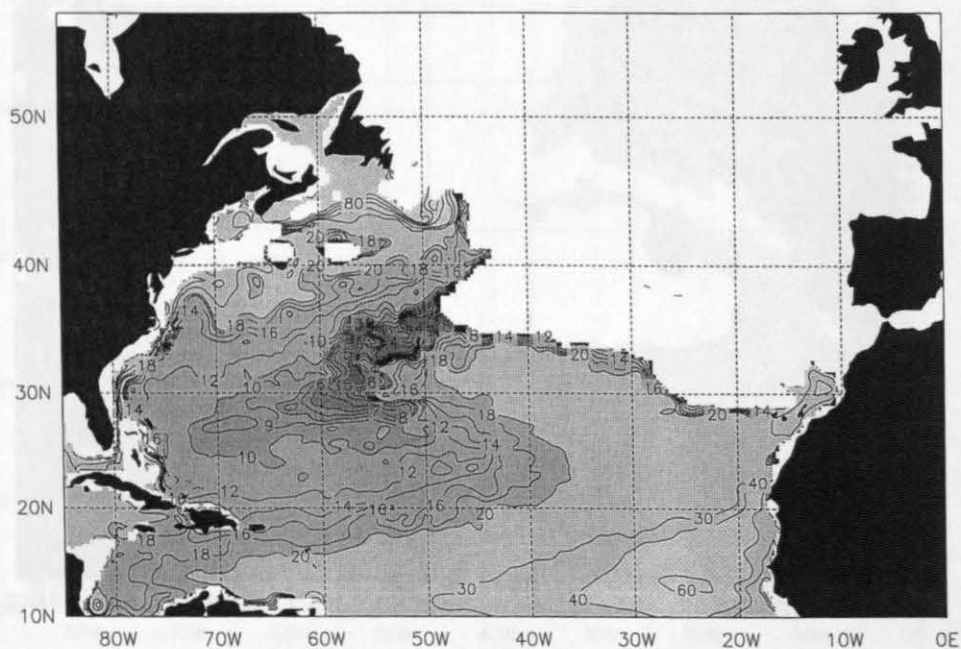


Figure 7.5: Potential vorticity ($\times 10^{-11} \text{ m}^{-1} \text{ s}^{-1}$) on isopycnal surface 26.18 (ISOPYCNIC layer 5). Contours at values of 1, 2, 3, 4, 5, 6, 7, 8, 9, 10, 12, 14, 16, 18, 20, 30, 40, 60, 80, and 100.



(a) Initial state for ISOPYCNIC, and all models



(b) winter climatological means for LEVEL

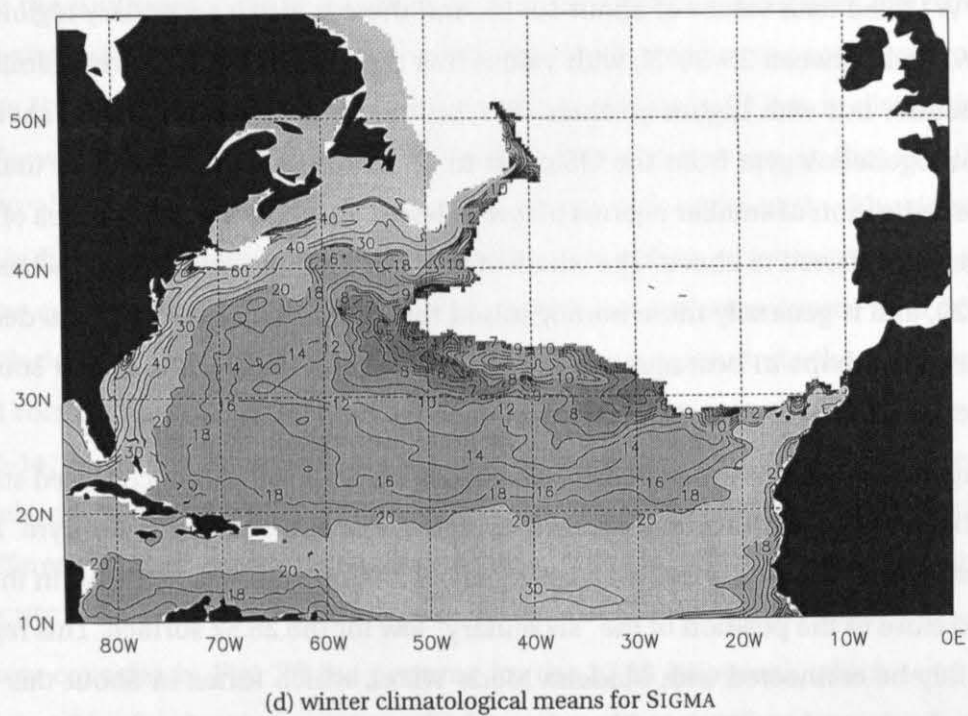
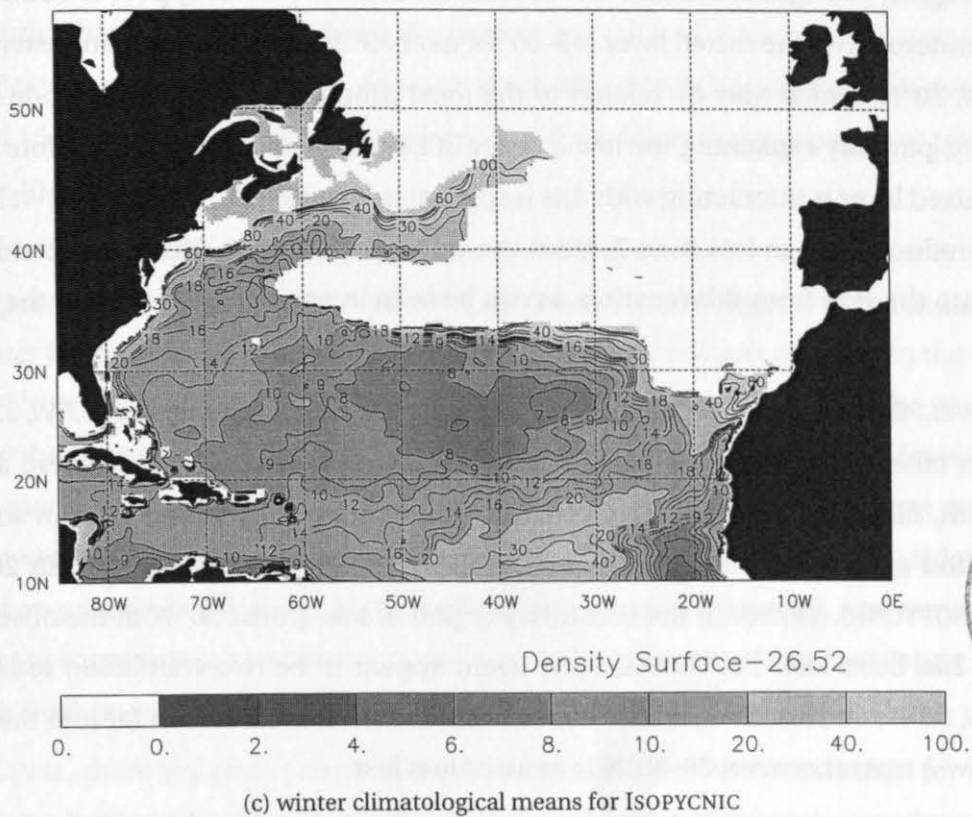


Figure 7.6: Potential vorticity ($\times 10^{-11} \text{ m}^{-1} \text{ s}^{-1}$) on isopycnal surface 26.52 (ISOPYCNIC layer 6). Contours at values of 1, 2, 3, 4, 5, 6, 7, 8, 9, 10, 12, 14, 16, 18, 20, 30, 40, 60, 80, and 100.

density is slightly too light in the SS.). The sources for the low- q water appear to be both on the northern outcrop into the mixed layer (45–50°W, near 35°N), and also from an eastern source near 30°W, 30°N, which may be related to the local production of Madeira Mode Water in this vicinity, partially explaining the low- q water in Levitus near this location. (Note however that the mixed layer is interacting with this isopycnal in this vicinity, so that the q -values here are being reduced (i.e. to less than 7) from the values (about 8–9) which are actually being injected into the gyre from this location, as can be seen in an analogous plot for the summer case.)

For LEVEL, there is clearly a primary ventilation source for this layer near 50°W, 35°N, and ventilation takes place along an obvious pathway more or less to the southwest, and then to the south, filling the western portion of the gyre with typical q -values of 10 or so. This is in quite good agreement with Levitus and the mean pattern between isopycnals 26.18 and 26.52 for ISOPYCNIC. However, the secondary region of low- q near 30°W in the observations of Levitus has been lost. For SIGMA, there again appear to be two ventilation sources, one near 50°W, 35°N, and another near 30°W, but ventilation does not reach far into the gyre, so that the low- q water between 20–30°N is more or less lost.

For this density surface (actually for the 26.40 surface), K shows the Sargasso Sea (out to about 50°W) filled with values of about 10–15, and there is also a secondary region of low- q near 30°W, and between 25–30°N, with values less than 25, being somewhat similar to the Levitus picture, but with higher q -values. SW, on the other hand (for 26.50), show a more or less homogeneous gyre from the US coast to about 40°W, with values less than 10, but with some indication of smaller regions of low- q (less than 10) in the general area of the “secondary” region referred to above. The whole of the gyre between 20–35°N in SW has q -values less than 20, and is generally more homogenised than in K. In summary for this density surface, LEVEL is perhaps in best agreement with the various observational data sources, but ISOPYCNIC and SIGMA are not too dissimilar.

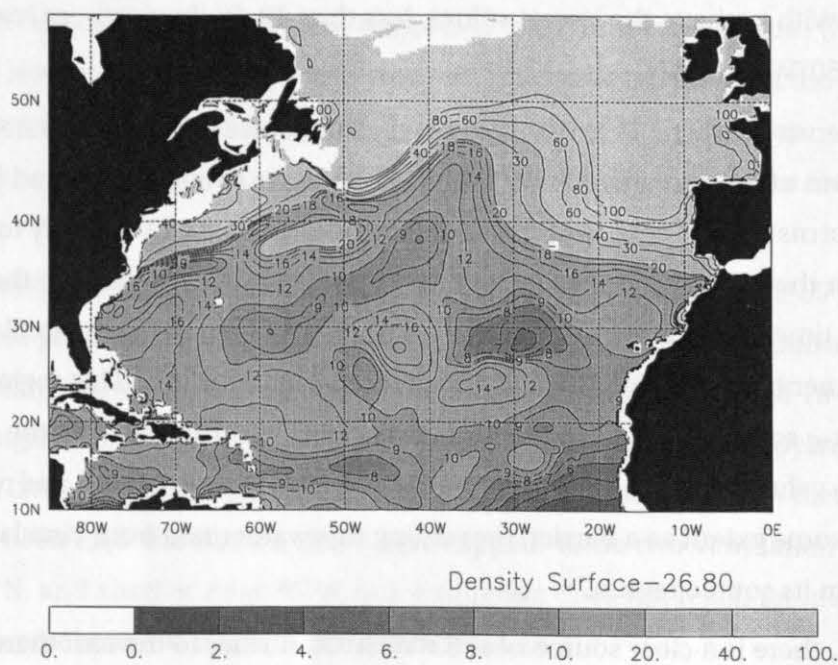
Moving now to the density surface 26.80, Fig. 7.7 shows a somewhat confused state in the Levitus observations, with regions of low and high- q interspersed across the gyre. However, the area of lowest values (less than 6) is again near 30°W, 30°N, south of the AC in the eastern basin, and close to the position of the “secondary” low for the 26.52 surface. This region may also possibly be connected with Madeira Mode Water, which forms in about this location. There are also two other regions of low- q near 40°W, 40°N and 60°W, 30°N (values less than 8) which may indicate a ventilation source somewhere towards the northwest of the gyre. We also note, broadly speaking, a ridge of somewhat higher q values running across the gyre

between 15–25°N, separating the lower- q regions further north from the low- q regions further to the south which result mostly from the decreasing value of f towards the equator. K and MRK indicate that most of the gyre, down to about 10–15°N, is homogenised between values of 10 and 15, with perhaps the lowest values, less than 10, in the northern/central region of gyre near 40–50°W, 30–40°N.

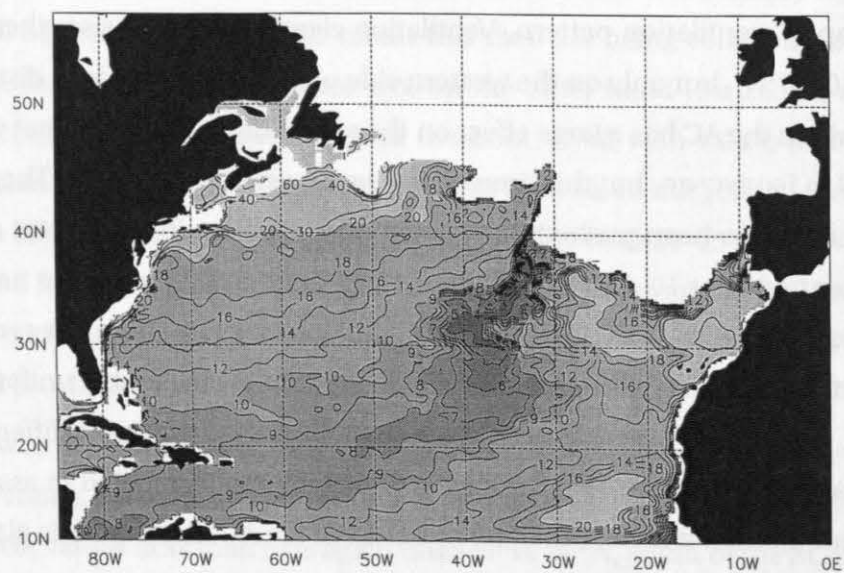
For this density surface, ISOPYCNIC shows a clear source of lowest- q water in the north-western portion of the gyre, near 50°W, 35°N, between the two regions noted in Levitus. The low- q water forms a small pool near this source region, and advects strongly to the east along about 35°N in the AC system. The low- q water appears to move across to the south side of the AC by the time it has crossed the mid-Atlantic ridge, where it then recirculates in an anti-cyclonic manner between 25–35°N in the eastern side of the basin. This region contains the area of lowest- q south of the AC in the Levitus dataset. We also note that the ridge of somewhat higher- q values between 15–25°N has been preserved in the model, and remark that this would act to some extent as a barrier, preventing this water mass from circulating directly to the south from its source region.

For LEVEL, there is a clear source near 32°W, 38°N, further to the east than for ISOPYCNIC (indicating a lighter mixed layer). Ventilation then occurs initially to the southwest, turning slightly to the southeast at 30°N, and then back to the southwest and west near 25°N, forming an “S-shaped” ventilation pattern. Ventilation clearly reaches the southernmost regions of the gyre (10–20°N), but only on the western side of the basin. This is in distinction to ISOPYCNIC, for which the AC has a large effect on the ventilation pattern, so that ventilation also reaches 20°N in ISOPYCNIC, but this time on the eastern side of the basin. The ridge of higher q -values in LEVEL has been pushed further to the south than in ISOPYCNIC and in Levitus, and is now centred near 10–15°N. For SIGMA, there is a ventilation source near 38°W, 38°N, and ventilation occurs to the southeast, but again does not penetrate the gyre very far. The potential vorticity in most of the gyre south of about 30°N is reasonably uniform, with values about 12–14. In summary, on this density surface, there are significant differences between the models, and although the observations are not sufficiently detailed to assess the realism of the different models, it is clear that the presence of the AC-like feature is playing a key role in ISOPYCNIC.

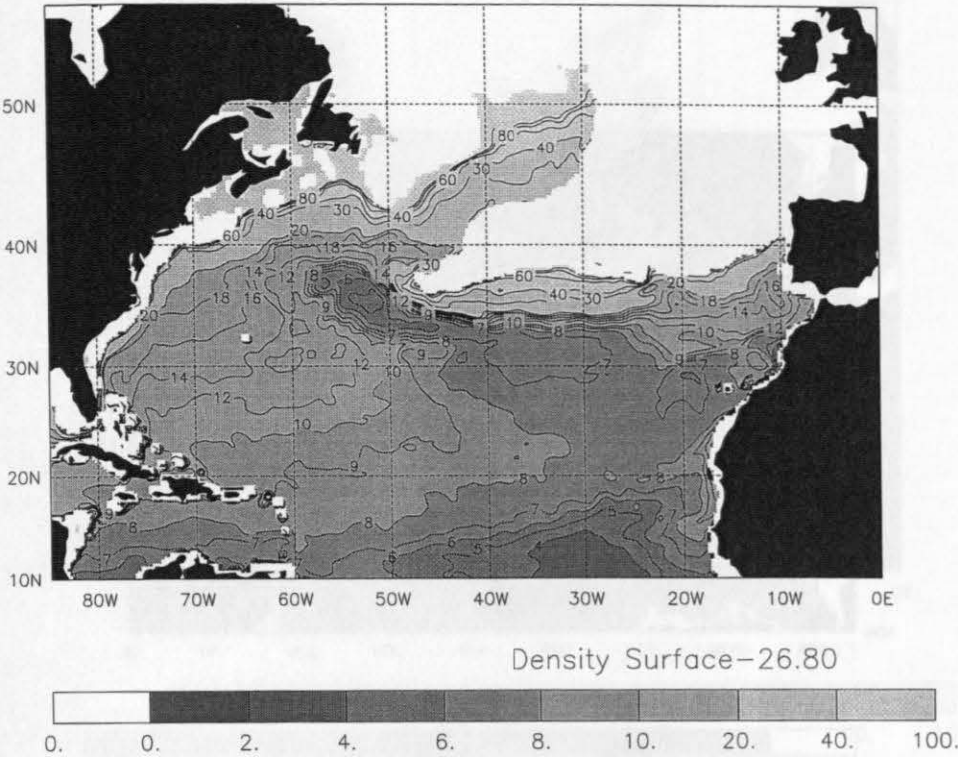
We now consider in Fig. 7.8 the patterns for the 27.03 isopycnal, which is in the upper range of densities for the mode waters which are thought to ventilate from the Bay of Biscay (BB) area, and which we will call Eastern North Atlantic Water, or “ENAW” (after POLLARD et al., 1996). Levitus (the initial model state) shows a clear region of low- q in the northeastern



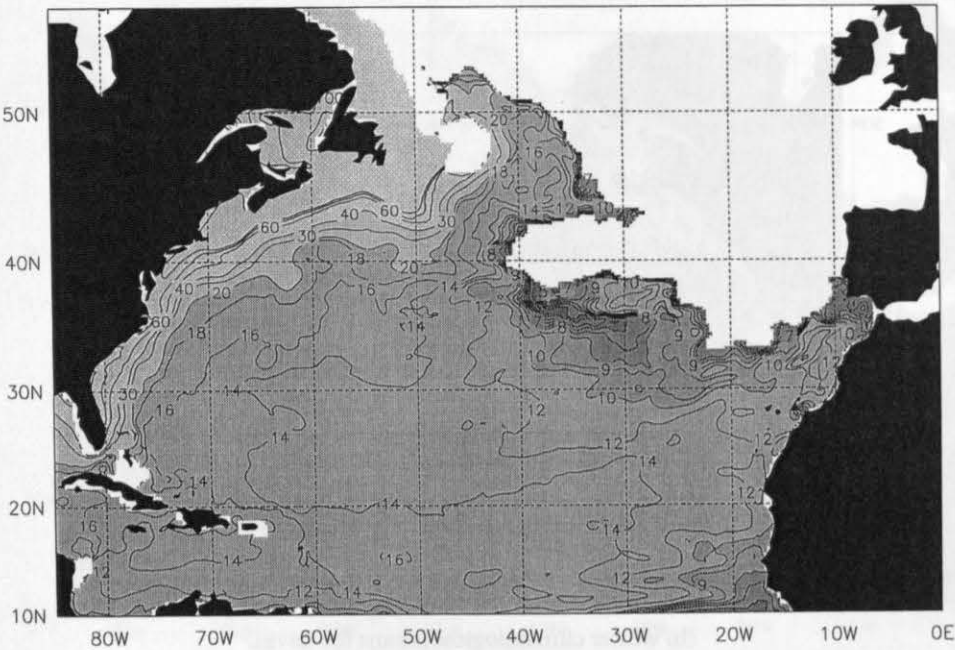
(a) Initial state for ISOPYCNIC, and all models



(b) winter climatological means for LEVEL

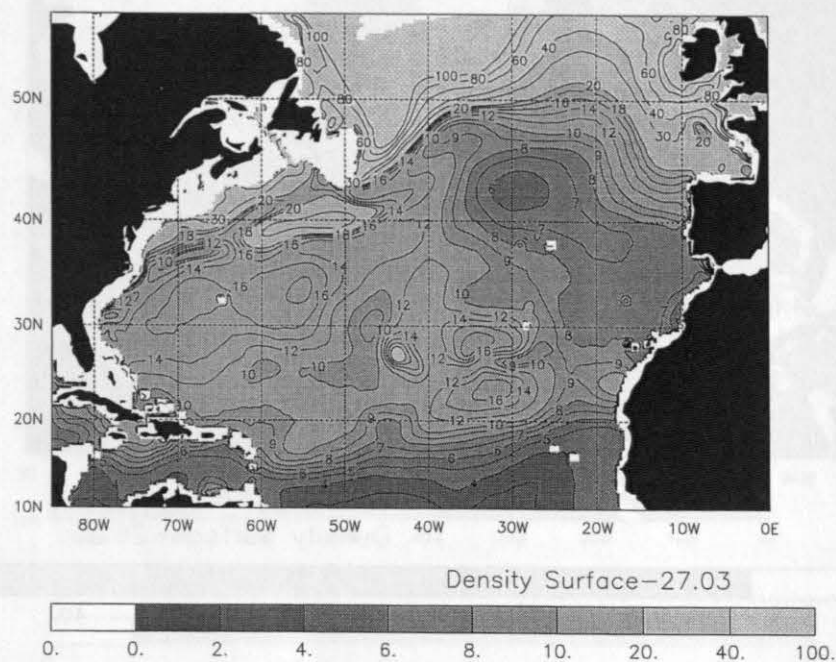


(c) winter climatological means for ISOPYCNIC

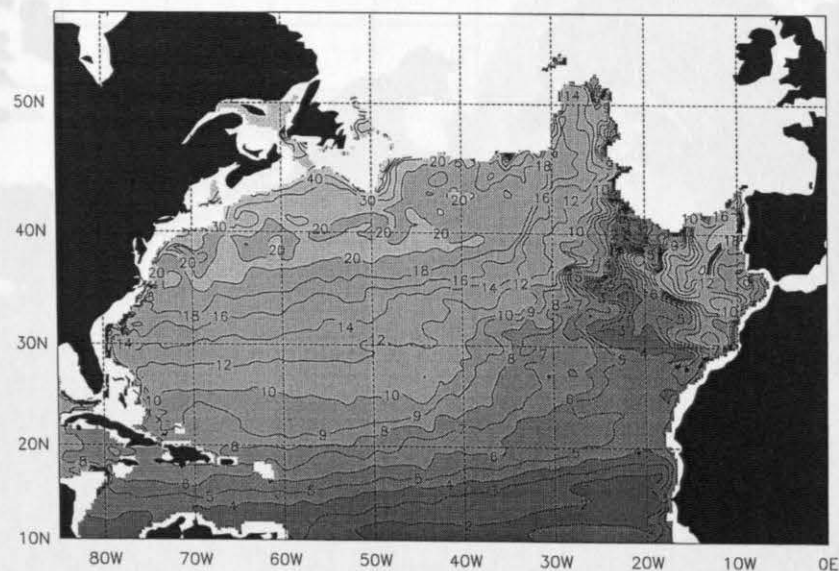


(d) winter climatological means for SIGMA

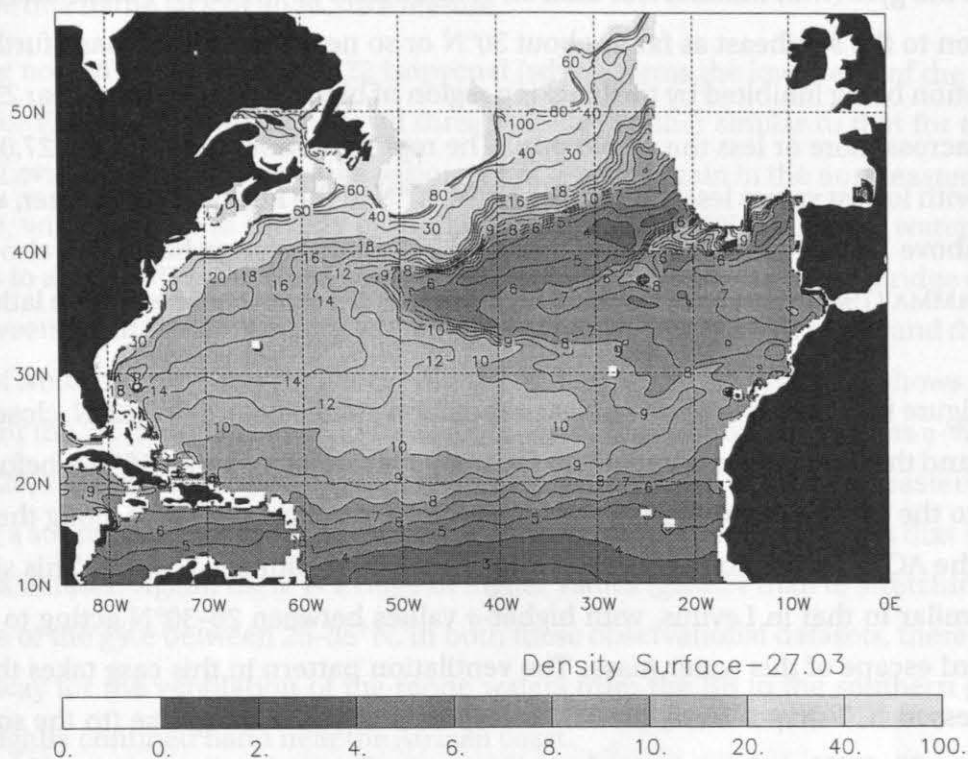
Figure 7.7: Potential vorticity ($\times 10^{-11} \text{ m}^{-1} \text{ s}^{-1}$) on isopycnal surface 26.80 (ISOPYCNIC layer 7). Contours at values of 1, 2, 3, 4, 5, 6, 7, 8, 9, 10, 12, 14, 16, 18, 20, 30, 40, 60, 80, and 100.



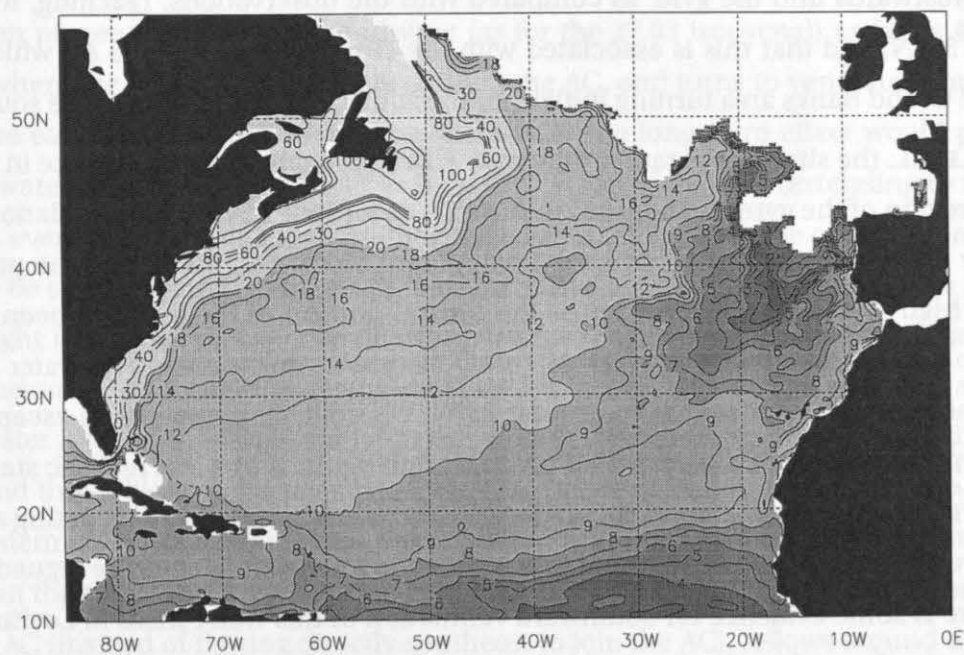
(a) Initial state for ISOPYCNIC, and all models



(b) winter climatological means for LEVEL



(c) winter climatological means for ISOPYCNIC



(d) winter climatological means for SIGMA

Figure 7.8: Potential vorticity ($\times 10^{-11} \text{ m}^{-1} \text{ s}^{-1}$) on isopycnal surface 27.03 (ISOPYCNIC layer 8). Contours at values of 1, 2, 3, 4, 5, 6, 7, 8, 9, 10, 12, 14, 16, 18, 20, 30, 40, 60, 80, and 100.

region of the gyre (with minima less than 6), centred near 30°W , 42°N . This seems to indicate ventilation to the southeast as far as about 30°N or so near the African coast, further southward motion being inhibited by the blocking region of high q values centred near 25°N which extends across more or less the whole gyre. The representation in SW for the 27.0 surface is similar, with lowest values less than 8 near 30°W , 40°N in the northeastern corner, and higher values (above 10) further to the south, near $25\text{--}30^{\circ}\text{N}$ in the eastern basin. We also note here that STRAMMA (1984) reveals a "blocking high" on the 27.1 isopycnal near these latitudes ($26\text{--}34^{\circ}\text{N}$).

The figure for ISOPYCNIC shows a clear ventilation source near 20°W , 42°N , close to that in Levitus, and that ventilation is initially to the west-southwest (to about 50°W), before turning sharply to the east on encountering the AC, and then running eastwards along the northern edge of the AC to fill the northeastern portion of the gyre with low- q water. This situation is rather similar to that in Levitus, with higher- q values between $20\text{--}30^{\circ}\text{N}$ acting to block the southward escape of this water mass. The ventilation pattern in this case takes the form of a compressed "C"-shape. Here, the AC corresponds with the sharp rise (to the south) of q -values near $32\text{--}35^{\circ}\text{N}$, and appears to be acting as an effective barrier to the southward ventilation of this water mass. We also note, however, that the water mass in the model is pushing too far westwards into the gyre, as compared with the observations, reaching, for instance 50°W at 35°N , and that this is associated with the current branch of the AC which extends from the Grand Banks area turning initially to the southwest rather than to the southeast.

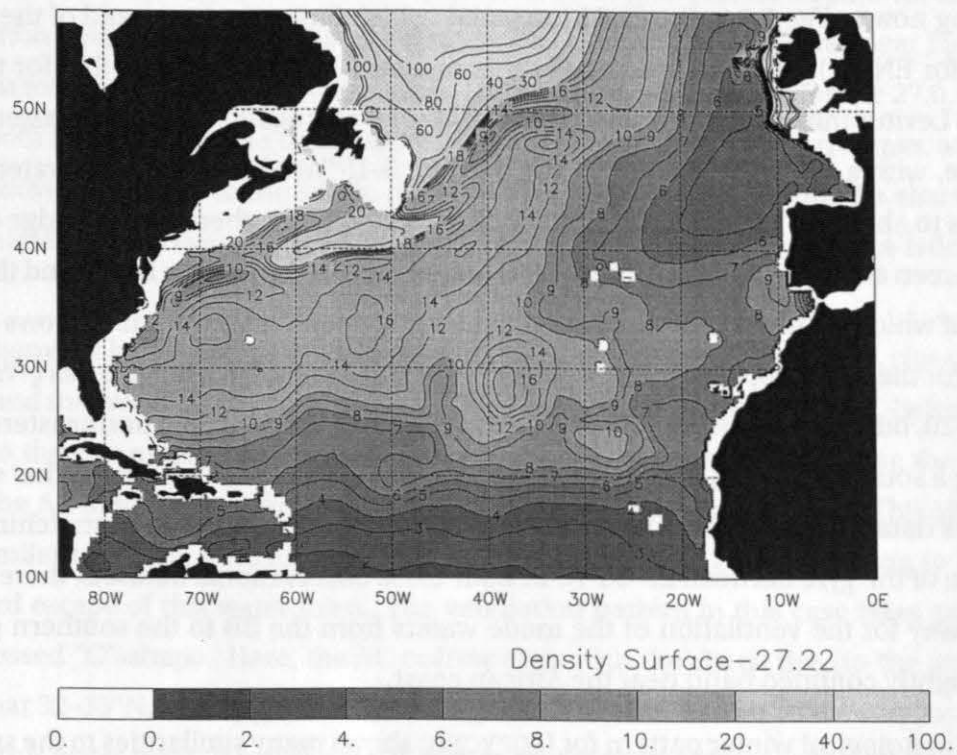
For LEVEL, the situation is rather different. Although there is again a source in the northeastern region of the gyre (again near 20°W , 42°N , as for ISOPYCNIC), the ventilation pathway is nearly directly to the south. There is no apparent block near 30°N , and the pronounced ridge of high- q values stretching across the central portion of the gyre has been lost. This seems to be associated with the lack of an AC-feature in this model. The water mass ventilates more or less southwards to at least 25°N , where it then appears to escape into the southernmost regions of the gyre. This probably corresponds to a less realistic state than for ISOPYCNIC, and the significant effect of the AC is becoming clear, effectively acting as a barrier to the southward ventilation of water masses from the BB region. It could be argued, however, that there is some evidence for southward ventilation of this water mass in Levitus near the African coast, but only extending as far south as about 27°N .

For SIGMA, the situation is rather similar to that for LEVEL, with ventilation occurring southwards from the BB region. Here again, the ridge of high- q values has been lost, and ventilation into the southernmost portion of the gyre appears to be taking place. This again

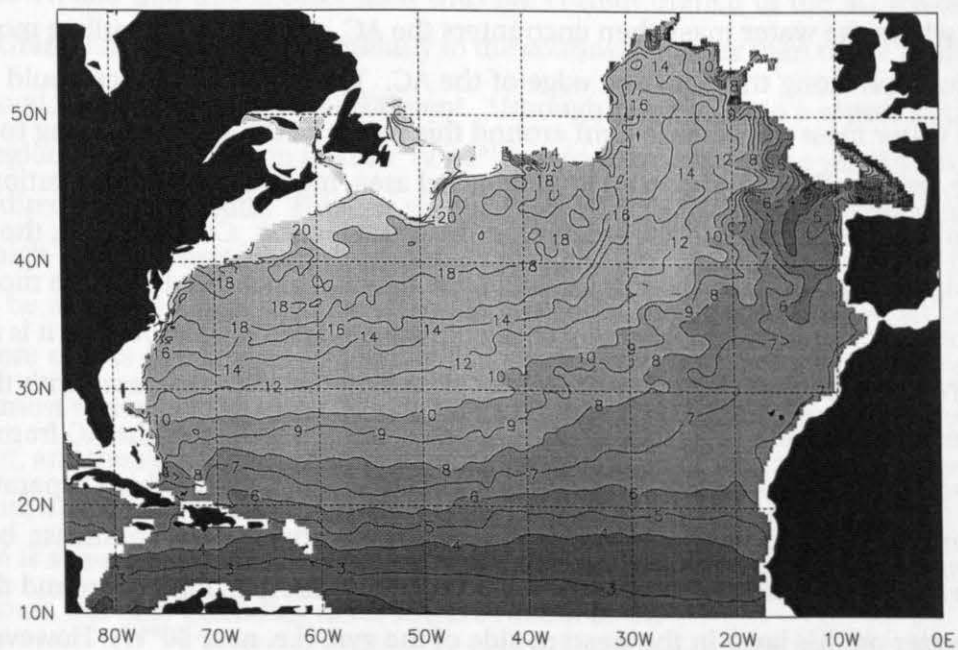
seems to be due to the lack of an AC-like feature.

Turning now in Fig. 7.9 to the 27.22 isopycnal (which forms the lower end of the range of densities for ENAW), the situation for all three models is rather similar to that for the 27.03 layer. The Levitus initial state reveals a region of low- q water again in the northeastern region of the gyre, with a source in the Bay of Biscay, near $5\text{--}15^\circ\text{W}$, 45°N . The low- q water extends westwards to about 30°W , and southwards to about 35°N . Again, there is also a ridge of high- q water between about $20\text{--}35^\circ\text{N}$, which extends across most of the eastern basin, and the northern limit of which more or less coincides with the latitude of the AC system. K shows a similar situation for the 27.15 isopycnal. The western portion of the subtropical gyre has q -values between 10–20, but there is a region of low- q (with values less than 6) in the northeastern corner, indicating a source near $10\text{--}15^\circ\text{W}$, 45°N , and occupying about the same area as that shown in the Levitus dataset. Again, there is a ridge of higher values (greater than 8) stretching across the middle of the gyre between $25\text{--}35^\circ\text{N}$. In both these observational datasets, there is a possible gateway for the ventilation of the mode waters from the BB to the southern gyre, but only in a tightly confined band near the African coast.

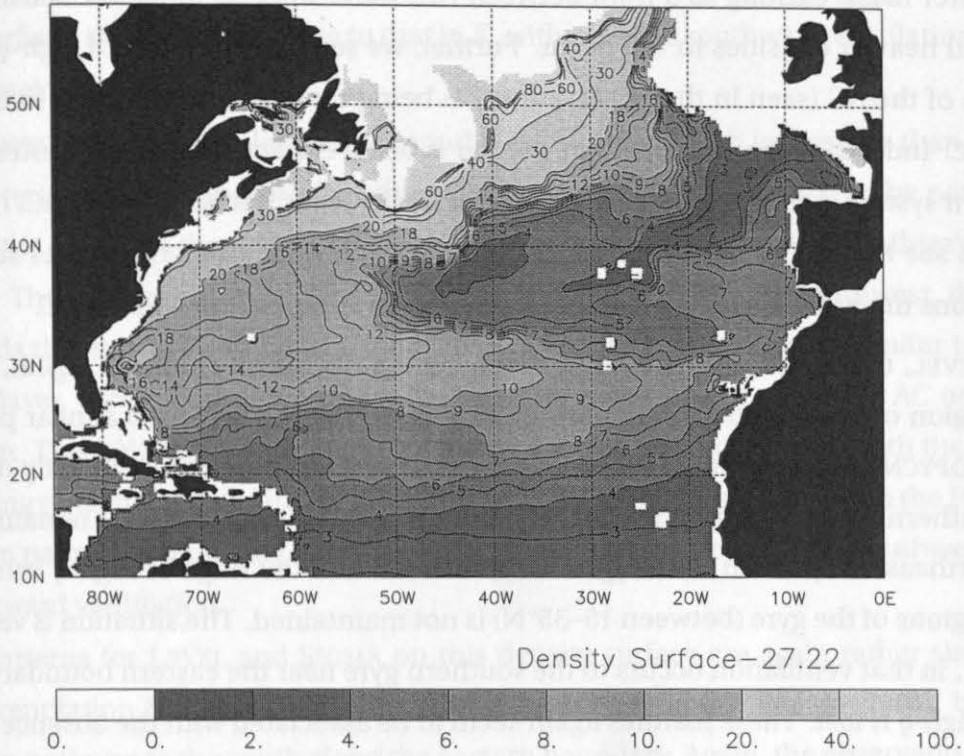
The climatological winter pattern for ISOPYCNIC shows many similarities to the structures in the observations. There is a clear source near 15°W , 45°N , with q -values less than 3. Ventilation then proceeds to the west-southwest (as for the 27.03 isopycnal) as far as $40\text{--}50^\circ\text{W}$, $33\text{--}35^\circ\text{N}$, where the water mass then encounters the AC, and turns to ventilate more or less directly due east along the northern edge of the AC. The long-term effect would probably be for the water mass to circulate right around this region of the gyre (extending to the eastern coast), eventually resulting in an homogenised area, much as in the observations. There could also be some leakage to the south near the African coast. Consequently, the model is giving insight into how this water mass ventilates the real ocean (and how the more or less uniform region of low- q might be set up in the Levitus observations). However, it is also clear that the water mass again drives too far to the West in the model, compared with the observations, and this is likely to be associated with the poor separation of the AC from the Gulf Stream system. At least, it seems that the branch of the Gulf Stream which separates in the model from the Grand Banks, and flows to the southwest, then to the southeast, before entering the AC (instead of flowing directly southeast to join the AC), follows around the region of low- q water on this layer in the western side of the gyre (i.e. near 50°W). However, on the other hand, POLLARD et al. (1996) deduced from observations that the ENAW water mass did ventilate more or less directly west from its source region in the BB area. The model gives us the insight that this is probably because the AC acts to block the more southward ventilation



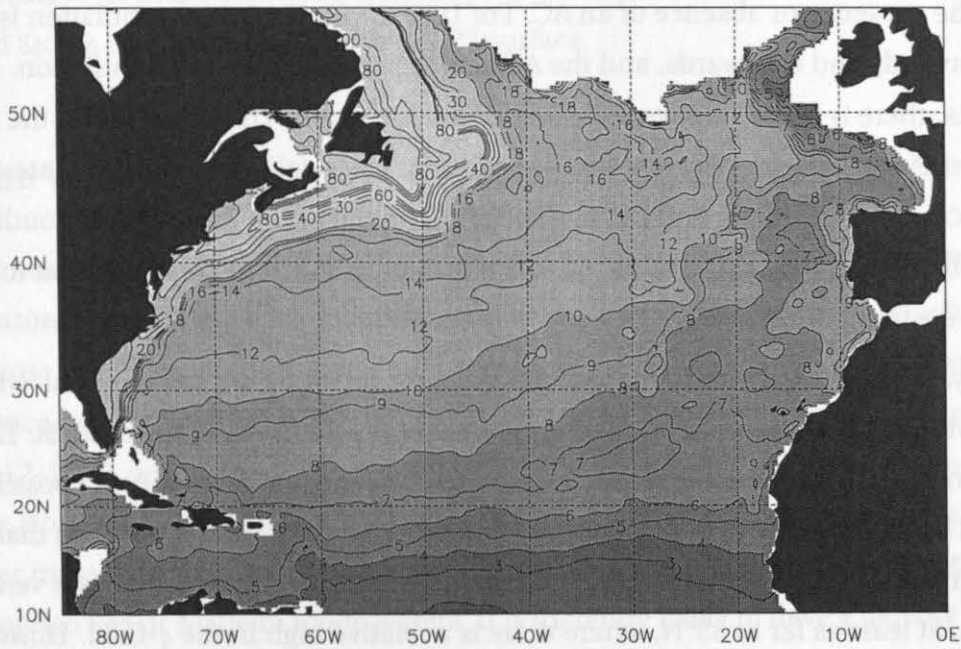
(a) Initial state for ISOPYCNIC, and all models



(b) winter climatological means for LEVEL



(c) winter climatological means for ISOPYCNIC



(d) winter climatological means for SIGMA

Figure 7.9: Potential vorticity ($\times 10^{-11} \text{ m}^{-1} \text{ s}^{-1}$) on isopycnal surface 27.22 (ISOPYCNIC layer 9). Contours at values of 1, 2, 3, 4, 5, 6, 7, 8, 9, 10, 12, 14, 16, 18, 20, 30, 40, 60, 80, and 100.

of this water mass, existing as a front between two water masses, of lighter densities to the south, and heavier densities to the north. Further, we see that the ridge of high- q values to the south of the AC (seen in the observations) is being maintained, and even intensified in ISOPYCNIC. Indeed, it appears that high- q water is being extracted from the western boundary current system, and being brought eastwards by the (southern side of the) AC, near 30°N . Again, we see the model has given insight into how the ridge of high- q values seen in the observations might be formed and maintained, and its relationship with the AC.

For LEVEL, the situation is similar to that for the 27.03 density surface. Again, there is a source region of low- q water in the northeastern region of the gyre, at a similar position to that in ISOPYCNIC, but the ventilation pathway is thereafter more or less directly due south, to the southern regions of the gyre. Consequently, this water mass does not remain confined to the northeastern portion of the gyre in this model, and the ridge of high- q values in the central regions of the gyre (between $15\text{--}35^\circ\text{N}$) is not maintained. The situation is very similar for SIGMA, in that ventilation occurs to the southern gyre near the eastern boundary, and the ridge of high- q is lost. These features again seem to be associated with the absence of the AC in these models.

In summary for this layer, there are again significant differences between the models, related to the presence or absence of an AC. For ISOPYCNIC, the initial ventilation is primarily southwestwards and westwards, and the AC acts to prevent southerly ventilation. For LEVEL and SIGMA, there is no AC, and ventilation occurs due south. The situation for the real world (in the somewhat smooth observations of Levitus at least) falls between the states shown by ISOPYCNIC on the one hand, and LEVEL and SIGMA on the other, with initially southwestward ventilation and some blocking at the AC latitude, but also with some ventilation to the south along the eastern boundary.

Finally, in Fig. 7.10, we show the ventilation patterns for the 27.38 isopycnal, which is the densest which affects the ventilation of the subtropical gyre in any of the models. The Levitus observations show the lowest- q values northwest of Ireland and in the BB, the possible source regions. The eastern side of the gyre then contains generally lower values (less than 10) than the western side, which points to the possibility that some of this water mass is ventilating to the south, at least as far as 35°N , where there is a relative high in the q -field. However, there is also a relative low near 33°W , 37°N , which, if connected to region of low- q to the southeast, would provide some evidence that this water mass could be partially escaping to the south of (i.e. by going underneath) the AC. K gives the indication of southward ventilation on the 27.40 surface, on the eastern side of the gyre, with values less than 10, extending as far as 30°N at

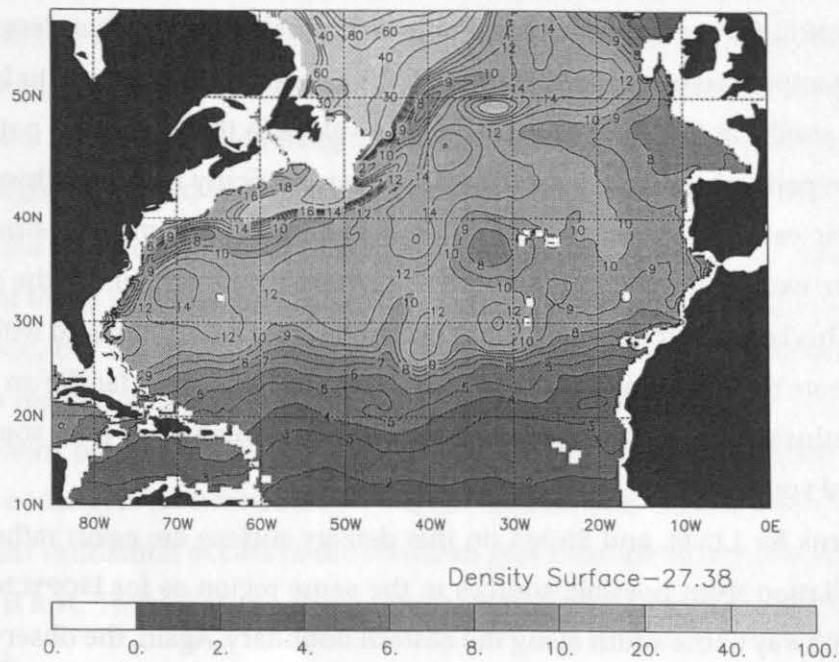
least, and possibly much further, although the contouring interval is rather sparse. SW (for the 27.5 surface) show a similar state to that in K, with possible southward ventilation into the southern regions of the gyre.

For ISOPYCNIC, we see a clear source southwest of Ireland with values less than 2. These source waters appear to be partially trapped in this area, but also appear to be partially escaping to the south (in the first instance), since q -values in the core of the pathway are only around 7. The pathway then forms a "C"-shape, moving firstly to the southwest, then turning towards the east and southeast near 35°N. This pathway is somewhat similar to that for the 27.22 layer, except that the route for the southward ventilation under the AC now seems more open. This behaviour does not seem too unrealistic when compared with the observations, taking note that the minimum in Levitus at 33°W, 37°N does in fact lie on the ISOPYCNIC ventilation pathway, coinciding approximately with the turning point from southwestward to southeastward ventilation.

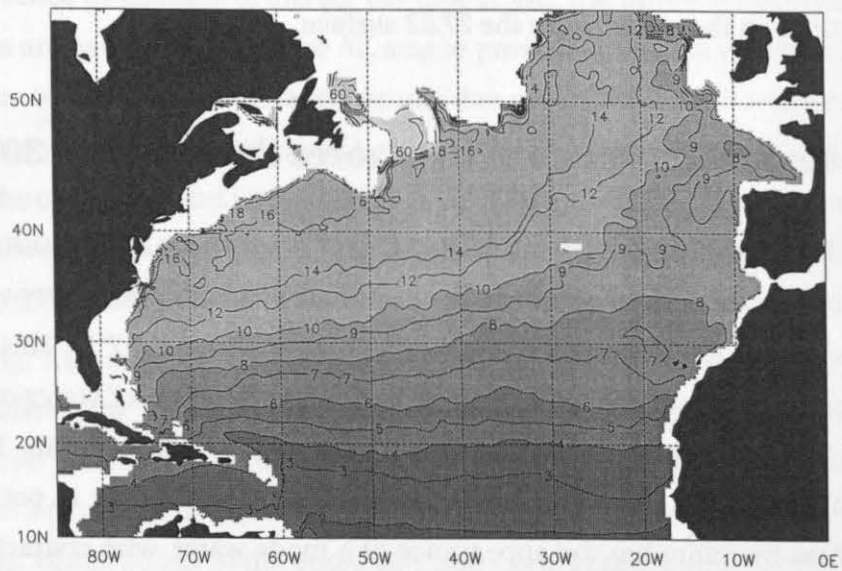
The patterns for LEVEL and SIGMA on this density surface are again rather similar, and indicate ventilation from possible sources in the same region as for ISOPYCNIC, but with a ventilation pathway to the south along the eastern boundary. Again, the observations are not sufficiently clear to enable an unambiguous assessment of the models' behaviour, but the real world appears to lie somewhere between the pattern for ISOPYCNIC on one hand and that for LEVEL and SIGMA on the other, as for the 27.22 surface.

7.5 The Vertical Structure of the Azores Current Near 30° W

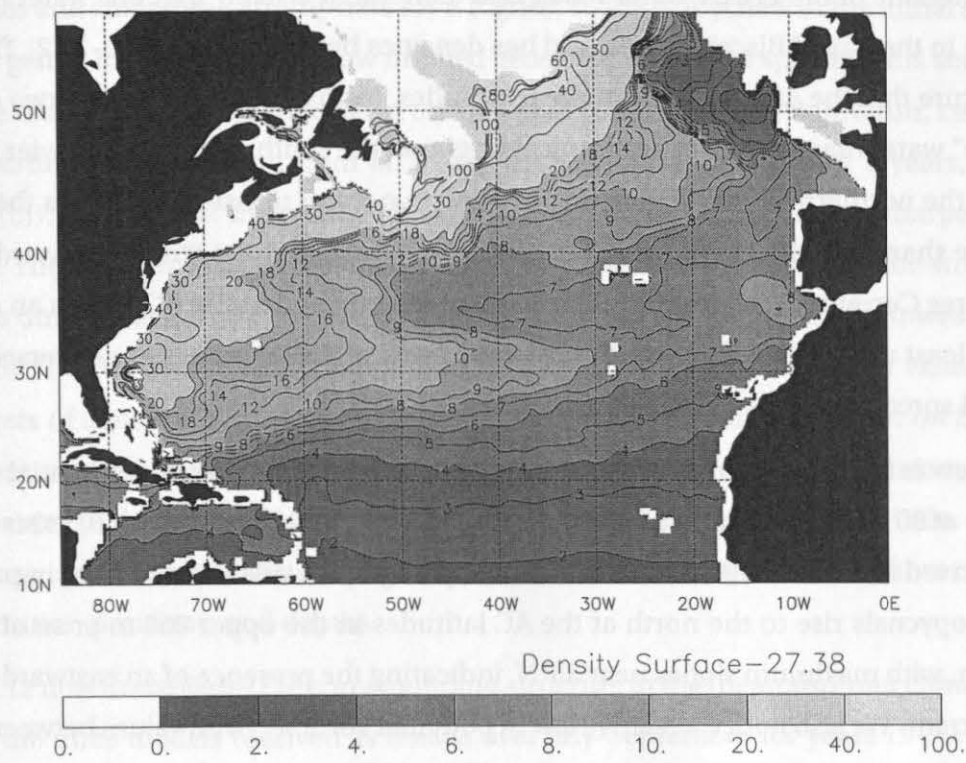
We now consider the vertical structure of the Azores Current near 30°W. GOULD (1985) shows a temperature section derived from a high-resolution hydrographic survey which cut diagonally across the AC from approximately 40°W, 30°N to 27°20'W, 37°N. This clearly reveals the presence, on the southern side of the AC, of a large volume of water of temperatures between 17–19°C, occupying the water column between 100–300 m depth. From the spacing of the isotherms, it is clear that this corresponds to a relative low in potential vorticity. This water mass therefore has the appearance of a mode water, with characteristics typical of the Sargasso Sea or Madeira mode waters. It is therefore likely to have a density of around 26.5–26.8. This water mass, however, is almost entirely absent to the north of the AC in this section. Instead, we observe the presence of another mode water, between temperatures of 10–13°C, which occupies the water column between 300–700 m depth on the northern side of the AC front. This again corresponds to a region low potential vorticity. These temperatures



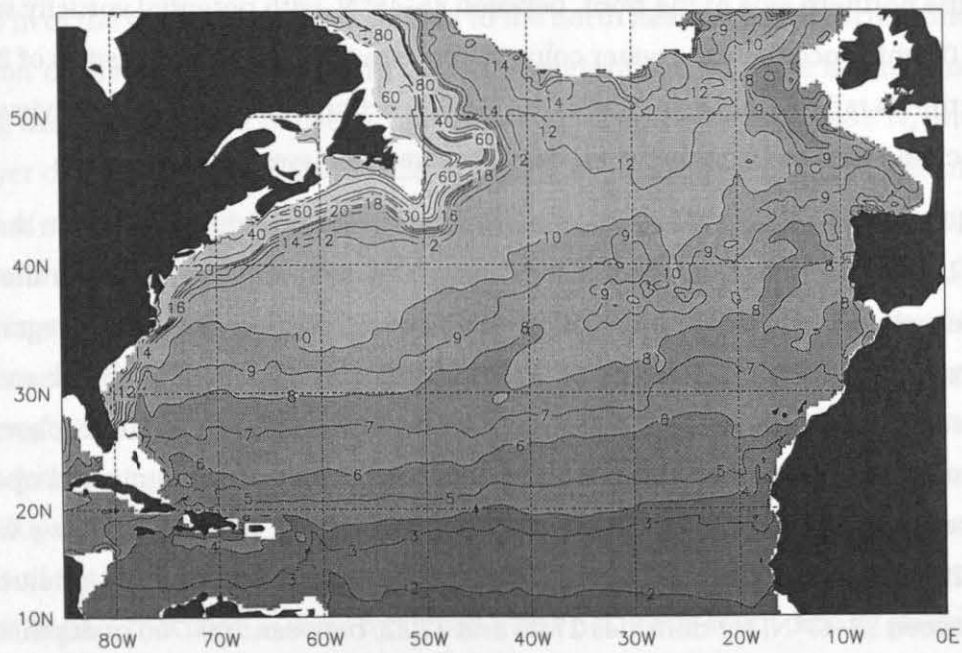
(a) Initial state for ISOPYCNIC, and all models



(b) winter climatological means for LEVEL



(c) winter climatological means for ISOPYCNIC



(d) winter climatological means for SIGMA

Figure 7.10: Potential vorticity ($\times 10^{-11} \text{ m}^{-1} \text{ s}^{-1}$) on isopycnal surface 27.38 (ISOPYCNIC layer 10). Contours at values of 1, 2, 3, 4, 5, 6, 7, 8, 9, 10, 12, 14, 16, 18, 20, 30, 40, 60, 80, and 100.

are characteristic of the ENAW water mass, and therefore it is likely that this water mass has originated in the Bay of Biscay region, and has densities between about 27.0–27.2. This gives us the picture that the AC, at least at these longitudes, forms the front between two competing “mode” water masses, one of subtropical origin on the south side, and a heavier mode of ENAW on the northern side. The meeting of these two water masses then forces the isopycnals to rise sharply to the north, which implies (by geostrophy) the strong eastward motion in the Azores Current. This structure also implies, of course, that the AC acts as an effective barrier, at least near 30°W, to the southward ventilation of ENAW, and also, conversely, to the northward spreading of the lighter water mass.

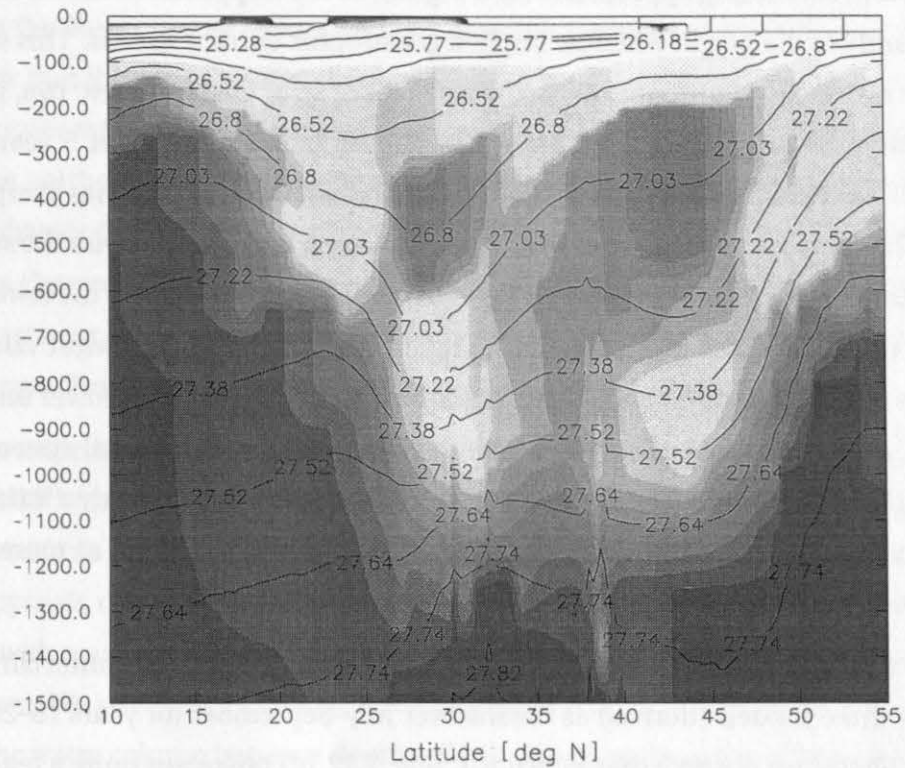
This view is further reinforced by a south-north section of density and potential vorticity (in winter) at 30°W (actually, an average between 27.5–32.5°W) presented by BECKMANN et al. (1994), derived from the ROBINSON et al. (1979) hydrographic atlas. We observe in particular that the isopycnals rise to the north at the AC latitudes in the upper 800 m or so of the water column, with maximum slopes near 35°N, indicating the presence of an eastward-flowing Azores Current. We also notice a relative low in potential vorticity (with values between 10–15) occupying the water column between depths of 150–300 m, at densities of between 26.5–26.9, just to the south of the AC system, between about 27–33°N. In contrast, there is a deeper mode water on the northern side of the front, between 35–45°N, with potential vorticity values between 5–10, which occupies the water column between 350–700 m, at densities of 26.9–27.3. This structure is rather similar to that in the Gould section, and reinforces the view that the AC is associated with the front between these two water masses.

Fig. 7.11 now investigates the development of the structure of the AC region in the spin-up phase for ISOPYCNIC. We show sections of density and potential vorticity from the summer (September, when the mixed layer is shallowest) of certain years in the model integration near 30°W (actually an average between 27.5–32.5°W to remove the effect of eddies and waves). Firstly, the initial model state (Fig. 7.11(a)) is derived from the LEVITUS (1982) observational dataset and is the same for all three models. We notice the features remarked upon above in the observations presented by Gould and BECKMANN et al., namely, the low- q values, for densities 26.52 and 26.80, between 25–35°N and 150–500m depth, and low- q values further north, between 35–47°N, for densities 27.03 and 27.22, between 200–700 m depth. (We note in passing that this structure implies that the AC will be baroclinically unstable, since the horizontal south-north potential vorticity gradient reverses sign in the vertical here.) We also note that the isopycnals in the upper 700 m of the water column rise to the north between these two water masses, but also remark that since Levitus is a rather smooth dataset (with

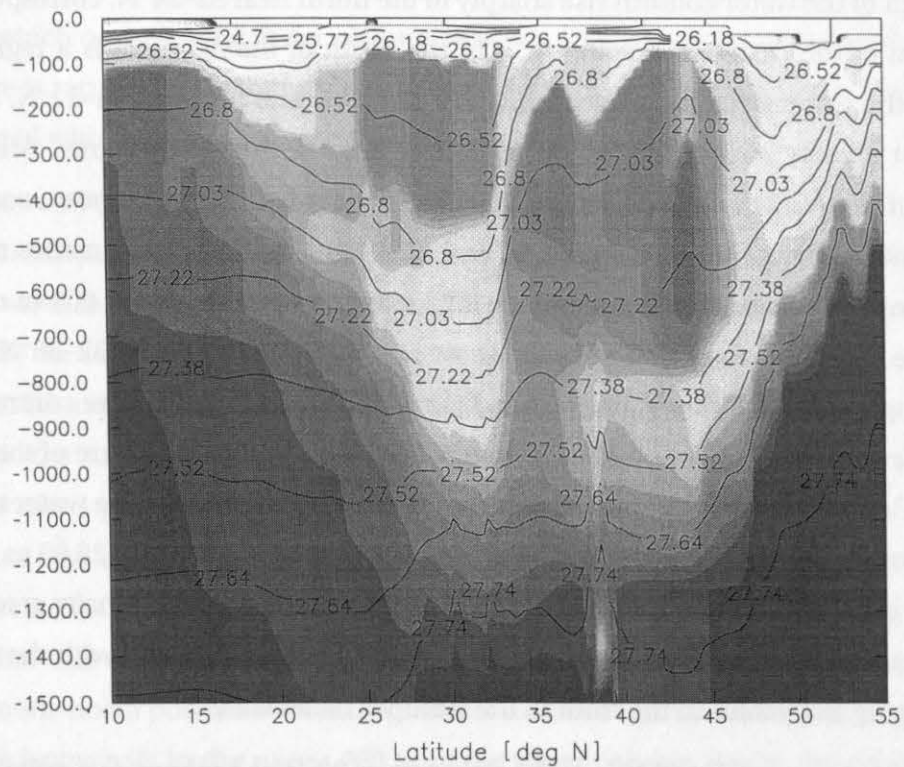
data-values and smoothing appropriate for a 1° grid), so the isopycnals in the initial state only rise fairly gently to the north, with low implied geostrophic current speeds. This seems to be why there is no readily identifiable AC in the first year or so of the ISOPYCNIC run, i.e. because we are starting the integration from an overly-smooth initial state. After 5 years, however (Fig. 7.11(b)), we note that the contrast between these two water masses has sharpened considerably. There is now a strong front near $32\text{--}34^\circ\text{N}$, which is associated with the strong AC at about this time in the model run (see Fig. 7.4). On the south side of the AC, the lowest q -values are now for the 26.52 water mass, whereas to the north of the front the lowest values are still in the layers of densities 27.03 and 27.22. The lowest values of q are now lower on both sides of the front, and this may be associated with the sharpening of the frontal system itself (i.e. the steepening of the isopycnals). By year 10, the situation has changed only a little. The front is still sharp, and the mode water masses either side of the front are still at more or less the same densities, positions, and depths.

Fig. 7.12 now investigates the corresponding structure in the mean summer climatological states of the three models (derived as means over July–September for years 15–20 of the integrations). Firstly, we observe that ISOPYCNIC (Fig. 7.12(b)) possesses quite a realistic structure, i.e. as compared with the initial “Levitus” state in Fig. 7.11(a). The isopycnals in the upper 700 m of the water column rise sharply to the north near $32\text{--}34^\circ\text{N}$, corresponding with the location of the eastward flowing AC. To the south of the AC there is a region of low- q occupying the water column between 100–450 m depth and between $25\text{--}32^\circ\text{N}$, and for primarily layer density 26.80, but also for 26.52, much as in the observations. Meanwhile, to the north of the AC, we note the presence of the denser ENAW mode water, occupying the water column between 100–800 m depth, and $32\text{--}44^\circ\text{N}$, and for layer densities of 27.03 and 27.22 (again much as in the observations). The isopycnals in the upper 800 m of the water column rise sharply to the north between these two water masses, from $32\text{--}36^\circ\text{N}$, giving rise to the strongly eastward-flowing AC. Thus ISOPYCNIC has maintained the contrast between these two “competing” water masses, so that the AC is a significant feature of the model circulation. (Compared with the state in year 10, Fig. 7.11(c), we see that the water mass on the south side of the front has shifted to slightly heavier densities, primarily 26.80 as opposed to 26.52. This implies that there is some reduction in the net north-south density gradient across the front, viewed in an average sense, and this appears to be associated with the slightly less steeply sloping isopycnals in the front in the summer mean state.)

For LEVEL, however (Fig. 7.12(a)), the structure at 30°W is perhaps not quite so realistic. The vertical section shows the absence of the lighter mode water mass in the upper water



(a) Initial state (September)



(b) Year 5 (September)

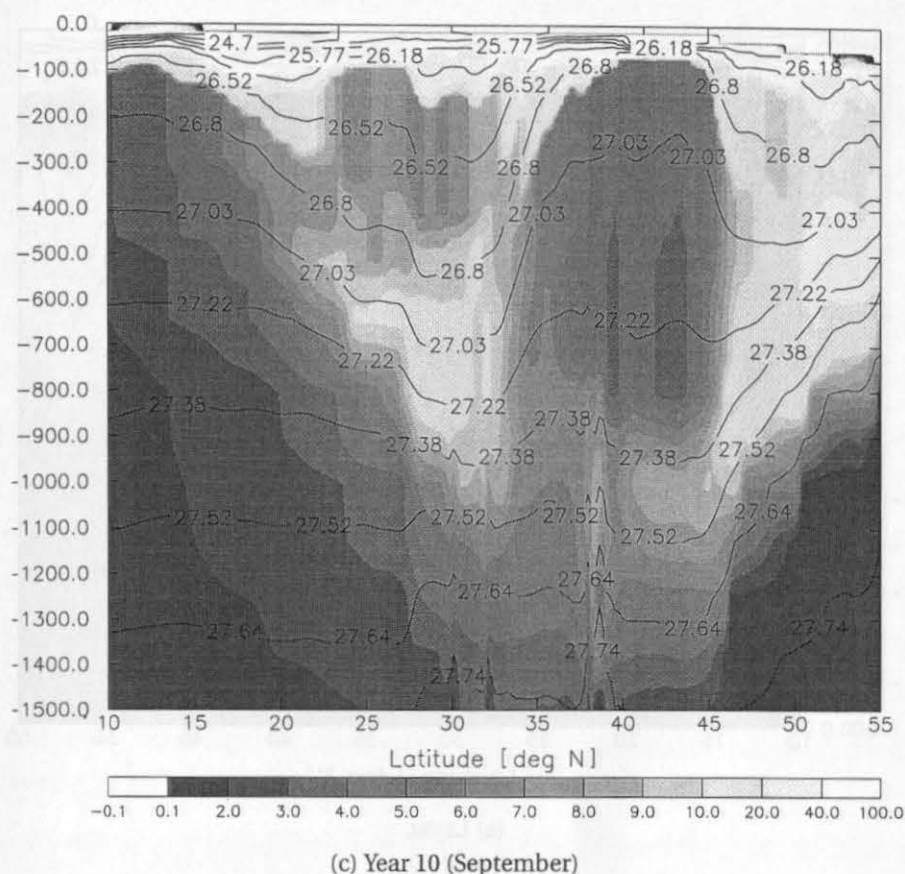
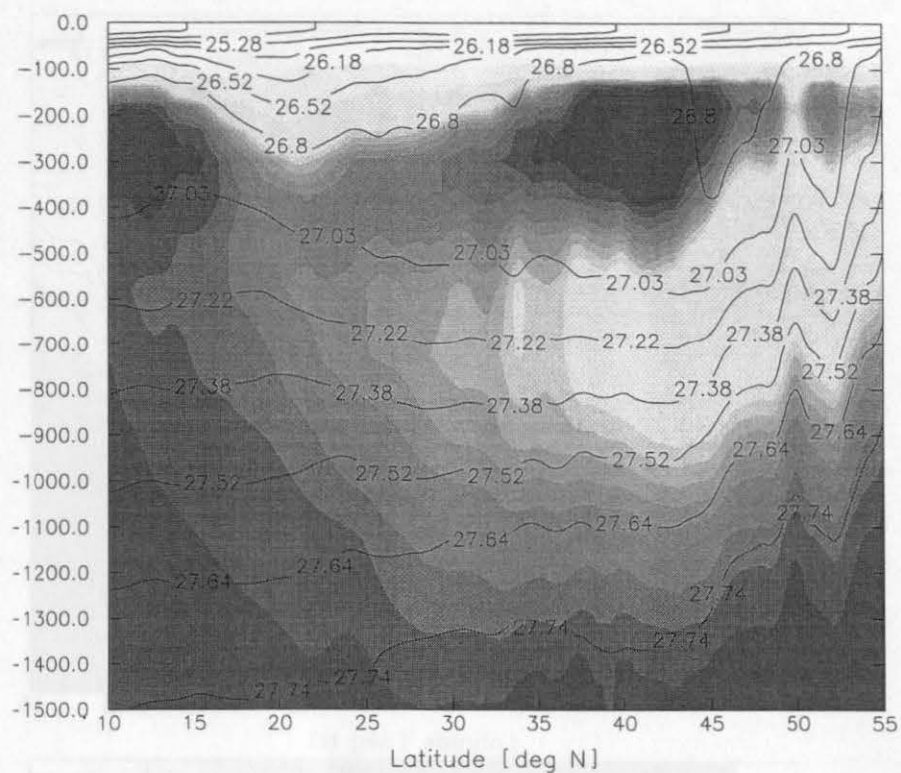
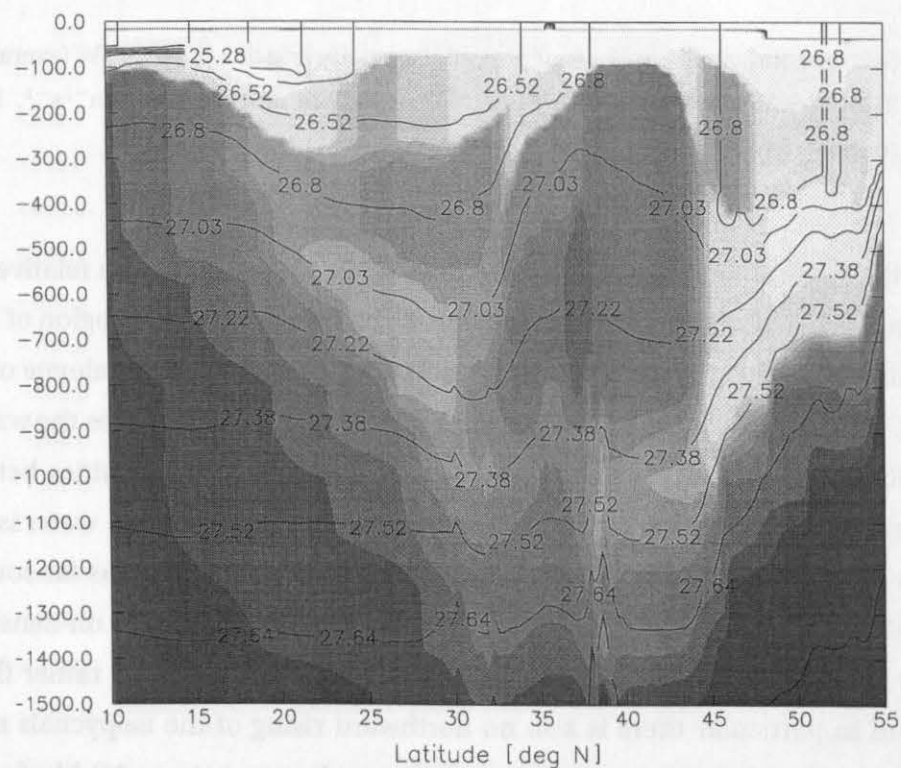


Figure 7.11: Sections showing snapshots of potential vorticity and density at 30°W (averaged between 27.5–32.5°W) for ISOPYCNIC. Potential vorticity in units of $10^{-11} \text{ m}^{-1} \text{ s}^{-1}$. Density contours at densities of ISOPYCNIC layers.

column on the southern side of where the AC should be. In fact, there is a relative high in the q -field down to 250 m depth in the region 25–35°N. There is, however, a region of low- q water which ventilates southwards from a northern source, representing an analogue of the ENAW water mass. North of where the AC should be (i.e. near 35°N) this occupies the water column between 150–450 m (higher up than in the observations), and for densities between 26.8–27.0 (lighter than in the observations). It is also apparent that this mode water is ventilating southwards through the position of the AC in the real world, reaching as far south as 24°N at least (at this longitude), in correspondence with the above maps of q on density surfaces (Figs. 7.7(c) and 7.8(c)). The isopycnal surfaces below about 300 m are rather flat between 25–45°N, and in particular there is also no northward rising of the isopycnals near the AC latitudes, and correspondingly no pronounced eastward currents in an AC-like feature in this model (Fig. 7.3(a)). In summary, it appears that there is no AC in LEVEL because it is not able



(a) LEVEL



(b) ISOPYCNIC

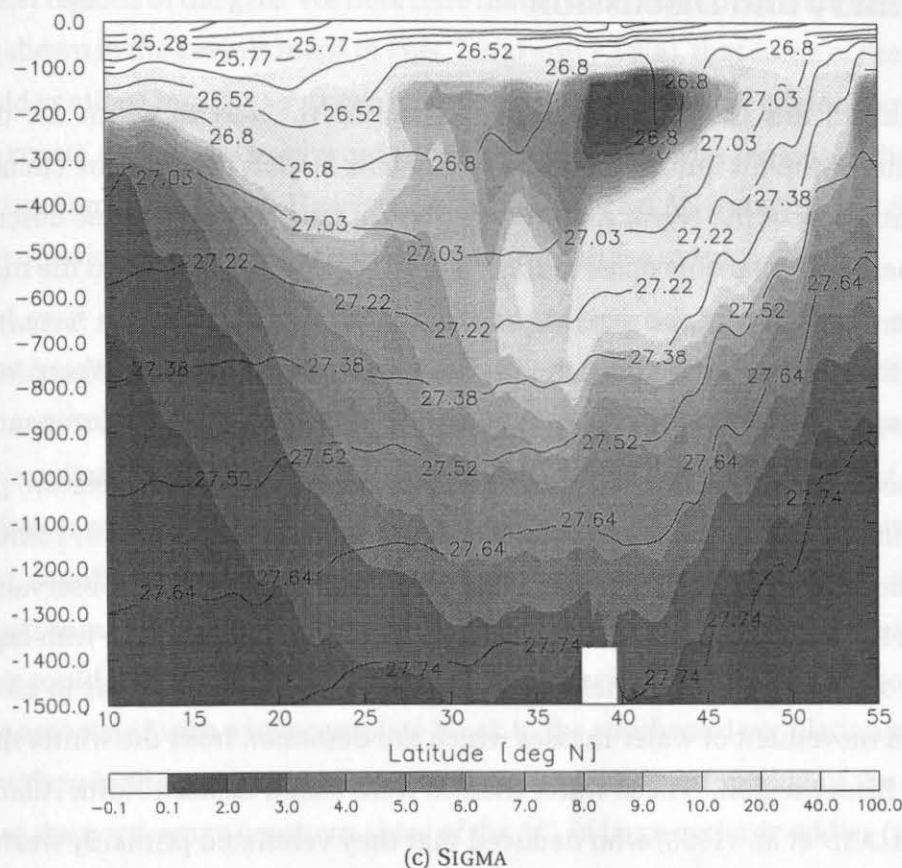


Figure 7.12: Sections showing potential vorticity and density at 30°W (averaged between 27.5–32.5°W for ISOPYCNIC) for summer. Potential vorticity in units of $10^{-11} \text{ m}^{-1} \text{ s}^{-1}$. Density contours at densities of ISOPYCNIC layers.

to support the contrast between the mode water masses on either side of the AC, so that the isopycnals do not rise to the north at the AC latitudes.

For SIGMA (Fig. 7.12(c)), the situation is similar to that for LEVEL. In particular, there is no low potential vorticity water in the upper water column on the south side of the AC latitudes, although there is a mode water to the north. This mode water, as for LEVEL, occupies the water column between about 100–350 m, and densities of 26.8–27.0, again, higher and lighter than in the observations. This mode water extends to the south, but only as far as 30°N (i.e. not so far south as for LEVEL), which is also consistent with the maps of potential vorticity on the isopycnic layers shown above. We also note that, as for LEVEL, the isopycnals below this water mass (i.e. below about 300 m depth) are almost flat between 25–45°N, again corresponding with the lack of an AC-like feature.

7.6 Summary and Discussion

The main goals of this chapter have been to describe the way in which the three high-resolution state-of-the-art numerical ocean circulation models describe the circulation patterns and ventilation of the North Atlantic subtropical gyre, to assess these descriptions by comparing them with available observations, and to seek new insights into the mechanisms governing the ventilation of the gyre in the real world. Throughout, we have laid special emphasis on the Azores Current, and the ENAW (Eastern North Atlantic Water) water mass, which have a special relevance for the oceanography of the seas near the European margins.

We have seen, primarily, that the presence of an Azores Current-like feature plays a key role in determining the ventilation patterns into the model gyres. For ISOPYCNIC, a strong AC exists in the eastern basin at latitudes of $32\text{--}35^\circ\text{N}$ (which agrees with observations of the AC), although its formation in the western basin is perhaps not fully in line with expectations derived from observations. Nonetheless the AC acts as an effective barrier in ISOPYCNIC to the southward movement of water masses which are detrained from the winter mixed layer in the Bay of Biscay region. These water masses were called Eastern North Atlantic Water, ENAW, by POLLARD et al. (1996) who deduced that they ventilated primarily westwards and southwestwards after formation, rather than southwards. This agrees with the initial ventilation direction of these water masses in ISOPYCNIC, which ventilate westwards and southwestwards until reaching latitudes of near 35°N , where they encounter the AC and are turned to the east. Although it appears that these water masses push too far westwards into the ISOPYCNIC model gyre (i.e. to near 50°W , which may be partly related to poor representation of the formation of the AC), we have gained the insight that the westward and southwestward ventilation of these water masses observed by POLLARD et al. (1996) is perhaps because the AC in the real world acts to some extent as a barrier to their southward ventilation. South of the AC in ISOPYCNIC, there are lighter mode waters which have characteristics similar to those of Sargasso Sea or Madeira mode waters. Thus the AC acts as a barrier separating these two water masses in this model. This parallels the situation in the real world quite closely. Alternatively, we may perhaps view the AC as existing precisely because these two ventilating water masses meet at about this latitude ($32\text{--}35^\circ\text{N}$ in the eastern portion of the gyre). PINGREE (1997) also provides further observational evidence that the AC acts as such a barrier, at least between $25\text{--}30^\circ\text{W}$.

For LEVEL and SIGMA, there is no feature like the AC system, and the ventilation of the northern mode waters of ENAW type takes place in a more or less southerly direction to the

southernmost regions of the gyre. We note here that there is some observational evidence, for instance as shown in the Levitus maps in Figs. 7.9(a) and 7.10(a), that some of the ENAW water masses could ventilate into the southern regions of the gyre along the eastern boundary (near the African coast), so that the southward ventilation of these water masses in these models is not wholly unreasonable either. However, the absence of an AC in LEVEL and SIGMA means that their ventilation patterns are rather different from those in ISOPYCNIC.

On balance, it seems to us that the ventilation patterns for these ENAW water masses in the real world probably fall between the states represented by ISOPYCNIC on the one hand, and LEVEL and SIGMA on the other, with the AC acting as at least a partial barrier to their southward ventilation, in particular away from the eastern boundary, but that some southward ventilation could occur near the African coast. The AC certainly exists in nature, and may extend zonally as far as the Moroccan coast (e.g. see STRAMMA, 1984, and PINGREE, 1997), though some authors (SY, 1988) report that the AC turns to the south near 20°W . Consequently, it could be that, in the mean, the AC is somewhat weaker east of about 20°W , and this may be associated with a less complete block to the southward ventilation of these water masses. Further, in the real world, there seems to be significant mixing of the ENAW water masses from the northern to southern sides of the AC, in large cyclonic eddies (up to 200–300 km in diameter) which form from loops of the AC system itself (GOULD, 1985; PINGREE et al., 1996). In ISOPYCNIC (and LEVEL and SIGMA), no such eddies form, probably because of the lack of resolution in the model(s), although unstable waves are present (in ISOPYCNIC). The absence of the transfer of ENAW southwards across the AC in ISOPYCNIC may be one reason why this water mass builds up on the northern side of the AC, and drives too far into the western regions of the gyre.

However, the general structure of the AC near 30°W seems to be better represented in ISOPYCNIC than in LEVEL and SIGMA, with the AC forming between two regions of low potential vorticity water which force the isopycnals to rise to the north. All models start from the same initial state, in which we have seen there is a contrast in water mass properties across the AC region (near 30°W) in the Levitus dataset, although the isopycnals rise only rather gently to the north in this overly-smooth dataset. It is apparent that ISOPYCNIC is able to maintain, and indeed sharpen, the contrast between these two water types, so that the isopycnals rise more steeply as time proceeds, and the AC develops a reasonably strong velocity field. LEVEL and SIGMA, however, do not seem to be capable of maintaining this contrast between the water masses, so that the north-south isopycnal slopes in the AC region are gradually lost in these models, with the result that there are no significant eastward velocities at these latitudes in

the mean spun-up states of these models.

We might initially conjecture this that difference could perhaps be due to the way in which the mixing schemes are implemented in the respective models. For ISOPYCNIC, the mixing is strictly isopycnic-diapycnic, so that water mass properties are correctly diffused along isopycnals. For LEVEL and SIGMA, however, constant mixing diffusivities are set in the horizontal and vertical directions. In the presence of a front, with sloping isopycnals, this could mean that the water mass properties are spuriously diffused across the isopycnals by the imposed horizontal diffusivity. It does not seem implausible that this horizontal diffusion could act over periods of years to decades to gradually destroy the structure of the AC in LEVEL and SIGMA. However, KÄSE and KRAUSS (1996) show the presence of an AC-like feature near 30°W in a run with the CME model at about 1/3° resolution: this is a level model similar to LEVEL. The horizontal diffusivities for this CME run are comparable to those for LEVEL, so that AC-like features are possible with models of this type. Nonetheless, the maximum current speeds for the AC shown in these CME results are only about 3 cm/s, so the feature is rather weak: the above figures showing the surface circulation patterns for the three present models have a velocity cutoff off 3 cm/s, so it is possible that a weak AC exists even in LEVEL. This however, is clearly not a significant enough feature to be associated with any noticeable northward rise in the isopycnals in the shown section near 30°W. However, both LEVEL and SIGMA are capable of maintaining steeply sloping isopycnals in other areas. We also report that BECKMANN et al. (1994) show that a 1/6° resolution CME model possesses a stronger AC feature, of about perhaps 10 cm/s on average, but this does not appear to be directly connected to the Gulf Stream system. In summary, level models are capable of showing AC-like features, but at 1/3° resolution, these appear to be rather weak. The question of why the AC-feature in the present ISOPYCNIC model is so much stronger than in the other models must at this stage remain somewhat of an open question.

In summary, we have shown that the presence (in ISOPYCNIC) or absence (in LEVEL and SIGMA) of an Azores Current feature has a critical effect on the way in which the subtropical gyres ventilate in the respective models. The ventilation patterns in the real world of the ENAW water masses, which are produced near the European margins, probably fall between the states shown by ISOPYCNIC on the one hand, and LEVEL and SIGMA on the other, but we have gained the important insight that the AC in the real world acts as at least a partial barrier to the southward ventilation of these water masses, and this seems to explain recent observations showing the westward and southwestward ventilation of these water masses. It also appears that ISOPYCNIC is better able to represent the upper ocean structure in the

eastern basin (near 30°W) by maintaining the water mass contrast across the AC front, but the exact reason for this remains somewhat of an open question at the moment. Overall, we feel we have gained significant insights into the way in which the subtropical gyre is ventilated in the real world, and have also learnt important lessons about the abilities of the various models to represent this process in a realistic fashion.

Chapter 8

Eddy Variability

8.1 Introduction

The existence of mesoscale variability (waves, meanders, eddies) as features of the general ocean circulation has been known to oceanographers for a long time from many observations in the Gulf-Stream System (FUGLISTER, 1972), and in many other parts of the world ocean. Observations and analysis of historical data performed in the 70's indicated that eddies can be found everywhere in the ocean, and provided evidence that the geographical distribution of fluctuating energy is strongly inhomogeneous, with highest levels occurring in strong mean currents and their extension (WYRTKI et al. 1976, DANTZLER 1977). Observational programs carried out in the last 20 years, including long-term current meter moorings (DICKSON, 1983, ZENK and MÜLLER, 1988, ARHAN et al., 1989), satellite-tracked drifting buoys (BRÜGGE, 1995, KÄSE and KRAUSS, 1996), and satellite (Geosat, TOPEX/POSEIDON, ERS-1) altimetry (LE TRAON et al., 1990, STAMMER and BÖNING, 1992, HEYWOOD et al., 1994), allowed to quantify more accurately the distribution, characteristic scales and amplitude of eddy activity.

At the same time, eddy-resolving ocean models have been developed. Their application to idealized problems has increased dramatically our understanding of the dynamical role of eddies in the large-scale circulation. The importance of barotropic and baroclinic instabilities as generating mechanisms, and of eddy-mean flow interactions as processes shaping the large-scale circulation were clearly demonstrated (see HOLLAND, 1985 for a review). High resolution models were also applied to simulating the wind-driven and thermohaline circulation in realistic basins. Major efforts are the Community Modeling Effort (CME) for the North Atlantic (BRYAN and HOLLAND 1989, BECKMANN et al., 1994a, DÖSCHER et al. 1994), the Fine Resolution Antarctic Model (FRAM) in the Southern Ocean (WEBB et al., 1992) and the global

modelling efforts of SEMTNER and CHERVIN (1992), of STAMMER et al. (1996), and the OCCAM project (GWILLIAM et al., 1995).

Sources of variability in these models are both external, caused by the seasonal cycle of the atmospheric forcing (a significant signal in the tropics), and internal, through eddy generating instability processes which dominate at mid-latitudes. The sinks of variability are viscosity and diffusivity, parameterized by simple harmonic or biharmonic operators.

Comparisons of variability statistics (geographical distribution, amplitude, frequency spectra, spatial scales) produced by model simulations with similar quantities obtained from surface drifters or altimetry in the North Atlantic, indicate that numerical model experiments have begun to simulate the major eddy characteristics with some realism (BECKMANN et al., 1994a). However, model simulations still exhibit too weak eddy activity in mid-latitude and northeastern basins, despite significant efforts to correct deficiencies by considering bottom topography roughness (BÖNING, 1989, BARNIER and LE PROVOST, 1993), increased horizontal resolution (BÖNING and BUDICH, 1992, BECKMANN et al., 1994a,b), and high frequency forcing (see STAMMER and BÖNING, 1996).

The DYNAMO project is not especially designed to improve the representation of eddy energy levels in the eastern basin, because both the horizontal and vertical resolutions of DYNAMO models are similar to those used in most model studies cited above. However, it can be expected to give some additional insight into the variability in the Greenland-Iceland-Scotland ridge area due to a northward extended model domain and higher (isotropic) resolution. Also, it enables us to evaluate influence of vertical model coordinate in a systematic way. Since the extratropical eddy field is largely related to instability processes of mean currents and fronts, differences in eddy activity will, to a large degree, reflect the different time-mean solutions proposed by the various models for the general circulation in the North Atlantic.

The general circulation produced by the three models has been discussed in Chapter 4. Significant differences between model solutions are noticed, relevant to the dynamics of the Gulf Stream, the North Atlantic Current (NAC) and the Azores Current (AC), which may have an impact on eddy statistics. Another region of interest is the seasonally forced North-Brazil Current (NBC) area.

Just as for the general circulation, one expects to find differences in eddy variability due to the use of different vertical coordinates, and different subgrid-scale parameterizations. ISOPYCNIC, for example, uses harmonic isopycnal and diapycnal diffusion (a Laplacian operator), whereas SIGMA and LEVEL have biharmonic horizontal and harmonic vertical diffusion.

The present Chapter compares and discusses the characteristics of mesoscale variability

produced by the three models over the five years of the intercomparison phase. The geographical distribution of the near surface eddy energy is investigated in section 8.2. Model solutions are compared to each other, and to independent estimates from surface drifters, long-term current meter moorings and satellite altimetry. Variation of eddy energy with depth is described in section 8.3. Finally, section 8.4 synthesizes and discusses the above results and addresses the role of mesoscale eddies in large scale circulation. An attempt is made to explain the differences noticed between models, and between models and observations.

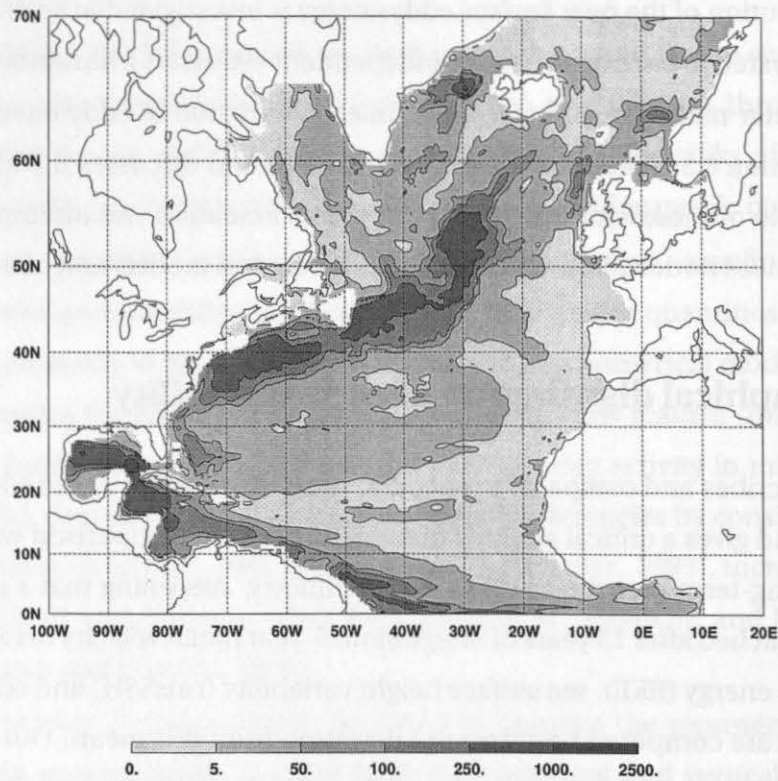
8.2 Geographical distribution of eddy variability

This section describes and compares the geographical distribution of the eddy energy in the three models, and gives a critical analysis of models results in comparison with observations from drifters, long-term moorings and satellite altimetry. Assuming that a statistical steady state has been reached after 15 years of integration, 5-year mean velocity fields are calculated, and eddy kinetic energy (EKE), sea surface height variability (rmsSSH) and eddy potential energy (EPE) fields are computed based on the deviation from this mean. Our eddy variability thus represents statistics over five years of model results. As in previous studies of model variability, a 3-day sampling rate was chosen. Note that this differs from the temporal resolution of the observational data.

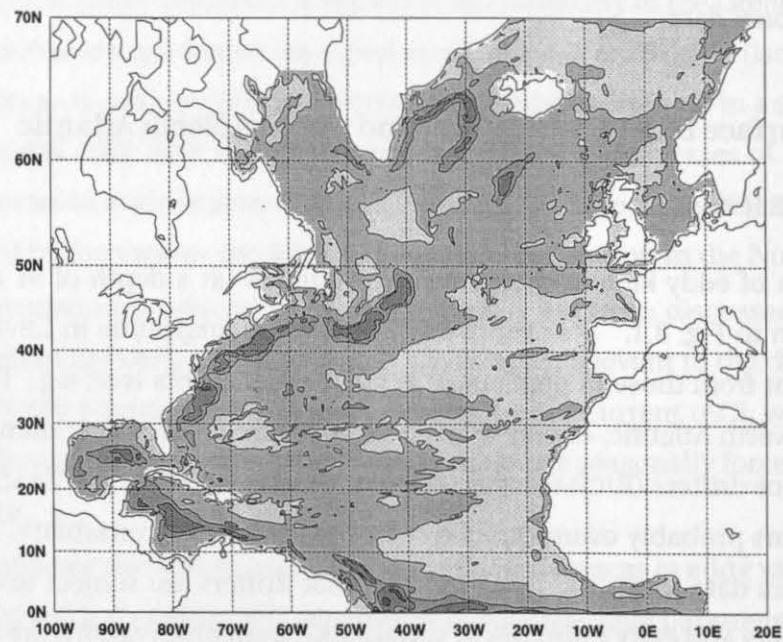
8.2.1 Near surface EKE in the tropical and western North Atlantic

Overview of EKE levels

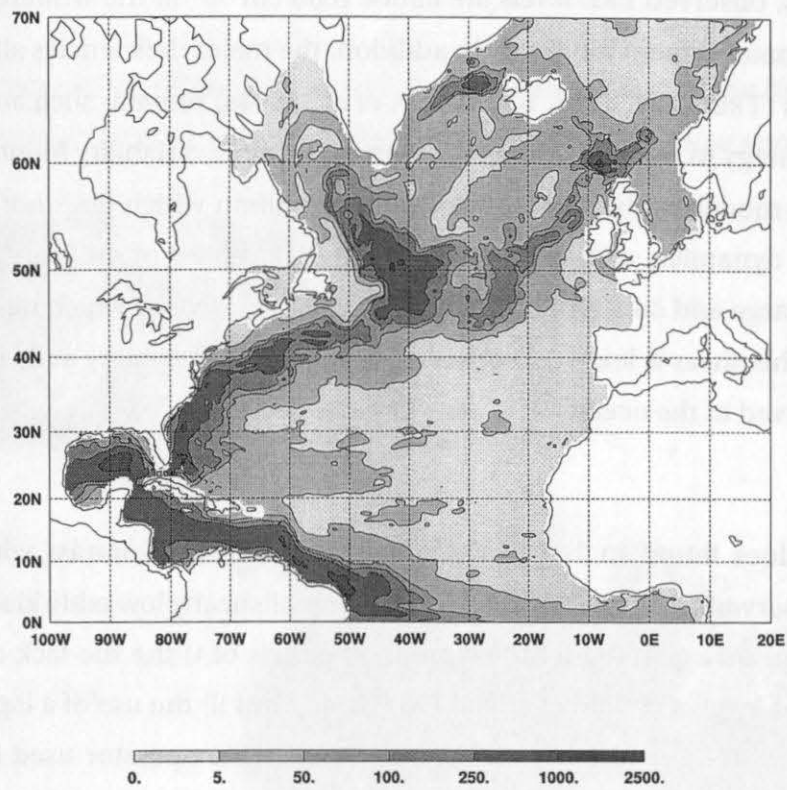
The distribution of eddy kinetic energy near the surface (at a depth of 91 m) for the three models is shown in Fig. 8.1. Its overall distribution and amplitude in LEVEL and SIGMA is not very different from those in previous $1/3^\circ$ CME experiments (see, e.g., TREGUIER, 1992). In the western North Atlantic, energy levels near $1000 \text{ cm}^2/\text{s}^2$ are lower than those observed from early surface drifters (RICHARDSON, 1983) or Geosat altimeter (LE TRAON, 1990). These early observations probably overestimated the ocean mesoscale variability. Recent analyses of surface drifters data (BRÜGGE, 1995) indicate that drifters are subject to the influence of the wind variability and early estimates of surface EKE from observations are probably biased toward high values. The reduced noise in altimetric measurements from TOPEX/POSEIDON (STAMMER and BÖNING, 1996) or ERS-1 (HEYWOOD et al., 1994) also suggests lower EKE levels than those estimated with GEOSAT.



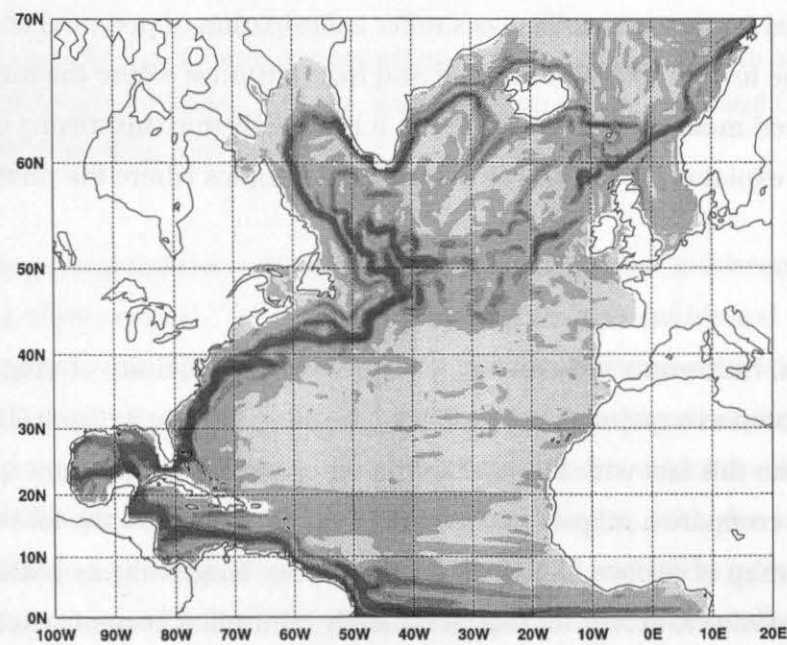
(a) LEVEL: EKE (cm^2/s^2) at -91.64 m.



(b) ISOPYCNIC: EKE (cm^2/s^2) at -91.64 m.



(c) SIGMA: EKE (cm^2/s^2) at -91.64 m.



(d) SIGMA: MKE (cm^2/s^2) at -91.64 m.

Figure 8.1: Near surface Eddy Kinetic Energy (cm^2/s^2) for LEVEL, SIGMA and ISOPYCNIC, and sub-surface Mean Kinetic Energy (cm^2/s^2) for SIGMA.

Nevertheless, observed EKE levels are above $1000 \text{ cm}^2/\text{s}^2$ in the western North Atlantic, and model estimates remain too weak. In addition, the major deficiencies already pointed in previous studies (TREGUIER, 1992, BECKMANN et al., 1994a) remain, such as the very abrupt decay of eddy energy to the east. A major reason for this low variability found in the DYNAMO (and also CME) models is the lack of horizontal resolution which does not allow a full resolution of eddy dynamics, and still requires a significant level of dissipation. Also, models use a relatively large and constant coefficient for vertical viscosity which tends to reduce the vertical shear. This shear is known to generate near surface variability and contributes to the variability observed in the ocean.

Low EKE values found in ISOPYCNIC (below $250 \text{ cm}^2/\text{s}^2$) contrast with values above $1000 \text{ cm}^2/\text{s}^2$ observed in SIGMA and LEVEL. This unrealistically low eddy kinetic energy level in ISOPYCNIC can be explained by the combined effects of i) the lack of velocity shear within the mixed layer, a characteristic of ISOPYCNIC, and ii) the use of a laplacian diffusion operator which is not as scale selective as the biharmonic operator used in other models (HOLLAND, 1978). Wind induced vertical shear are removed by vertical homogenization of the mixed-layer formulation, as would do a large vertical friction. As discussed by GENT et al. (1995), vertical friction generally acts similar a dissipation of potential energy which then could explain the lower EKE-values at mid and high latitudes where the mixed layer can be several of hundred meters in winter. However, it is unlikely that this mixing of momentum in the mixed layer explains for the low EKE level in the tropics where the mixed layer remains very shallow.

In all models, maximum eddy energy is observed in the vicinity of major currents. This feature is also noted as a major characteristic of the eddy field by BRÜGGE (1995) from drifter data. We illustrate this fact with SIGMA (but the other models would show qualitatively similar results) and compare a map of surface MKE (which represents the location of the mean currents) and a map of surface EKE (Figs. 8.1(c), 8.1(d)). Large values of MKE and EKE coincide almost everywhere, except for topographically controlled currents such as those in the Irminger and Labrador Seas. This suggests that model dissipation is still high, and that waves and eddies are dissipated not far from their place of generation. However, one shall see that this is not a general rule, and it would be misleading to conclude that eddies are not able to radiate energy far away from their regions of generation.

Tropical latitudes

In SIGMA and LEVEL, strong eddies are generated at the retroflection of the North-Brazil Current between 5°N and 10°N . Snapshots of the flow speed (Fig. 8.2) show strong anticyclonic

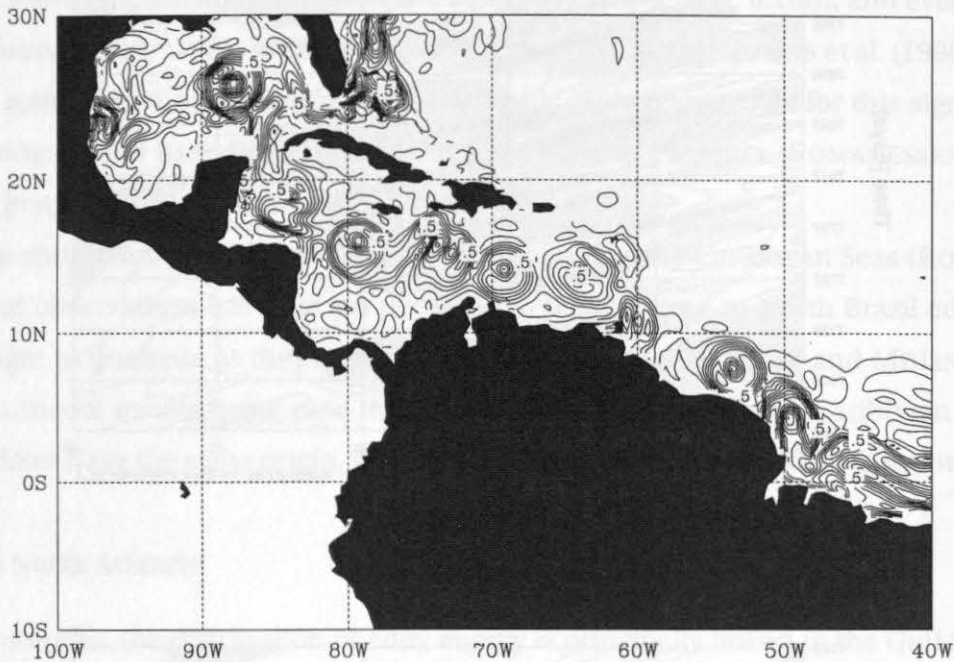
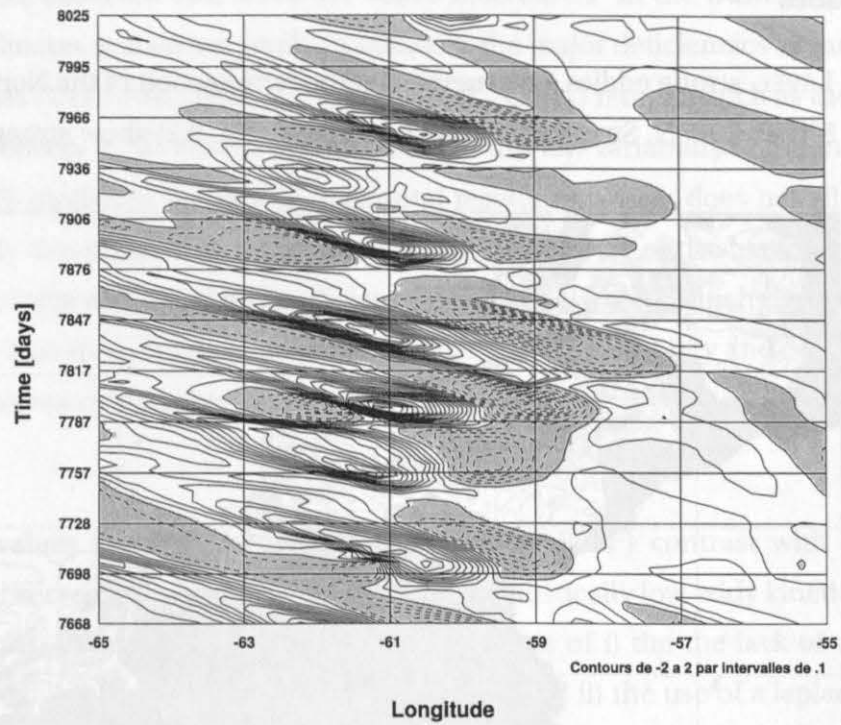


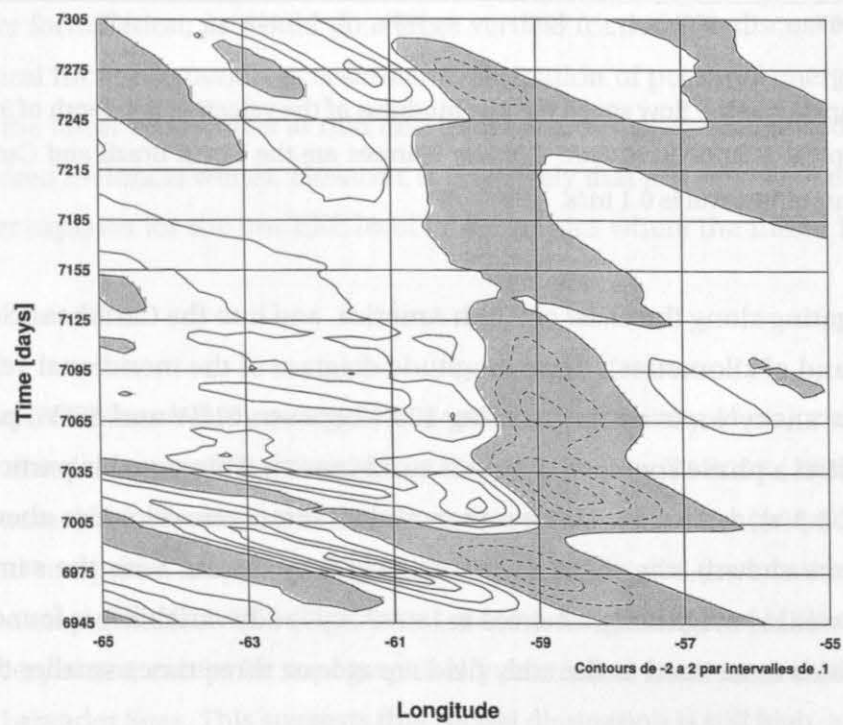
Figure 8.2: Snapshot of the flow speed (i.e. the modulus of the velocity) at a depth of 91 m in Western Tropical Atlantic in SIGMA. Circular features are the North Brazil and Caribbean eddies. Contour interval is 0.1 m/s.

eddies propagating along the coast of South America, and into the Caribbean Seas (thus over several thousand of kilometres). Time-longitude diagram of the meridional velocity at 12°N (Fig. 8.3) show anticyclonic eddies crossing 12°N between 61°W and 59°W , propagating to the north-west at a phase speed of 10 cm s^{-1} to 12 cm s^{-1} . This signal is particularly strong in SIGMA (Fig. 8.3(a)) with six eddies per year, and instantaneous velocities above 1.5 m/s . In LEVEL (no figure shown), the signal is qualitatively very similar, with the same number of eddies, but of weaker magnitude, whereas in ISOPYCNIC eddy variability is found only in winter, and velocities associated to the eddy field are at least three times smaller than in SIGMA (Fig. 8.3(b)).

The detachment of eddies from the North Brazil Current has been described by JOHNS et al. (1990) from a detail analysis of current meter data collected off the Guyana Plateau. They observed amplitudes in velocity records above 1 m/s , with a maximum variability at a nearly



(a) SIGMA



(b) ISOPYCNIC

Figure 8.3: Hovmuller diagram for the meridional component of the surface current (m/s) at 12°N in the western boundary. Contours from -9 to 1.8 , intervals of 0.1

two month period very similar to the period observed in the models. Johns et al. (1990) estimated an annual mean EKE of $1000 \text{ cm}^2/\text{s}^2$ with maximum EKE values of $1500 \text{ cm}^2/\text{s}^2$ from September to January and minimum EKE values of $800 \text{ cm}^2/\text{s}^2$ from February to June. These values are in a good quantitative agreement with SIGMA results (Fig. 8.1(c)). LEVEL exhibits a signal of lower amplitude, with EKE values below $500 \text{ cm}^2/\text{s}^2$ (Fig. 8.1(a)), and even lower values are found in ISOPYCNIC in these tropical regions (Fig. 8.1(b)). JOHNS et al. (1990) conclude that the retroflection of the North Brazil Current is likely responsible for this signal. Similar anticyclonic eddies have been inferred from sea surface elevation (ROMANESSEN, 1993), or satellite images (RICHARDSON et al., 1994).

Large anticyclonic eddies have also been observed in the Caribbean Seas (ROMANESSEN, 1993), but observations have not yet permitted to related these to North Brazil eddies which are thought to dissipate as they approach the lesser Antilles (SCHOTT and MOLINARI, 1996). DYNAMO model results bring new insight and strongly suggest that Caribbean and North Brazil eddies have the same origin, in the retroflection of the North Brazil Current.

Western North Atlantic

In mid-latitudes, the distribution of eddy energy is principally linked to the Gulf Stream system (Fig. 8.1). The differences in EKE along the path of the western boundary current can be related to conceptual model differences.

For example, SIGMA presents much larger EKE values in the Florida Current between 25°N and 35°N than LEVEL and ISOPYCNIC (values range between $500 \text{ cm}^2/\text{s}^2$ and $1000 \text{ cm}^2/\text{s}^2$). In SIGMA, this high variability originates in the main branch of the Gulf Stream near Bahamas Banks. However, this topographic feature has been deepened to a depth of 500 m in SIGMA, and the Florida Current oscillates between positions east or west of the Banks. This unrealistic oscillation generates meanders in the stream which propagate northward, and are largely responsible for the high variability observed in SIGMA off the coast of the southeastern United States. The variability of the Florida Current in the three models obviously needs to be further investigated, but the distribution of eddy energy, as well as the differences seen in the mean transport through the Florida Strait, (30 Sv in SIGMA, and 15 Sv in LEVEL and ISOPYCNIC, as shown in Fig. 4.15, page 61 in Chapter 4), already suggests that different behaviours will be found. As in BÖNING et al. (1991) the variability of the Antilles Current will have to be considered at the same time.

In LEVEL as well as in SIGMA, regions of high variability are found along the main path of the Gulf-Stream and east of the Grand Banks, but the pattern differs enough between models to suggest a different dynamics of the jet. In LEVEL, cores of maximum variability (above $500 \text{ cm}^2/\text{s}^2$) are seen in the Gulf Stream along 40°W . They are located between the large and quasi-permanent inertial eddies which characterize the jet in most numerical simulation carried out with the GFDL numerical code (see Fig. 4.15, page 61 in Chapter 4). They correspond to areas of favoured eddy generation. In SIGMA, similar regions of high variability are also observed, but their locations are slightly different. They also correspond to regions of preferred eddy generation at the extremity of inertial recirculation cells, in the main path of the Gulf Stream (at 62°W for example). In Figs. 8.1(c), 8.1(d), the area of maximum EKE at (40°N , 62°W) coincides in fact with a minimum MKE, thus outside of the main Gulf-Stream path.

Thus, in both models, the distribution of eddy kinetic energy is clearly linked to inertial dynamics of the jet. However, inertial recirculations cells which characterize the jet at mid-latitude are the results of complex eddy-mean flow interactions (HOLLAND, 1978). Differences in EKE between the two models are in fact associated with different patterns of the recirculations cells, which are more elongated in SIGMA, as in idealized quasi-geostrophic simulations (see for example BARNIER et al., 1991), and do not exhibit the standing-eddy like pattern observed in LEVEL (see Fig. 4.15, page 61 in Chapter 4). Therefore, it is likely that differences in EKE between LEVEL and SIGMA are caused by a different dynamical equilibrium of the jet (including eddy mean flow interactions), and that the use of different coordinate systems could explain for these differences. A more detailed look at these issues will be presented in the discussion section of this Chapter.

ISOPYCNIC has a spatial distribution of EKE somewhat similar to SIGMA (with high variability in the Florida Current for instance), but with a much smaller magnitude (EKE values are below $250 \text{ cm}^2/\text{s}^2$). The low levels of EKE in ISOPYCNIC limit the reach of a detail comparison with the other models in the region of the Gulf Stream.

However, a particularity of ISOPYCNIC is the region of intensified variability which extends eastward across the subtropical gyre approximatively between 30°N and 35°N , in relation with the strong eastward current which crosses the gyre at this latitude (see Fig. 4.18, page 67 in Chapter 4). EKE values are near $50 \text{ cm}^2/\text{s}^2$ with extrema of $70 \text{ cm}^2/\text{s}^2$. Because this structure does not branch out from the Gulf Stream at the Newfoundland Ridge, it is difficult to call it an Azores Current, but there are similarities to it in the eastern Atlantic.

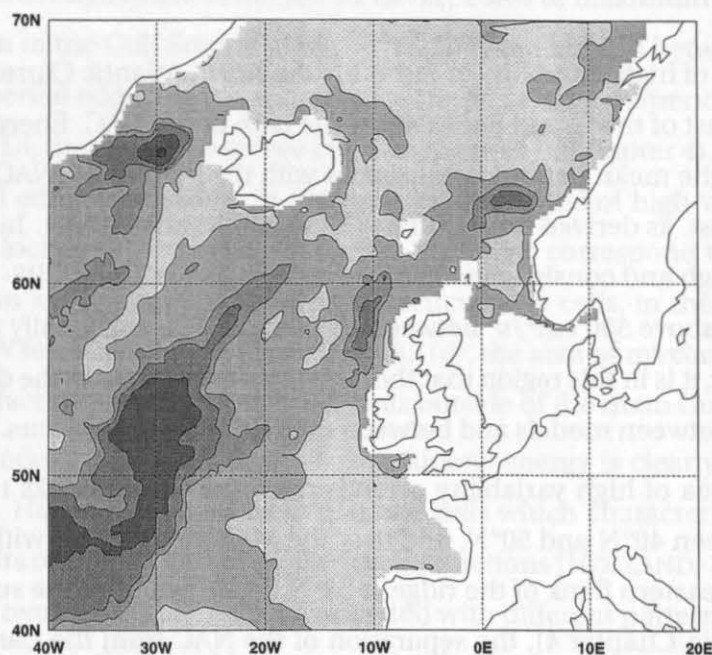
The other models show a weaker (between $10 \text{ cm}^2/\text{s}^2$ and $50 \text{ cm}^2/\text{s}^2$) but similar feature

of intensified variability 10° more to the south, between 20°N and 30°N , in regions of a weak westward mean flow.

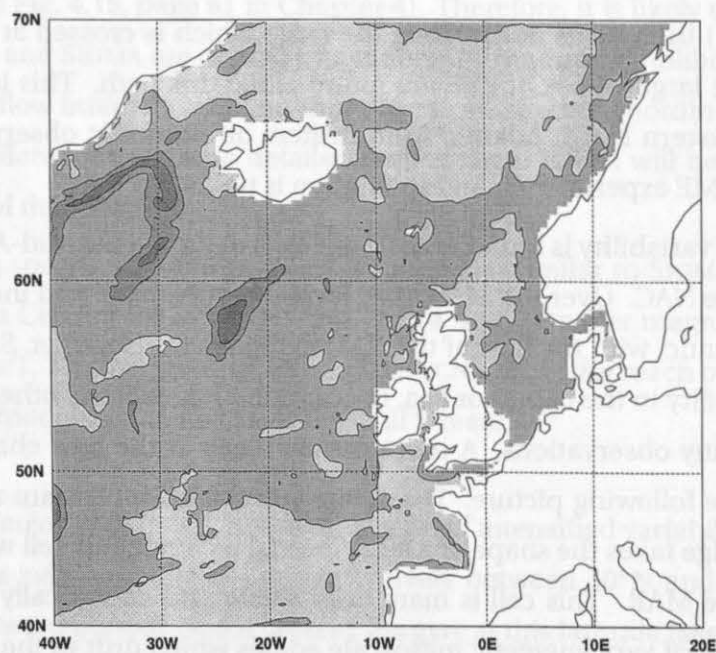
Another region of high variability in Fig. 8.1 is the North Atlantic Current. All models show large EKE values east of the Grand Banks along the path of the NAC. Energy levels are still low in ISOPYCNIC, but the mean pattern is consistent with the path of the NAC around the Banks as it turns to the east, as derived from drifters (KÄSE and KRAUSS, 1996). In SIGMA and LEVEL, energy levels are high and consistent with observations derived from ERS-1 (HEYWOOD et al., 1994), with values above $500 \text{ cm}^2/\text{s}^2$ between 45°N and 52°N , and locally above $1000 \text{ cm}^2/\text{s}^2$ in SIGMA. However, it is in this region that the largest discrepancies in the distribution of eddy energy are found between models and between models and observations.

In LEVEL, an area of high variability extends from the Grand Banks to the Mid-Atlantic Ridge (MAR) between 40°N and 50°N , and over the MAR along 30°W , with a maximum over $500 \text{ cm}^2/\text{s}^2$ on the eastern flank of the ridge at 53°N . As shown from the surface velocity field (Fig. 4.18, page 67 in Chapter 4), the separation of the NAC from the Canadian continental slope in LEVEL occurs at 45°N , at least 5° to the south of its usual location as suggested by surface drifters (BRÜGGE, 1995). At this latitude, the mean surface current flows eastward to the MAR (30°W) then turns north along the ridge which is crossed at 53°N at the Gibbs fracture zone. The large values of EKE are found along this path. This latter feature is not observed in the eastern North Atlantic from drifters or altimetric observations, nor was it seen in previous CME experiments. An explanation is unknown.

In SIGMA, eddy variability is found high from Flemish Cap to the Mid-Atlantic Ridge, with the branches of the NAC. Over the MAR, EKE levels sharply drop, and increase again in the Eastern North Atlantic, with the flow of the NAC to the north. However, SIGMA has an unexpected high variability in the Labrador Sea, in contradiction with the other models, a feature not sustained by any observations. A more detailed look at the flow characteristics in this region revealed the following picture: The extension of the Gulf Stream after it reaches the Newfoundland Ridge takes the shape of a large inertial recirculation cell which extends from Flemish Cap to the MAR. This cell is marginally stable and periodically grows and breaks into a large number of very energetic mesoscale eddies which drift to the northwest and invade the Labrador Sea. These eddies are very coherent in the vertical and can survive more than a year, and their signature is not smoothed out in the 5-year mean streamfunction (see Fig. 4.15, page 61 in Chapter 4). As a consequence, these eddies bring warm and salty subtropical waters into the Labrador Sea. We do not understand yet why this feature occurs in



(a) LEVEL



(b) ISOPYCNIC

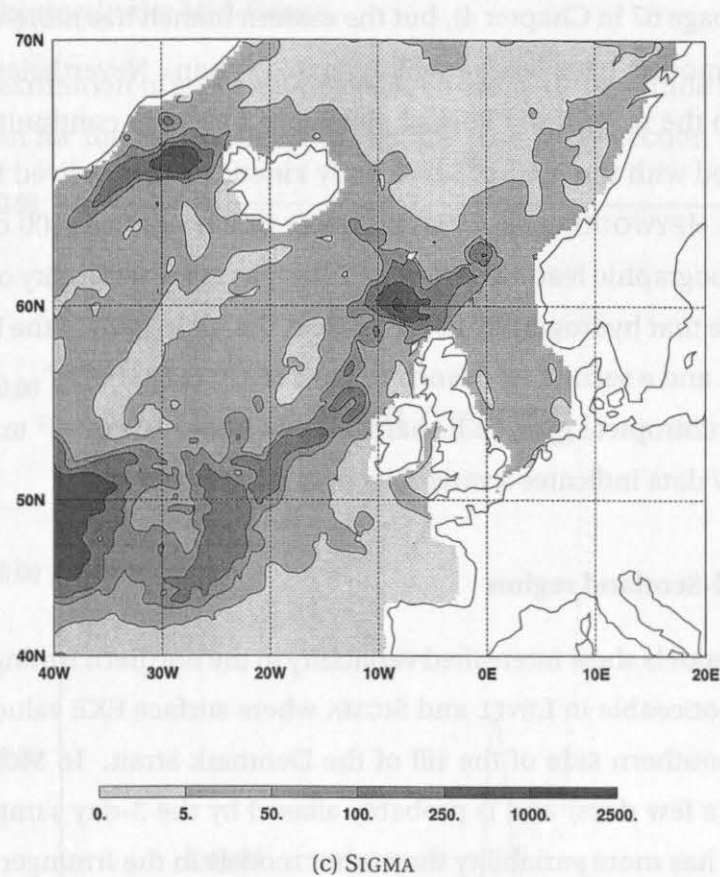


Figure 8.4: Near surface (91.64 m depth) Eddy Kinetic Energy (cm^2/s^2) in the eastern North Atlantic.

SIGMA. It may be a consequence of the stability of the jet which appears different from other models. It is unlikely, however, that the local topographic control of the flow is responsible, because the feature occurs in deep waters.

8.2.2 Eddy kinetic energy in the eastern North Atlantic

Eastern North Atlantic

In the eastern part of the subtropical gyre (Fig. 8.4), all models have a variability significantly lower than observed. None of the models has been able to overcome this deficiency, but this was not expected given the model configuration (resolution and forcing). But there are still interesting differences between the models in the Eastern North Atlantic.

In SIGMA, EKE values over $100 \text{ cm}^2/\text{s}^2$ are found east of the ridge between 42°N and 52°N , and to the east of the Rockall Plateau. Again, this is related to the branching of the NAC as it passes the MAR and before it flows to the northeast. The NAC flows on each side of the

Plateau (Fig. 4.18, page 67 in Chapter 4), but the eastern branch has more variability.

The two other models have less variability in this region. Nevertheless, significant EKE values are found to the west of the Rockall plateau in LEVEL, in continuity with the pool of large EKE associated with the NAC at 30°W. Eddy kinetic energy derived from altimetry (LE TRAON et al., 1990, HEYWOOD et al., 1994) indicates EKE levels near 100 cm²/s² or more on both side of this topographic feature. ISOPYCNIC also has more variability on the western side of the Plateau. Note that hydrography usually places the main path of the NAC to the west of the Rockall Plateau and a secondary branch to the east (ELLETT, 1993).

In the eastern subtropical gyre, EKE sharply drops under 10 cm²/s² in all models, where TOPEX/POSEIDON data indicates a variability over 50 cm²/s².

Greenland-Iceland-Scotland region

Further north, all models show intensified variability in the northern Irminger Basin (Fig. 8.4). This is especially noticeable in LEVEL and SIGMA where surface EKE values over 500 cm²/s² are found on the southern side of the sill of the Denmark Strait. In SIGMA this variability is high frequency (a few days) and is probably aliased by the 3-day sampling of the model output. ISOPYCNIC has more variability than other models in the Irminger Current along the Reykjanes Ridge, and in the East Greenland Current.

Only SIGMA has elevated levels of EKE along the Iceland-Faroe Rise (above 50 cm²/s²). This can be explained by the fact that SIGMA has a much better vertical resolution than the other models in this shallow area (depth between 300 m and 600 m) since it keeps 20 vertical levels in any depth. The variability produced by the model could be quite realistic, but a more thorough investigation should be performed. SIGMA also shows quite large surface EKE values North of the Scotland Shelf associated to the flow entering the Norwegian Sea. This variability has been observed to be high frequency (4 days) and could be attributed to local excitation of topographic waves. In this latter region, the bottom topography presents several features (Anton Dohrn Seamount, Rosemary Bank, Lousy Bank, Faroe Bank, ...). It could be that the smoothing of the topography reduces the topographic control of the current in this area and allows current meandering to resonantly excite high frequency topographic modes, in a process similar to the one proposed by MILLER and al. (1996) to explain for variability observed over the Iceland-Faeroe Ridge. But this point has to be investigated further.

In all models, strong slope currents such as the West Greenland Current and the Labrador Current do not present large eddy variability. These currents are stabilized dynamically by a large vertical coherency and the topographic constraint.

Meridional distribution in the Mid-Ocean

The meridional distribution of surface EKE averaged over a 10° longitude band between 30°W and 40°W is shown for the three models in Fig. 8.5. The 30°W section has become a stan-

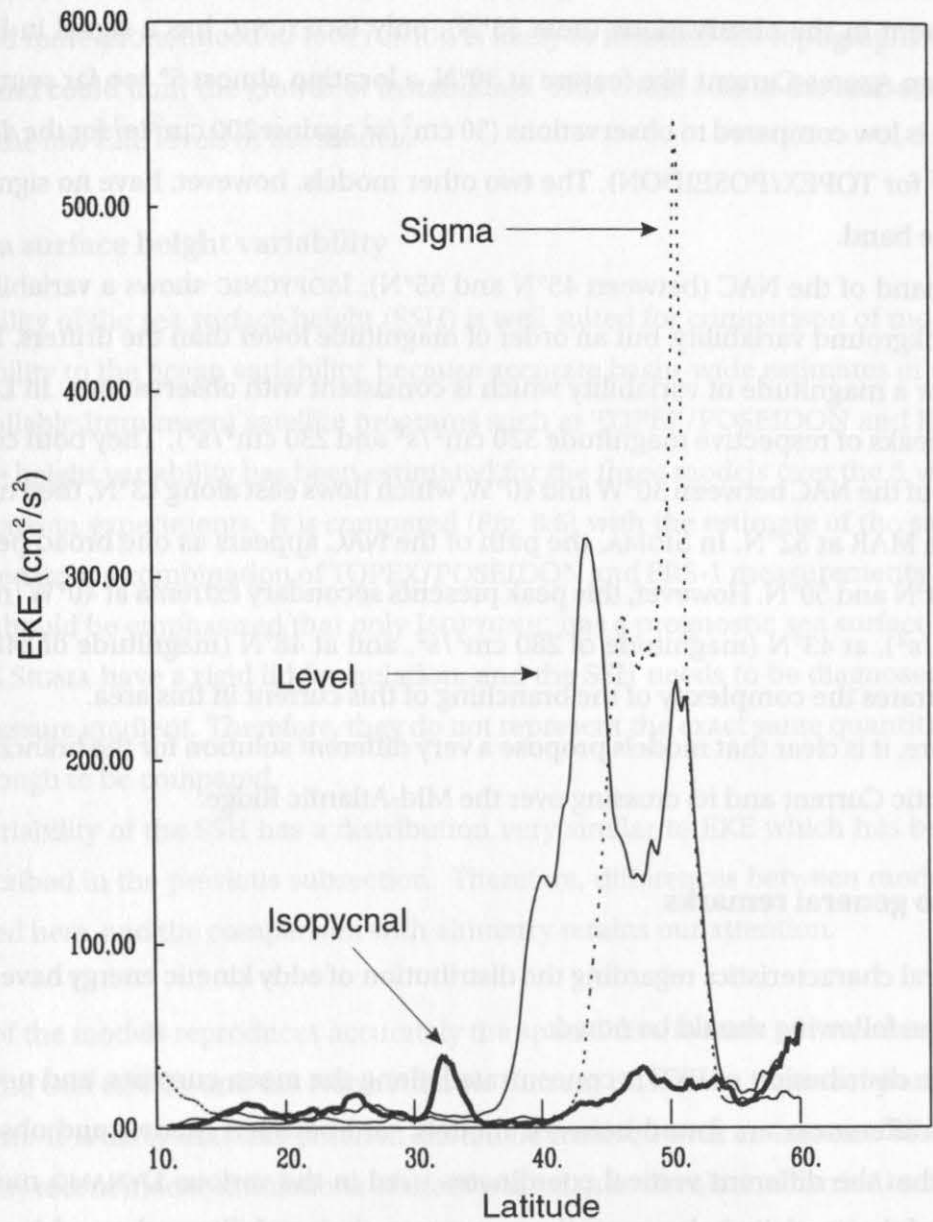


Figure 8.5: Zonal average between 40°W and 30°W of near surface Eddy Kinetic Energy (cm^2/s^2) at 91 m for the three models.

dard diagnostic quantity for North Atlantic models (see, e.g., the review article by STAMMER and BÖNING, 1996) where EKE is compared to estimates obtained with surface drifters or TOPEX/POSEIDON data. From the observations we expect to see a banded structure of the

variability in the eastern North Atlantic, as the Gulf Stream extension to the east of the Newfoundland Ridge is splitted into two major branches, corresponding to the Azores current and the NAC. In contradiction with drifter data, altimetric data suggest a weaker central branch.

Model solutions are somewhat different here. In the latitude band corresponding to the Azores current in the observations (near 35°N), only ISOPYCNIC has a signal in EKE which resembles an Azores Current like feature at 30°N , a location almost 5° too far south, and the magnitude is low compared to observations ($30\text{ cm}^2/\text{s}^2$ against $200\text{ cm}^2/\text{s}^2$ for the drifters and $300\text{ cm}^2/\text{s}^2$ for TOPEX/POSEIDON). The two other models, however, have no signal at all in this latitude band.

In the band of the NAC (between 45°N and 55°N), ISOPYCNIC shows a variability higher than its background variability, but an order of magnitude lower than the drifters. LEVEL and SIGMA show a magnitude of variability which is consistent with observations. In LEVEL, EKE show two peaks of respective magnitude $320\text{ cm}^2/\text{s}^2$ and $230\text{ cm}^2/\text{s}^2$. They both correspond to the path of the NAC between 30°W and 40°W , which flows east along 43°N , then turns north to cross the MAR at 52°N . In SIGMA, the path of the NAC appears as one broad peak of EKE between 40°N and 50°N . However, this peak presents secondary extrema at 40°W (magnitude of $140\text{ cm}^2/\text{s}^2$), at 43°N (magnitude of $280\text{ cm}^2/\text{s}^2$, and at 48°N (magnitude of $540\text{ cm}^2/\text{s}^2$), which illustrates the complexity of the branching of this current in this area.

Therefore, it is clear that models propose a very different solution for the branching of the North Atlantic Current and its crossing over the Mid-Atlantic Ridge.

8.2.3 Two general remarks

If two general characteristics regarding the distribution of eddy kinetic energy have to be emphasized, the following should be noted:

First, the distribution of EKE is concentrated along the mean currents, and nevertheless significant differences are found between models, and between models and observations. It is likely that the different vertical coordinates used in the various DYNAMO models have an impact of the vorticity balance on these currents, their stability and on eddy-mean flow interactions.

Second, it appears that interactions of the flow with the large-scale bottom topography could be a limiting factor of the eddy variability. In all models, highest energy levels are indeed found in deep waters, and the variability is found to decrease above significant topographic features such as continental slopes or the Mid-Atlantic Ridge, even in the presence of strong mean flows. This is the case for the Greenland and Labrador Currents, where lit-

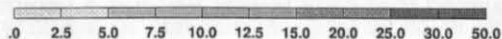
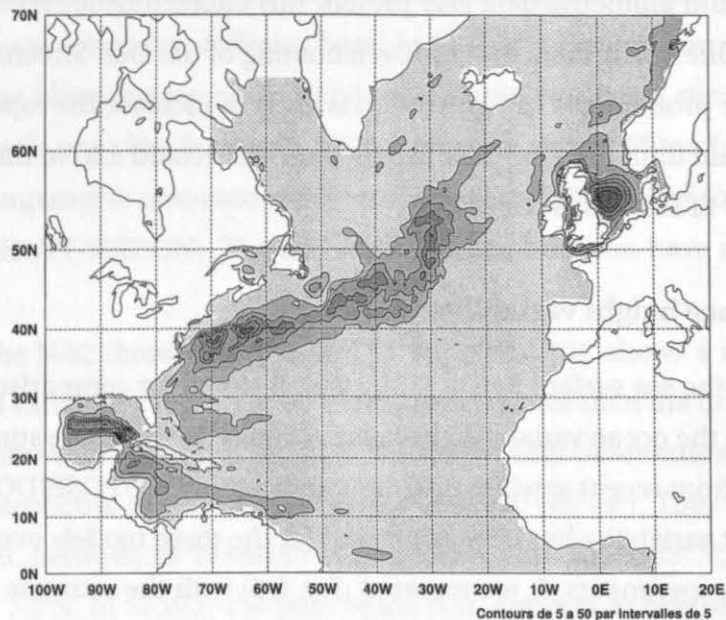
the variability is found. The variability in the NAC is also reduced over the mid-ocean ridge. This is confirmed in a following section which investigates the vertical distribution of eddy energy. Drifters and altimetric data also present this characteristic (HEYWOOD et al., 1994, BRÜGGE, 1995). One could think that the overshooting of the Gulf Stream observed in every model, (and more pronounced in ISOPYCNIC), is likely to increase the topographic influence of the jet, and could limit the growth of instabilities. This could add to the lack of resolution to explain the low EKE levels of the models.

8.2.4 Sea surface height variability

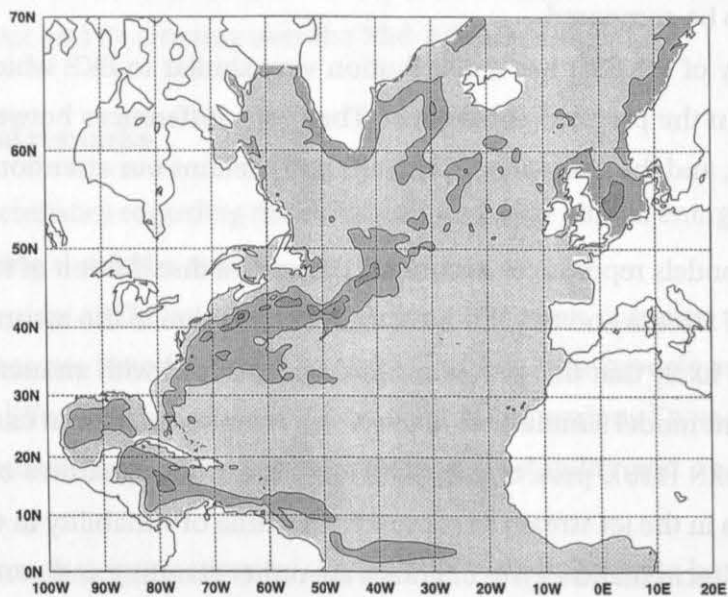
The variability of the sea surface height (SSH) is well suited for comparison of model generated variability to the ocean variability, because accurate basin-wide estimates of this quantity are available from recent satellite programs such as TOPEX/POSEIDON and ERS-1. The sea surface height variability has been estimated for the three models over the 5 years of the intercomparison experiments. It is compared (Fig. 8.6) with the estimate of the same quantity obtained from a combination of TOPEX/POSEIDON and ERS-1 measurements (DYNAMO, 1995). It should be emphasized that only ISOPYCNIC has a prognostic sea surface elevation. LEVEL and SIGMA have a rigid lid formulation, and the SSH needs to be diagnosed from the surface pressure gradient. Therefore, they do not represent the exact same quantities, but are similar enough to be compared.

The variability of the SSH has a distribution very similar to EKE which has been extensively described in the previous subsection. Therefore, differences between models are not emphasized here, and the comparison with altimetry retains our attention.

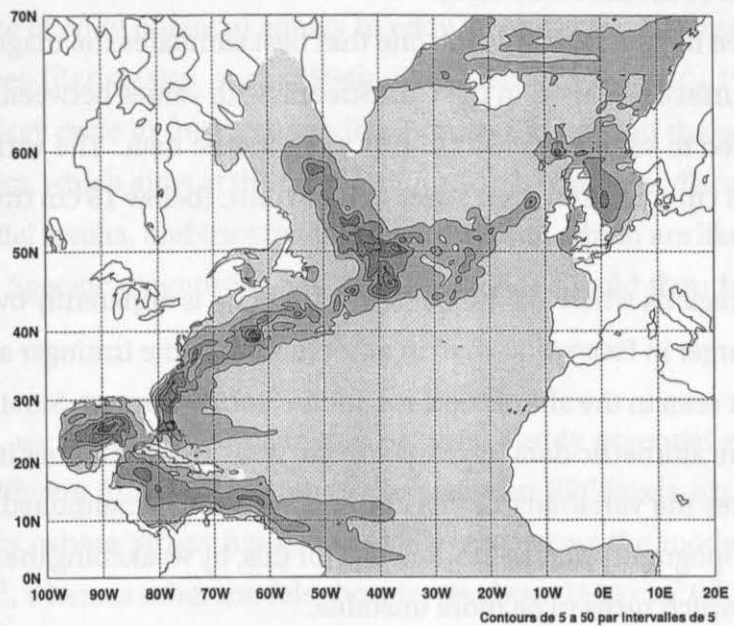
None of the models reproduces accurately the spatial distribution of rms sea surface elevation in the Gulf Stream and the North Atlantic Current due to the incorrect position of the Gulf-Stream. It is likely that this problem should be resolved with an increase resolution, as indicated by recent model simulations of the North Atlantic circulation carried-out at a $1/10^\circ$ resolution by BRYAN (1997, pers. comm.). All models exhibit signatures of inertial eddies or recirculation cells in the jet stream as successive maxima of variability in the SSH. This indicates that inertial recirculation gyres or eddies are rather standing and permanent features in models, as already discussed in the eddy kinetic energy section. The distribution of SSH variability is more homogeneous in altimetric data (Fig. 8.6(d)), and it is not obvious to identify inertial recirculations in the jet. This could mean that the inability of models to reproduce the correct levels of variability of the Gulf Stream comes from the fact that these stationary struc-



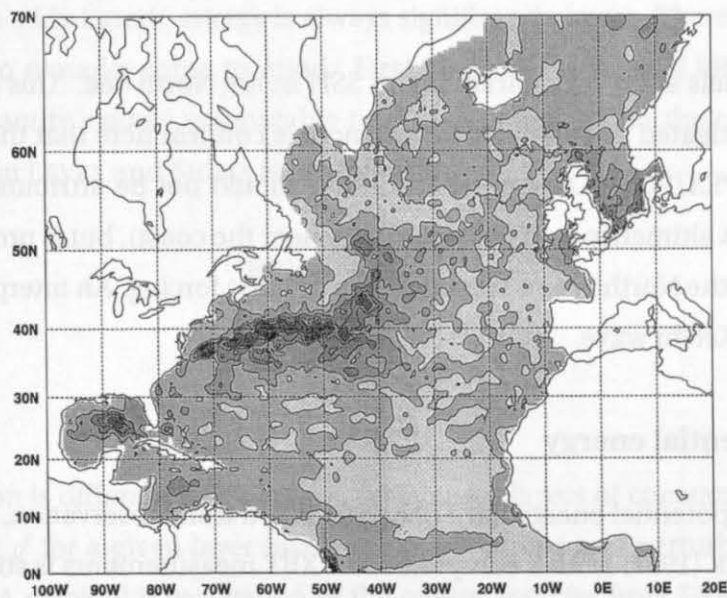
(a) LEVEL



(b) for ISOPYCNIC



(c) SIGMA



(d) TOPEX/POSEIDON and ERS-1 combined

Figure 8.6: Sea-surface height variability (the rms of the sea level elevation, in cm).

tures are model artifacts. We expect that increased horizontal and vertical resolution should improve this aspect of the model solution.

Among the three models, LEVEL is the one that best simulates the magnitude of the variability of the sea surface elevation in the Gulf Stream, with values between 20 cm and 30 cm rms, to be compared to values over 30 cm rms in altimetric data. The variability is lower in SIGMA (10 cm to 25 cm rms), and even lower in ISOPYCNIC (below 15 cm rms).

There are also regions where the model SSH variability is apparently overestimated: The rms of the SSH is larger in ISOPYCNIC than in other models in the Irminger and Labrador Currents, a pattern not seen in the altimetric data. In the Florida Current, SIGMA has a variability of 20 cm rms, where altimetric data have only 10 cm rms. This is another indication that the model overestimates the variability of this current. As already mentioned, the topographic smoothing of the topography may be responsible for this, by weakening the topographic control of the current which turns to be more unstable.

The variability associated to the Loop Current in the Gulf of Mexico is well represented in SIGMA both in pattern and magnitude. This pattern is somewhat different but realistic in LEVEL. The signal here is rather weak in ISOPYCNIC, with no apparent extremum in the Loop Current.

Finally, all models show high variability in SSH in the North Sea. This phenomenon has not yet been investigated in detail. However, models confirm here that this signal, which is also strong in TOPEX/POSEIDON and ERS1 data, should not be attributed to aliased tidal signal remaining in altimetric data (excepted very near the coast), but is probably dominated by the response of the North Sea to seasonal atmospheric forcing. An interpretation could be a large amplitude Kelvin wave.

8.2.5 Eddy potential energy

Few maps of eddy potential energy have been produced from observation, and the one published by DANTZLER (1977) from a compilation of XBT measurements is still a reference. Often, the distribution of EPE in models is not discussed since most of the information it provides is redundant with that obtained from EKE, as it can be seen in comparing Fig. 8.1 and Fig. 8.7.

However, the similarities in the distribution of EKE and EPE, and their association with mean currents is indicative of dominant eddy generating processes, which are linked to the

mean flow and stratification.

Potential energy is a useful quantity to understand eddy generating processes. In particular, the transfer rate of eddy potential energy to eddy kinetic energy characterizes baroclinic instability processes (BECKMANN et al., 1994b, STAMMER and BÖNING, 1996). A complete analysis of the energy cycle in the three models, however, is beyond the scope of this chapter on eddy statistics, which aims at the description and evaluation of discrepancies between the individual model results, and tries to identify the reasons which are likely responsible for these differences. Specific diagnostics and process studies should then follow for a deeper investigation.

In this section, we discuss the distribution of surface eddy potential energy (Fig. 8.7) in areas where it is different from EKE. All models have similar EPE levels, except in few specific areas in the tropics, where SIGMA has the lowest levels among the models, with no values above $1000 \text{ cm}^2/\text{s}^2$, whereas other models show levels above $1500 \text{ cm}^2/\text{s}^2$. LEVEL and SIGMA have very similar values in the Gulf Stream, in general below $500 \text{ cm}^2/\text{s}^2$, significantly lower than values proposed by DANTZLER (1977). Only ISOPYCNIC has values between $500 \text{ cm}^2/\text{s}^2$ and $1000 \text{ cm}^2/\text{s}^2$ in the Gulf Stream. This model exhibits a variability in potential energy generally similar or even larger as the other models, in particular in the North Brazil Current for example, although eddy kinetic energy is always significantly lower. There is no explanation at present, but two remarks come to mind. First, one may wonder if EPE as calculated in ISOPYCNIC is a quantity exactly comparable to EPE as calculated in the other models. The formulation used in LEVEL and SIGMA is the following

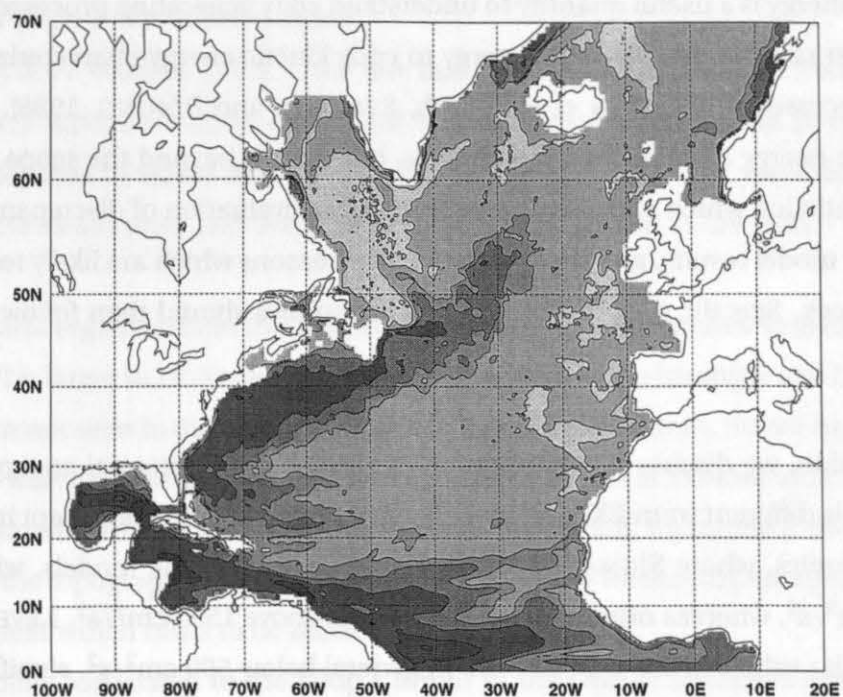
$$\text{EPE} = -\frac{1}{2} \frac{g}{\rho_0} \frac{\overline{\rho'^2}}{\overline{\rho_z^{xy}}} \quad (8.1)$$

with

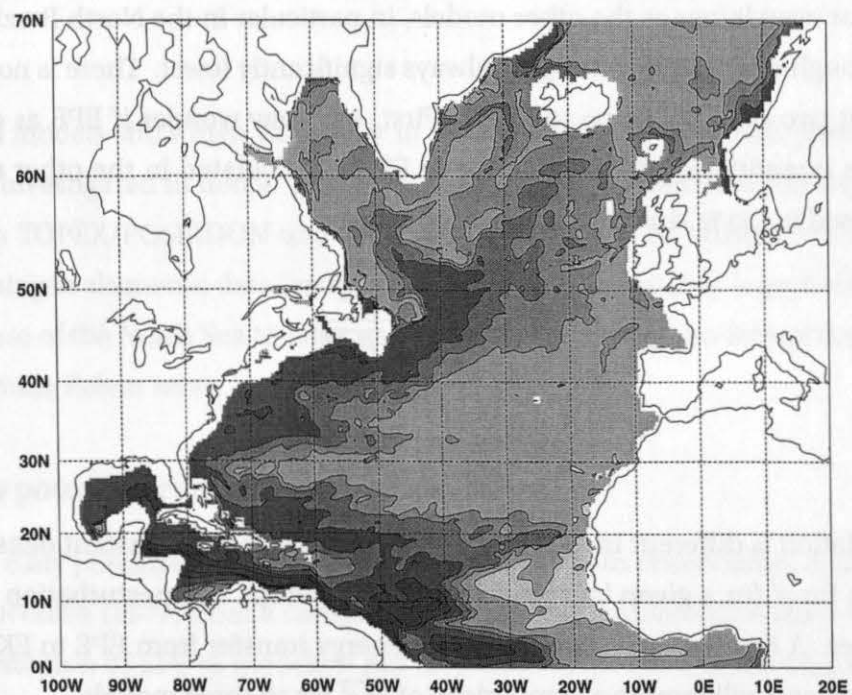
$$\overline{\rho_z^{xy}} = \frac{1}{S} \int_x \int_y \frac{\partial \rho}{\partial z} dx dy \quad (8.2)$$

The formulation is different in ISOPYCNIC which uses layers of constant density. A different expression for ρ' for a given layer involves density jumps and perturbation in elevation at the interfaces. A detailed investigation of the energy transfer from EPE to EKE should be carried out later, and will require a comparison of $\overline{w'\rho'}$ for all three models.

In SIGMA, low levels of EPE are noticed in the eastern North Atlantic in the path of the NAC to the north, despite significantly large EKE levels above $100 \text{ cm}^2/\text{s}^2$. It could be that



(a) LEVEL



(b) ISOPYCNIC

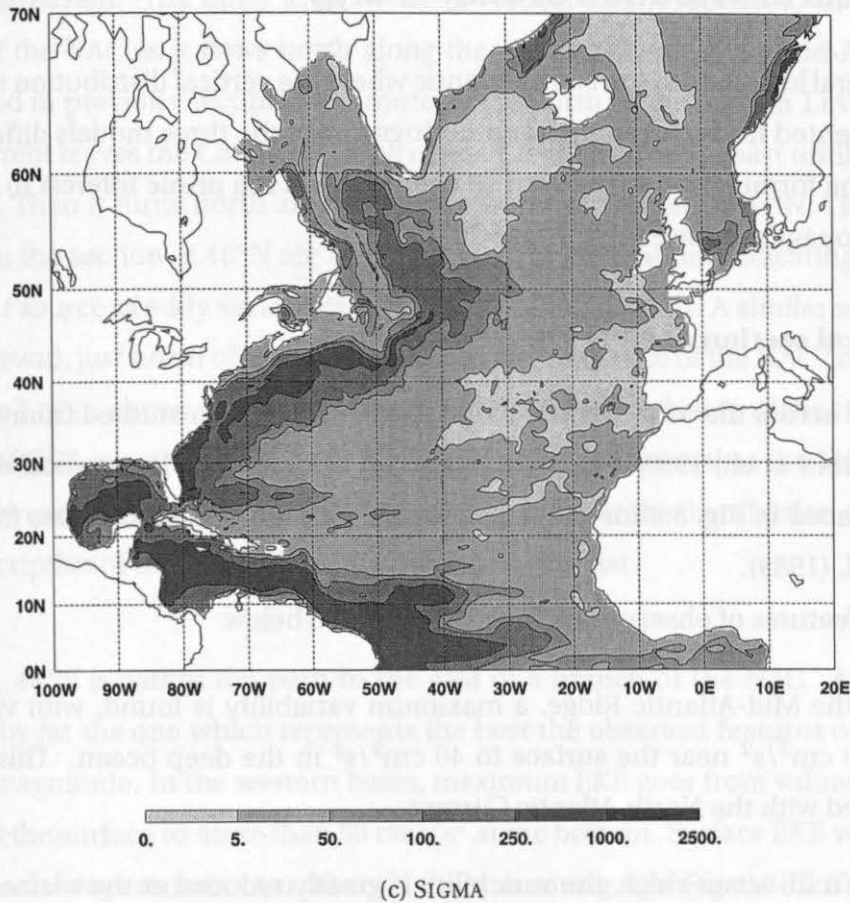


Figure 8.7: Near surface (91.64 m depth) Eddy Potential Energy (cm^2/s^2).

variability in that region is for a part driven by advection of eddies by the mean flow, or by horizontal shear instability of the NAC.

In LEVEL the most significant differences between EPE and EKE occur in the North Brazil Current. It seems that the model generates EPE but is not efficient to convert it into current fluctuations. This is consistent with the shallow aspect of the NBC and its variability which is confined to the near surface, as discussed in the next section.

In the overflow area EPE is low in all models, even when EKE is large. This is an indication that the variability here should be related to horizontal shear instabilities and current meandering.

Our final remark is that in LEVEL and SIGMA, the southwestern limit of the subtropical gyre (between 20°N and 30°N where a weak westward mean current is observed), is a place where a weak baroclinic instability generates significant levels of EKE and EPE.

8.3 Vertical distribution of eddy energy

There are several locations in the North Atlantic where the vertical distribution of eddy energy is well documented from current meter moorings. Since the three models differ mainly (but not only) by the formulation of the vertical coordinate, it is a prime interest to compare how the models propagate eddy energy at depth.

8.3.1 Vertical section at 48°N

The eddy flow across the Mid-Atlantic Ridge at 48°N have been studied from current meter moorings (ARHAN et al., 1989, COLIN DE VERDIÈRE et al., 1989). The vertical distribution of EKE is reproduced in Fig. 8.8 for the three models with the observed values from COLIN DE VERDIÈRE et al. (1989).

The gross features of observed EKE are summarized below.

- i) West of the Mid-Atlantic Ridge, a maximum variability is found, with values ranging from $350 \text{ cm}^2/\text{s}^2$ near the surface to $40 \text{ cm}^2/\text{s}^2$ in the deep ocean. This variability is associated with the North Atlantic Current.
- ii) Over the mid-ocean ridge, the variability is greatly reduced at the surface over the topography, and is very low at great depth on both flanks of the ridge ($5 \text{ cm}^2/\text{s}^2$ or less).
- iii) In the eastern basin, an intensified variability is found above the main thermocline ($100 \text{ cm}^2/\text{s}^2$ near the surface and $10 \text{ cm}^2/\text{s}^2$ at 1500 m), but a very low variability (below $5 \text{ cm}^2/\text{s}^2$) characterizes the great depths.

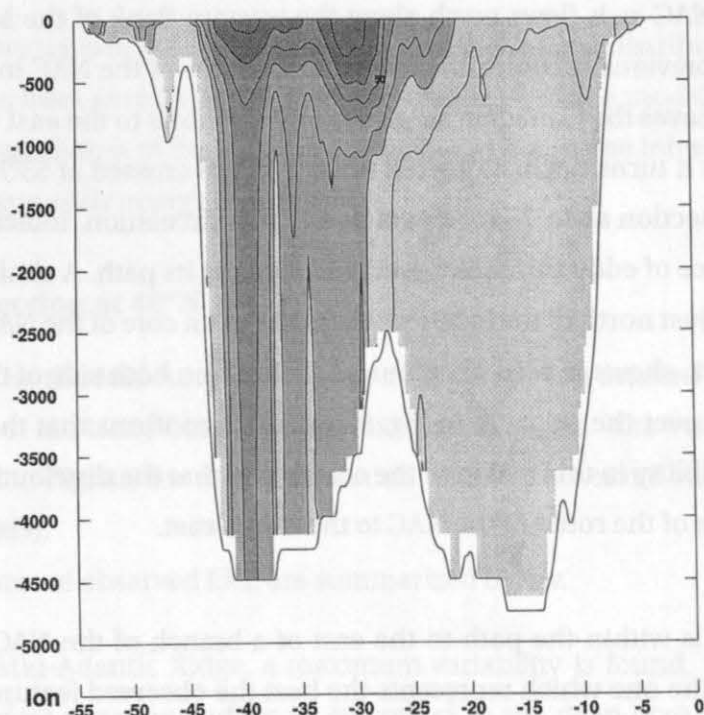
Because of low EKE levels everywhere, ISOPYCNIC can be compared to observations only qualitatively. The gross features are however reproduced. EKE is found to be largest in the upper ocean, west of the ridge in the NAC (at 40°W), and gradually decreases eastward over the mid-ocean ridge. Minimum EKE near the surface is found over the MAR. The vertical extension of eddy kinetic energy in the NAC remains shallow in ISOPYCNIC (the $10 \text{ cm}^2/\text{s}^2$ level does not reach 800 m), despite surface EKE values as large as $100 \text{ cm}^2/\text{s}^2$. A weakly intensified variability in the main thermocline ($10 \text{ cm}^2/\text{s}^2$) is observed in the eastern basin in ISOPYCNIC. However, the variability is quasi-inexistent below the main thermocline.

LEVEL has almost no variability in the eastern basin; EKE levels are less than $5 \text{ cm}^2/\text{s}^2$ near the surface and below $1 \text{ cm}^2/\text{s}^2$ at depths greater than 300 m. In the western basin, two regions of high variability are found. One at 40°W, which extends to the bottom is part of the

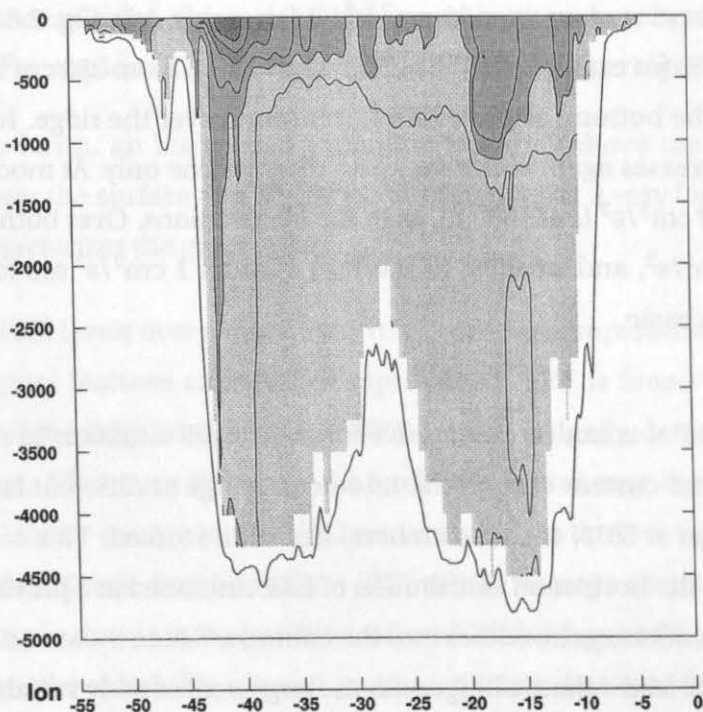
Gulf Stream extension. The other at 30°W has a vertical extent limited to the first 1500 m, and is part of the NAC as it flows north along the western flank of the Mid-Atlantic Ridge. As commented in previous sections, the route to the north of the NAC in LEVEL is unusual. When the current leaves the Canadian slope near 45°N it flows to the east until it reaches the MAR at 30°W . Then it turns north along the ridge which is crossed at 53°N . The two regions of high EKE in the section at 48°N are associated to this circulation, indicating that the NAC is a significant source of eddy variability everywhere along its path. A similar section at 55°N (figure not shown), just north of the location where the main core of the NAC crosses the mid-ocean ridge in LEVEL, shows indeed maximum EKE levels on both side of the ridge, as well as a minimum of EKE over the ridge, as in Fig. 8.8(d). This confirms that the NAC is the main source of eddy variability in this region of the ocean, and that the distribution of eddy kinetic energy is descriptive of the route of the NAC to the north-east.

In SIGMA, 48°N is within the path to the east of a branch of the NAC. At this latitude, the model is by far the one which represents the best the observed features of variability, in pattern and magnitude. In the western basin, maximum EKE goes from values largely above $500\text{ cm}^2/\text{s}^2$ at the surface to more than $50\text{ cm}^2/\text{s}^2$ at the bottom. Surface EKE values decrease to the east, but always remain over $50\text{ cm}^2/\text{s}^2$. At mooring A in Fig. 8.8(d) (from COLIN DE VERDIÈRE et al., 1989) for example (35°W), EKE values range from $250\text{ cm}^2/\text{s}^2$ near the surface to $25\text{ cm}^2/\text{s}^2$ near the bottom. Surface EKE is minimum over the ridge. In the eastern basin, eddy variability increases again above the main thermocline only. At mooring D for example (20°W), the level $10\text{ cm}^2/\text{s}^2$ is at 1500 m, as in the observations. Over both flanks of the ridge, EKE is below $10\text{ cm}^2/\text{s}^2$, and smallest EKE values of order $1\text{ cm}^2/\text{s}^2$ are found in the abyssal plain of the eastern basin.

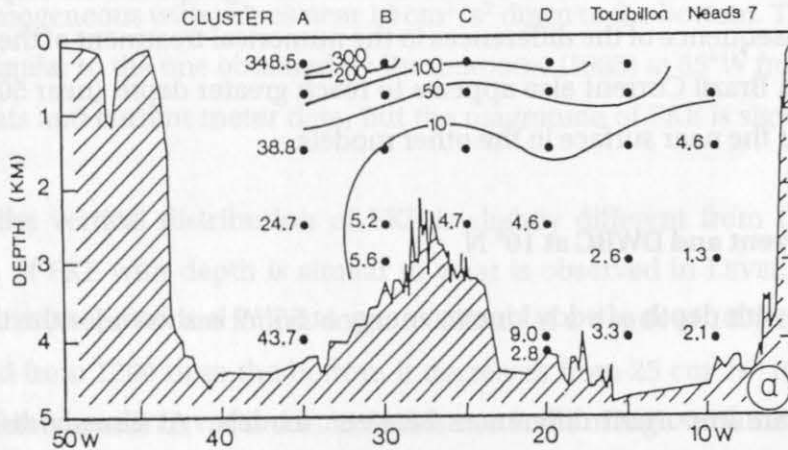
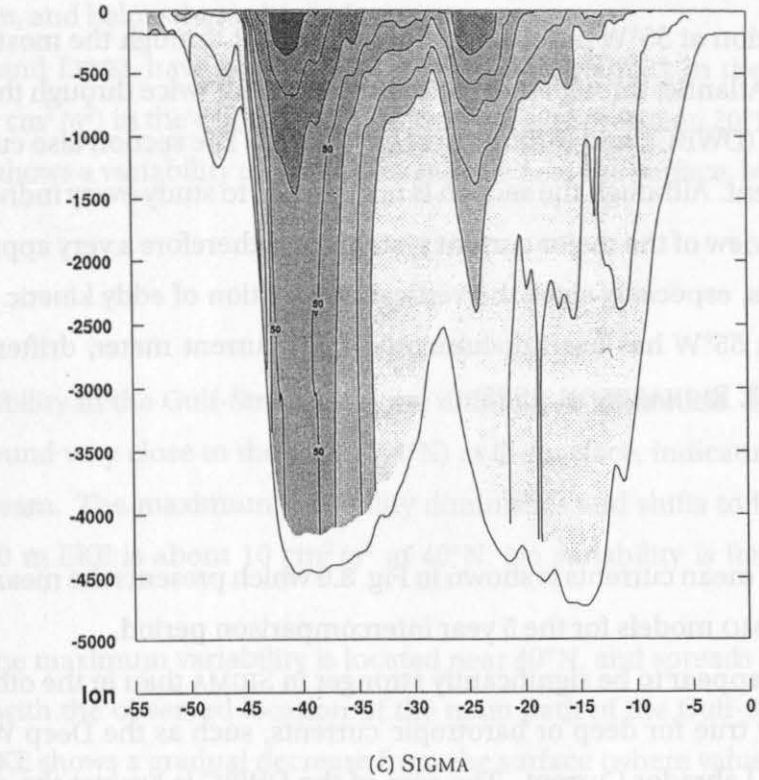
The section at 48°N is not representative for the overall situation in the NAC in the various models since the current crosses the mid-ocean ridge at different latitudes. Therefore, an additional section at 55°N (not shown here) has been studied. This section confirms the analysis made from the horizontal distribution of EKE discussed in a previous section, in particular the intrusion of energetic eddies into the Labrador Sea in SIGMA and the peculiar path of the NAC across the Mid-Atlantic Ridge with the large pool of eddy variability on the eastern flank of the ridge. In LEVEL with regard to the section at 48°N that we extensively discussed above, the vertical distribution of EKE at 55°N does not bring additional information relative to the fundamental ability of the models to propagate eddy variability at depth.



(a) LEVEL



(b) ISOPYCNIC



(d) Vertical distribution of EKE estimated from current meters moorings at this latitude

Figure 8.8: Vertical section of Eddy Kinetic Energy (cm^2/s^2) along 48°N . The vertical distribution of EKE estimated from current meters moorings at this latitude (COLIN DE VERDIÈRE et al., 1989) is also shown for comparison.

8.3.2 Vertical section at 55°W

A vertical EKE section at 55°W has the great interest to cut through the most important currents of the North Atlantic; through the North Brazil Current, twice through the Deep Western Boundary Current (DWBC), and through the Gulf Stream. The section also cut twice through the Labrador Current. Although the section is not optimal to study every individual current, it allows a synthetic view of the major current systems. It is therefore a very appropriate section to compare models, especially since the vertical distribution of eddy kinetic energy through the Gulf Stream at 55°W has been documented from current meter, drifter and float data (RICHARDSON, 1983, RICHARDSON, 1985).

Mean currents

The location of the mean currents is shown in Fig. 8.9 which presents the mean kinetic energy for the three DYNAMO models for the 5 year intercomparison period.

Mean currents appear to be significantly stronger in SIGMA than in the other two models. This is particularly true for deep or barotropic currents, such as the Deep Western Boundary Current or the Labrador Current. The core of the DWBC is against the slope at 2300 m in SIGMA, which is somewhat realistic, whereas it is a few gridpoints off-slope in LEVEL and ISOPYCNIC, a consequence of the differences in the numerical treatment of the bottom topography. The North Brazil Current also appears to reach greater depth (near 500 m) in SIGMA, but is confined to the near surface in the other models.

North Brazil Current and DWBC at 10° N

The distribution with depth of eddy kinetic energy at 55°W is shown for the three models in Fig. 8.10.

Again, there are important differences between models. As already discussed, SIGMA presents EKE values over $1000 \text{ cm}^2/\text{s}^2$ in the North-Brazil Current (at 10°N). Variability extends significantly deep, with values over $25 \text{ cm}^2/\text{s}^2$ at 1500 m depth. These values are quite consistent with the current meter estimates published by JOHNS et al. (1990) at 8.3°N, 52.1°W. In the DWBC, EKE is still over $10 \text{ cm}^2/\text{s}^2$ at 3000 m. Whether this variability is driven by the dynamics of the DWBC, or is in fact forced by the NBC above is not yet determined. The vertical time coherency of the signal will have to be investigated to answer that question.

In ISOPYCNIC as well as in LEVEL, the variability in the NBC is much weaker than in SIGMA and is confined near the surface (0 m to 500 m), in agreement with the shallow extent of the

mean current. The variability is near $5 \text{ cm}^2/\text{s}^2$ in the Deep Western Boundary Current in LEVEL at 2000 m, and below that value in ISOPYCNIC.

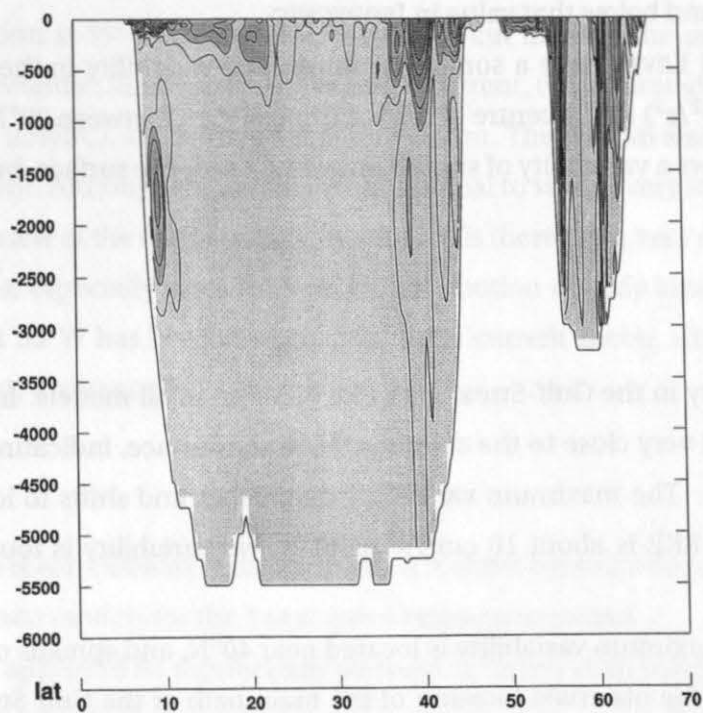
ISOPYCNIC and LEVEL have a somewhat intensified variability in the main thermocline ($5 \text{ cm}^2/\text{s}^2$ to $50 \text{ cm}^2/\text{s}^2$) in the centre of the subtropical gyre (between 20°N and 35°N). In this region, SIGMA shows a variability of similar magnitude near the surface, but it vanishes below 300 m.

Gulf Stream

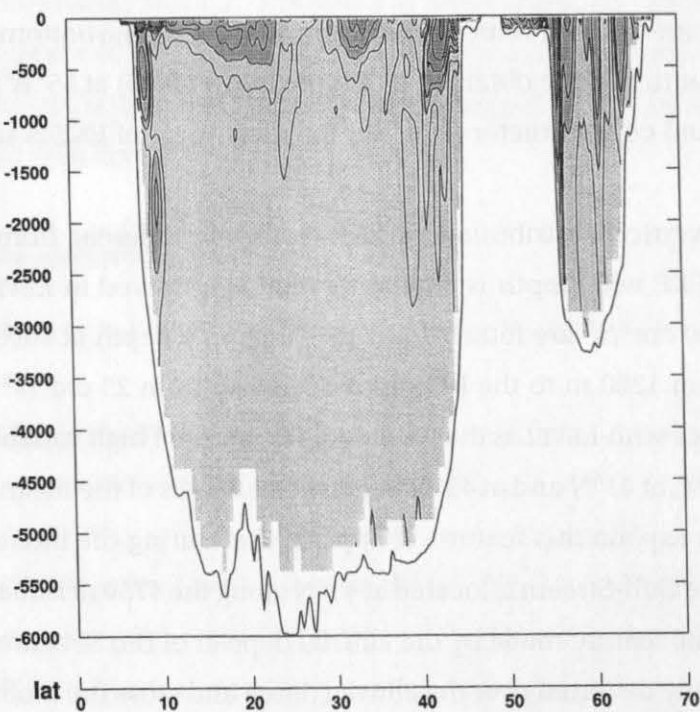
The eddy variability in the Gulf-Stream is quite different in all models. In ISOPYCNIC, maximum EKE is found very close to the coast (44°N) at the surface, indicating the overshooting of the Gulf-Stream. The maximum variability diminishes and shifts to lower latitudes with depth. At 1000 m EKE is about $10 \text{ cm}^2/\text{s}^2$ at 40°N . No variability is found at depth below 2000 m.

In LEVEL, the maximum variability is located near 40°N , and spreads over 10° in latitude, in agreement with the observed location of the main path of the Gulf-Stream. The vertical extension of EKE shows a gradual decrease from the surface (where values above $500 \text{ cm}^2/\text{s}^2$ are observed) to a depth of 1000 m (values there are $25 \text{ cm}^2/\text{s}^2$). Below that depth, EKE is vertically very homogeneous with values near $10 \text{ cm}^2/\text{s}^2$ down to the bottom. This distribution is qualitatively similar to the one obtained by RICHARDSON (1985) at 55°W from a combination of drifters, floats and current meter data, but the magnitude of EKE is significantly larger in the data.

In SIGMA the vertical distribution of EKE is slightly different from the other models. The reduction of EKE with depth is similar to what is observed in LEVEL. Values between $250 \text{ cm}^2/\text{s}^2$ and $500 \text{ cm}^2/\text{s}^2$ are found down to 400 m; at a depth of 1000 m EKE is still near $50 \text{ cm}^2/\text{s}^2$, and from 1200 m to the bottom it decreases from $25 \text{ cm}^2/\text{s}^2$ to below $5 \text{ cm}^2/\text{s}^2$. The major difference with LEVEL is that in SIGMA two cores of high variability are observed in the Gulf Stream area, at 41°N and at 43°N . A detailed analysis of the mean and eddy flows has been performed to explain this feature. It appears that during the intercomparison period, the main path of the Gulf-Stream is located at 41°N along the 4750 m isobath, just south of the peculiar topographic feature made by the alluvial deposit of the St Laurent River. Deep isobaths are significantly distorted over the alluvial dome and cross the main axis of the stream. Meanders of the jet often interact with this topographic feature; part of the flow goes north of the topography along the 3500 m, and a large variability is generated over the topography where there is no mean current but where the second core of high EKE is found. This specific



(a) LEVEL



(b) ISOPYCNIC

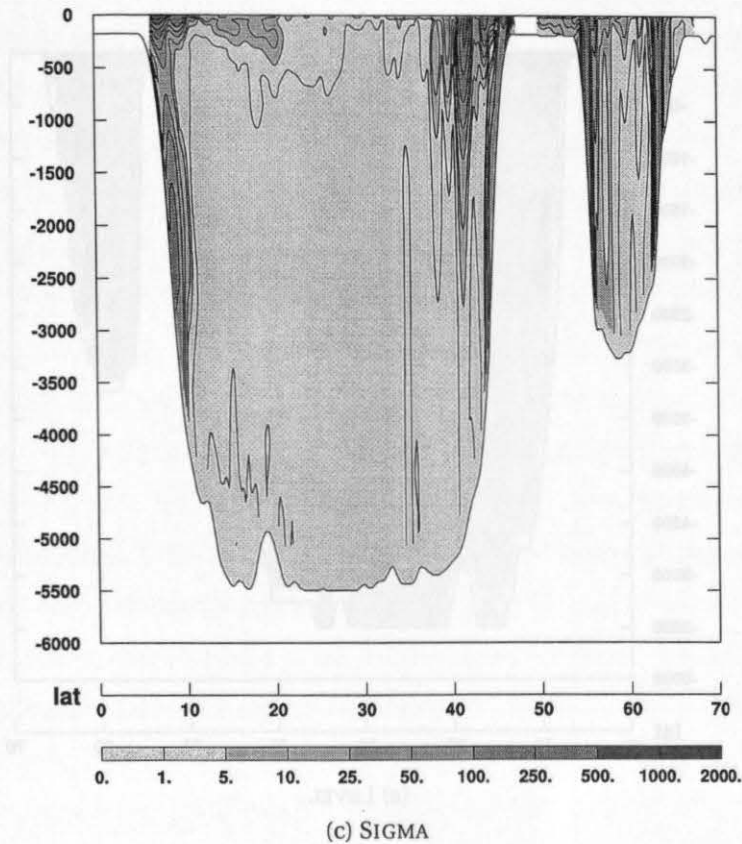


Figure 8.9: Vertical section of Mean Kinetic Energy (cm^2/s^2) along 55°W .

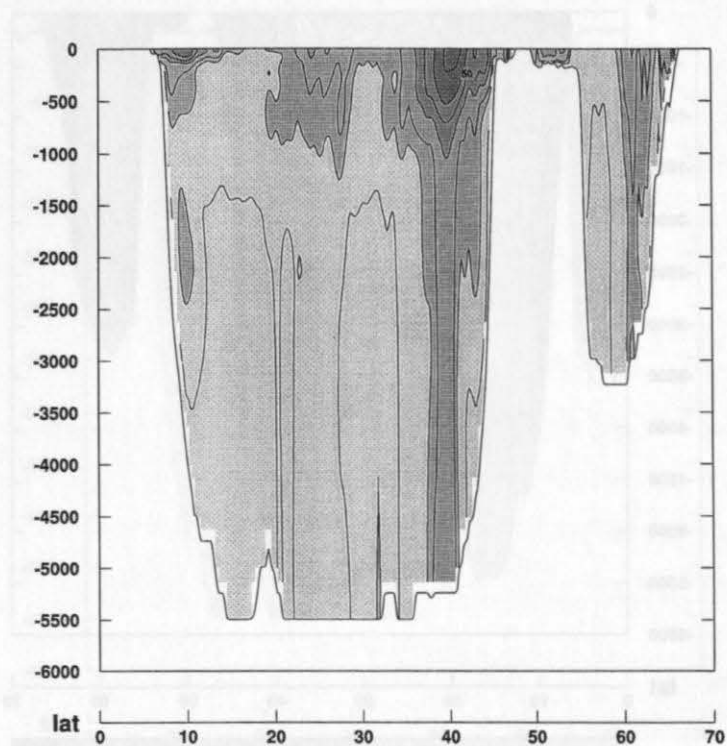
feature is a consequence of the slight overshooting of the Gulf Stream and may be amplified by the topographic smoothing which enlarged the continental slope.

Labrador Current

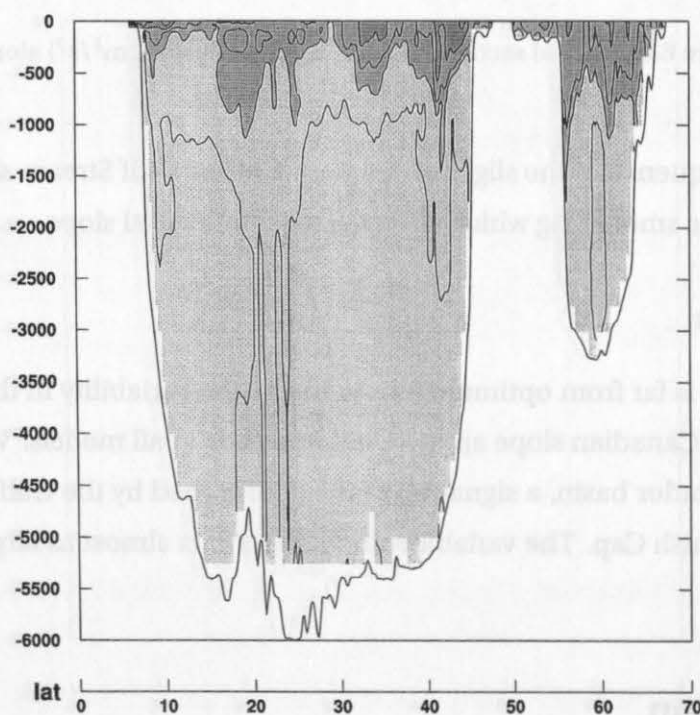
The 55°W section is far from optimum to investigate the variability in the Labrador Sea. The current along the Canadian slope appears rather steady in all models. Variability is found in SIGMA in the Labrador basin, a signature of the eddies shed by the Gulf Stream extension in the region of Flemish Cap. The variability in ISOPYCNIC is almost as large as in SIGMA in the Labrador Basin.

8.4 Discussion

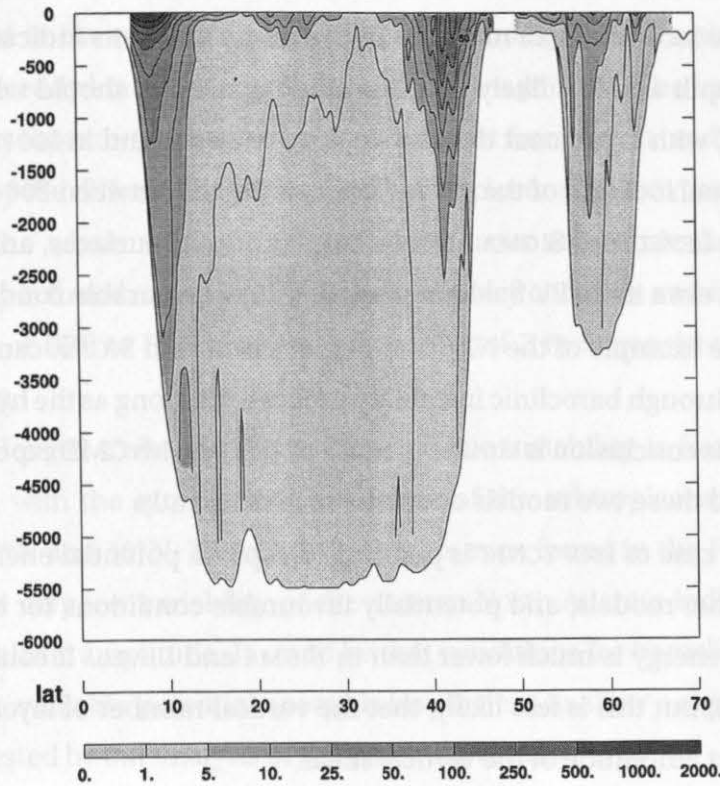
The description and preliminary analysis carried out in the preceeding sections pointed out significant differences in the geographical and vertical distribution of eddy energy between



(a) LEVEL



(b) ISOPYCNIC



(c) SIGMA

Figure 8.10: Vertical section of Eddy Kinetic Energy (cm^2/s^2) along 55°W .

the models. In agreement with observations, the distribution of eddy energy is concentrated along major mean currents, and in deep waters.

As briefly discussed above, local discrepancies in variability are related to differences in the general circulation produced by the various models, but also to the impact that model concepts have on eddy generating processes, and eddy mean flow interactions. In the following discussion, we are addressing several of the potentially relevant issues.

8.4.1 Eddy generating processes

One major source of eddies at mid-latitudes is the baroclinic instability. Instability theory (PEDLOSKY, 1979) relates the necessary condition for instability to the change in sign of the meridional gradient of potential vorticity (PV). PV sections for all three models have at 30°W have been shown and commented in Chapter 7 discussing the ventilation of the subtropical gyre (see Fig. 7.12, page 175 in that chapter). Potentially unstable conditions are found in the

upper thermocline (between 100 m and 400 m) in all models in the NAC (near 50°N, the NAC is not at the same location in all models). High density gradients indicate available potential energy at this depth and it is likely that baroclinic instability should take place. Favourable conditions in PV, with significant density slopes, are also found in ISOPYCNIC between 30°N and 35°N, the usual location of the Azores front, at depths between 200 m and 600 m. At this latitude of 32°N, LEVEL and SIGMA have rather flat density surfaces, and baroclinicity is not likely to develop, even if the PV field give a weak sign of favourable condition.

Therefore, the example of the NAC shows that LEVEL and SIGMA can generate significant eddy variability through baroclinic instability processes, as long as the hydrographic situation is favourable. This conclusion is similar to those obtained with CME experiments (BECKMANN et al., 1994b), and these two models do not behave differently.

However, the case of ISOPYCNIC is puzzling. Despite a potential energy of similar magnitude than the other models, and potentially favourable conditions for baroclinic instability, the eddy kinetic energy is much lower than in SIGMA and LEVEL. It could be that the model is too diffusive or, but this is less likely, that the vertical number of layers is not sufficient to allow for a correct amplitude of the vertical shear.

8.4.2 Eddy lengthscale

Still following the instability theory (Pedlosky, 1979), the ratio of eddy potential energy to eddy kinetic energy should correspond to the ratio of the eddy lengthscale to the internal radius of deformation in the following way:

$$\frac{\text{EPE}}{\text{EKE}} = \left(\frac{L}{L_D}\right)^2 \quad (8.3)$$

where L is the eddy lengthscale and L_D the first radius of deformation. This ratio has been calculated over the first 1500 m for the three models and is shown in Fig. 8.11.

Interpretation of this scale with regards to instability processes is delicate. It may be that the absolute magnitude of the ratio depends upon the depth for which the calculation is performed. In general, values significantly below 1 would indicate that the characteristic scale of the eddies is smaller than the radius of deformation, and would suggest that the variability does not take energy from the stratification. Values around 2 and 5 would indicate a good correlation of the eddy lengthscale with the characteristic scale of the baroclinic instability defined as the scale of the most unstable perturbation. Large values (more than 10) could be understood as an absence of variability at mesoscale.

A very low level of mesoscale variability is a striking characteristic of the ISOPYCNIC run.

Only the subpolar Gyre and the equatorial Atlantic seem to have mesoscale variability. In the subtropical Gyre and in the tropics, and in western boundary currents, the eddy potential energy overcome the eddy kinetic energy by an order of magnitude. The length scales of the instability process in ISOPYCNIC seem to be very different from LEVEL and SIGMA. Presumably, this is caused by the different lateral sub-grid scale closure in ISOPYCNIC.

In LEVEL, it is the whole subtropical gyre which lacks mesoscale variability. Where mesoscale variability is found, in particular in the boundary currents, and in the Gulf Stream extension, the ratio of EPE to EKE is often of the order of 2 to 5, consistent with an active baroclinic instability.

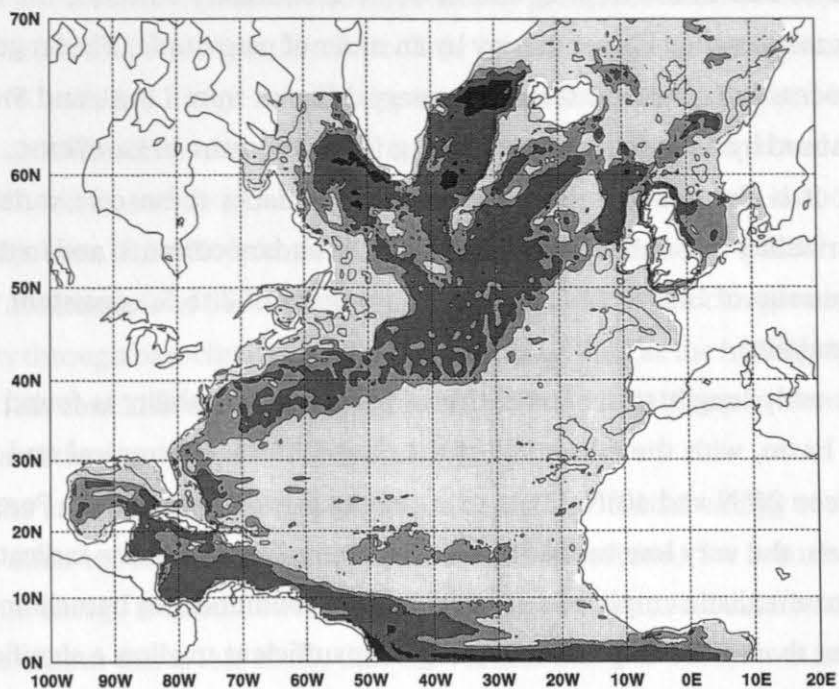
In SIGMA, eddy length scales indicative of baroclinic instability is found almost everywhere in the basin, with the exception of the centre of the subtropical and in the eastern Atlantic between 20°N and 40°N. Mesoscale activity is even found in the Porcupine Abyssal plain. However, the very low variability of the eastern North Atlantic indicates that eddies cannot grow to a realistic amplitude. It could be that conditions for baroclinic instability are favourable, but that available potential energy is insufficient to allow a significant growth of the eddies, as suggested by our analysis of the potential vorticity at 30°W.

In any case, models are quite different in eddy scale, reflecting the differences in the mean circulation (the path of the NAC for example), but also in the way they resolve eddy generating processes.

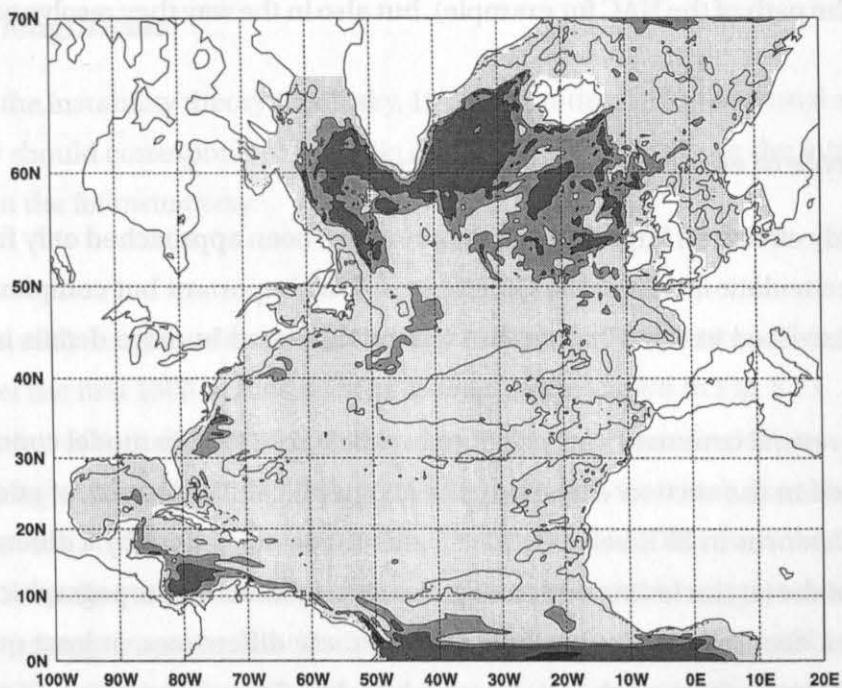
8.4.3 The role of eddies in the mean circulation

Aspects of eddy effects on large scale circulation have been approached only from the side of the inertial recirculation cells in the Gulf Stream. This important but complex subject is not thoroughly discussed in this Chapter, but will be discussed in more details in forthcoming papers.

However, several comments are worth to be made relatively to model concepts. As it has been suggested in the section discussing the geographical distribution of eddy energy, it is likely that differences in EKE between LEVEL and SIGMA are caused by a different dynamical equilibrium of the jet (including eddy-mean flow interactions and topographic control). The use of different coordinate systems could explain these differences, at least qualitatively. In LEVEL, the vorticity balance of the jet stream is largely influenced by lateral friction as long as the current feels the coastline or the stair-case bottom topography. On the contrary, the jet stream in SIGMA would be influenced by lateral friction only when the current flows along the land-sea mask. But the Gulf Stream is always several grid points away from the coast in the



(a) LEVEL



(b) ISOPYCNIC

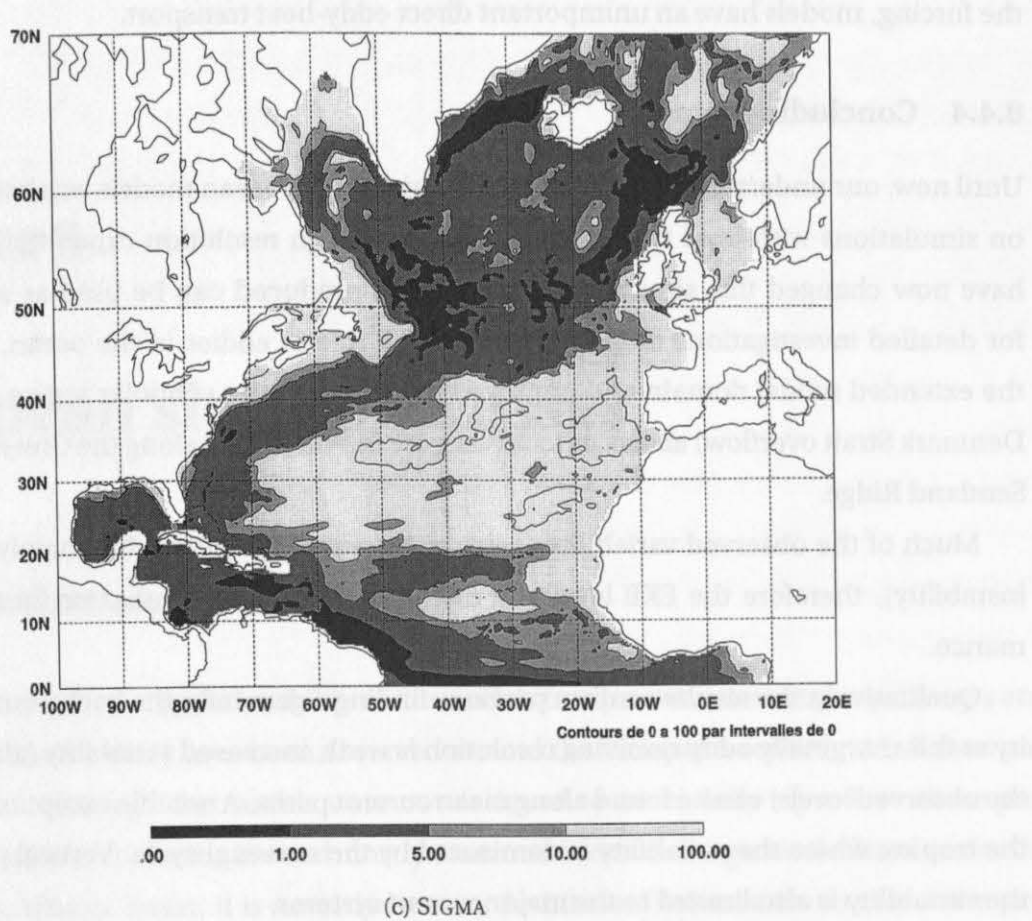


Figure 8.11: Non-dimensional Eddy Length estimated as the ratio of eddy potential to eddy kinetic energy over the first 1500 m.

simulations, and dominant processes involved in the dissipation of vorticity are the eddies and the bottom friction. Different numerics such as using different staggered grid (B-grid for LEVEL and C-grid for SIGMA) could also contribute to the differences in solutions for the WBC. The comparison with ISOPYCNIC is not relevant on this topic because the model has so few eddies, that no significant eddy-driven recirculation cells are generated in the Gulf-Stream system.

Another quantity that deserves attention is the eddy component of the meridional heat transport. The DYNAMO models do not bring fundamental new insight, and the direct eddy contribution is still low compared to the overall contribution of the mean flow (which includes the eddy driven-part). However, it is worth noting that ISOPYCNIC has much less eddy variability compared to SIGMA, but both models propose a similar meridional heat transport. This confirms that, with their present resolution, parameterization and implementation of

the forcing, models have an unimportant direct eddy-heat transport.

8.4.4 Concluding remarks

Until now, our understanding of mesoscale variability in ocean models was based exclusively on simulations with level type models. The three high resolution experiments in DYNAMO have now changed this situation. The data sets produced can be used as a broader base for detailed investigations of the generation and role of eddies in the ocean. In particular, the extended model domain and improved resolution in the subpolar region (including the Denmark Strait overflow) allows us to investigate the variability along the Greenland-Iceland-Scotland Ridge.

Much of the observed variability seems to be generated internally (mainly by baroclinic instability), therefore the EKE level and distribution is a good indicator for model performance.

Qualitatively, the results confirm previous findings: generally, the background eddy activity at this marginally eddy resolving resolution is weak, increased variability (almost reaching the observed levels) can be found along mean current paths. A notable exception is, of course, the tropics, where the variability is dominated by the seasonal cycle. Vertical penetration of the variability is also limited to the major current systems.

Large scale topographic features are found to have a stabilizing effect on the circulation, which results in a significant reduction of the eddy variability near continental slopes and over the Mid-Atlantic Ridge.

Quantitatively, the model solutions differ considerably, especially ISOPYCNIC, which has much less EKE than the other models, presumably mostly due to the less scale selective harmonic diffusion, but also because the near surface vertical shear is eliminated to a large degree by the mixed layer formulation. Regions where the variability in ISOPYCNIC is larger than those in the other two (like the Azores Current, or the West Greenland Current) will therefore be of particular interest.

Many more regional differences exist between the three models, and additional analyses will have to be performed, before detailed conclusions can be drawn.
